UNIVERSITÀ DEGLI STUDI DI PADOVA

DIPARTIMENTO DI INGEGNERIA INDUSTRIALE

CORSO DI LAUREA MAGISTRALE IN INGEGNERIA CHIMICA E DEI PROCESSI INDUSTRIALI

Tesi di Laurea Magistrale in
Ingegneria Chimica e dei Processi Industriali

EXPERIMENTAL AND MODELING-BASED EVALUATION OF ELECTRODIALYSIS FOR THE DESALINATION OF WATERY STREAMS

Relatore: Ing. Monica Giomo
Correlatore: Dott. Wim De Schepper

Laureando: DAVIDE ANDRIOLLO

ANNO ACCADEMICO 2013-2014

"Why does this magnificent applied science which saves work and makes life easier bring us so little happiness? The simple answer runs: Because we have not yet learned to make sensible use of it. [...] It is not enough that you should understand about applied science in order that your work may increase man's blessings. Concern for the man himself and his fate must always form the chief interest of all technical endeavours [...]. Never forget this in the midst of your diagrams and equations."

Albert Einstein, 1931

Riassunto

Nel presente lavoro di Tesi viene analizzato il processo di Elettrodialisi per la dissalazione di soluzioni saline ad alto contenuto organico. In particolare, vengono esaminati alcuni aspetti critici quali: la stima della corrente limite, il fenomeno di *fouling* delle membrane ed i consumi energetici. Lo studio si completa confrontando, in termini di efficienza, il processo considerato con soluzioni innovative quali l'*Electrodialysis Reversal* e *Continuous Electrodeionization*.

In questa breve sezione si vogliono riassumere le motivazioni che hanno condotto a questo studio, inquadrandole nel panorama scientifico di riferimento e nel contesto aziendale in cui si è svolto il lavoro sperimentale. Successivamente, per ciascun capitolo, vengono brevemente descritti i principali obiettivi ed risultati ottenuti.

L'Elettrodialisi (ED) è un processo elettrochimico per la separazione di sostanze ioniche da soluzioni attraverso l'impiego di membrane a scambio ionico, appositamente disposte, ed all'applicazione di un campo elettrico. Negli ultimi anni, questo processo è stato largamente utilizzato per la produzione di acqua potabile o acqua di processo da acqua salmastra o acqua di mare, nel trattamento di effluenti industriali, nel recupero di acidi organici o di altre sostanze, ecc.

Nel processo di *Electrodialysis Reversal* (EDR) la polarità degli elettrodi è periodicamente invertita, così come i flussi delle soluzioni concentrata e diluita. Questa variante rispetto al processo convenzionale comporta solamente alcune piccole modifiche costruttive, ma permette un azione auto-pulente delle membrane.

Il processo di separazione innovativo *di Continuous Electrodeionization* (CEDI) impiega invece resine a scambio anionico e cationico sotto forma di piccole perle all'interno di una cella convenzionale di elettrodialisi.

VITO, *Flemish Institute for Scientific Research*, è un importante centro di ricerca, con sede in Belgio, che sviluppa tecnologie innovative nei seguenti settori: chimica sostenibile, energia, salute, materiali e uso del territorio. La ricerca condotta da VITO ha come scopo quello di sostenere e potenziare la struttura economica e sociale delle Fiandre. Il progetto oggetto di questa Tesi è stato sviluppato all'interno dell'unità *Separation and Conversion Technology* che si occupa dell'integrazione tra tecnologie di conversione (anche biologica) e tecniche di separazione. Allo scopo VITO ha reso disponibile un impianto pilota di ED/EDR, un campione di acqua di rigenerato con alto contenuto salino e di materiale organico *(Natural Organic Matter*, NOM) e resine a scambio ionico.

L'attività sperimentale ha visto lo svolgimento di prove di tipo batch, con un'unità su scala di laboratorio, in diverse condizioni operative.

Utilizzando il software COMSOL Multiphysics, è stato sviluppato un modello che descrive il comportamento di una cella di dissalazione sotto l'azione di un campo elettrico. I risultati della simulazione, sono stati quindi confrontati con quelli ottenuti in laboratorio per le diverse condizioni di lavoro.

La Tesi si compone di quattro Capitoli: una trattazione teorica del processo di ED, una verifica di tipo sperimentale del modello proposto da Strathmann e Lee per la stima della densità di corrente limitante, parametro fondamentale per il processo in esame, il caso studio di un impianto di EDR ed una investigazione approfondita sul processo di CEDI.

Nel primo Capitolo vengono esaminati i principi teorici alla base del processo di ED, in particolare il trasporto degli ioni in soluzione ed attraverso le membrane, la concentrazione di polarizzazione e la densità di corrente limitante (*Limiting Current Density*, LCD). Problemi come la formazione di depositi in superficie ed all'interno delle membrane ed il flusso indesiderato di solvente attraverso le stesse vengono analizzati, mettendo in luce anche le proprietà elettrochimiche correlate. In questo Capitolo, con riferimento ai processi ED, EDR e CEDI, sono anche descritte le principali tecniche di progettazione ed i criteri per le valutazioni energetiche, le principali applicazioni industriali e le limitazioni che li caratterizzano.

Considerando che un'accurata previsione della LCD è importante per evitare perdite di energia o brusche variazioni di pH nelle soluzioni, lo studio è stato sviluppato partendo dall'analisi del modello per la determinazione della LCD da dati sperimentali proposto da Strathmann e Lee, come riportato nel Capitolo 2. I risultati ottenuti hanno permesso di formulare alcune modifiche al modello, che sono state verificate seguendo un approccio statistico. Il modello sviluppato considera come variabili la velocità lineare di flusso e la concentrazione di equivalenti di sali contenuti nella soluzione, che nel processo viene progressivamente diluita. La stima di tre parametri viene effettuata tramite una regressione non lineare a partire da un set di dati ottenuti utilizzando una specifica cella di elettrodialisi. Lo studio condotto ha quindi permesso di ottenere i valori dei parametri caratteristici per la configurazione adottata. Nel terzo Capitolo viene affrontata la progettazione e la valutazione economica di un impianto di trattamento di acqua di rigenerato attraverso un processo di EDR. Utilizzando l'impianto pilota ed il campione di acqua di scarico industriale messi a disposizione da VITO, quattro diversi esperimenti sono stati eseguiti in sequenza. Dapprima il rigenerato è stato sottoposto ad un processo di dissalazione; quindi è stato valutato l'effetto di una breve operazione di inversione della polarità del sistema. Con il terzo esperimento si è voluta testare l'efficienza del processo di EDR, eseguendo un'accelerata esposizione al NOM delle membrane. Infine le membrane sono state sottoposte ad un trattamento chimico con una soluzione caustica. Inoltre tra un esperimento ed il successivo, sono stati eseguiti test specifici in modo da evidenziare eventuali aumenti della resistenza allo scambio delle membrane. Sulla base dei risultati ottenuti, è stato proposto un impianto industriale con una capacità di 100 m^3/giorno, che raggiunge un tasso di dissalazione del 63%. Un'analisi economica che tiene conto del costo dell'elettricità consumata dalle celle,

dei costi di costruzione annualizzati, del costo per l'acquisto e il periodico ripristino delle membrane e del costo del personale, porta alla stima di un costo annuale totale pari a 135620 €/anno. Nell'analisi condotta si è tenuto conto che il contenuto di NOM nell'acqua di rigenerato utilizzata richiede l'esecuzione di un periodico trattamento chimico, per ripristinare le originali proprietà delle membrane. Inoltre, il flusso indesiderato di acqua attraverso le membrane è stato stimato essere il 15.5% della capacità dell'intero impianto.

Nell'ultimo Capitolo i due processi di ED e di CEDI vengono messi a confronto eseguendo una serie di esperimenti a breve e a lunga durata, adottando la stessa geometria della cella di elettrodialisi. Diverse concentrazioni di soluzioni acquose di cloruro di sodio sono state utilizzate per il calcolo dell'efficienza di corrente e del consumo energetico durante processi di dissalazione. È stata inoltre analizzata la LCD risultante nei due processi. Ottimi risultati sono stati ottenuti con il processo di CEDI, su ampi intervalli di concentrazione. Tale soluzione permette di ottenere anche una buona rimozione di NOM. Tra le limitazioni rilevate, si evidenzia in particolare una ricorrente ostruzione del flusso nelle celle dovuto ad uno spostamento delle perle di resina all'interno dei compartimenti dove sono inserite. La soluzione individuata per superare questo problema è l'utilizzo di resine di maggiori dimensioni.

Abstract

This study investigates some critical aspects of the desalination process by Electrodialysis (ED), focusing on three essential topics: the determination of limiting current density (LCD), the membrane's fouling and the energy consumption. The conventional ED process was compared with Electrodialysis Reversal (EDR) and Continuous Electrodeionization (CEDI) operations, through several batch experiments carried out using a lab-scale stack. The effects of different operative conditions were analysed using both salt aqueous solutions and regenerate wastewater. Moreover, a model representing a desalination process in an ED process was developed using COMSOL Multiphysics.

During the study, it has been developed an empirical model for the LCD prediction, starting from Lee - Strathmann model. The parameters, obtained by a multi-variables nonlinear regression, depend on the structure and the geometry of the stack.

The research presents also a design study and an economical evaluation of an EDR plant, which treats wastewater produced by a deionization system by ion-exchange resins. In particular, the effort was concentrated on undesired water transport and membrane's fouling.

Finally, CEDI and ED operations were compared in terms of LCD, current efficiency, energy consumption and removal organic matter. CEDI operation achieved excellent performances in most of the experiments, although some technical disadvantages must be overcome.

Acknowledgements

I have been very lucky to spend four months at VITO Research Centre in Belgium for the experimental activity of my Master Thesis. I could not succeeded without the invaluable support of several people. First and foremost I want to thank my supervisor Wim De Schepper for his guidance, support and hospitality during my time there. Wim has been helpful on multiple occasions and – at the same time - he gave me the possibility to work autonomously. I'm very grateful to Hans for lab assistance and technical support. Then, I am particularly indebted to Dennis Cardoen for helping me on the simulation modelling. I know that I could always ask them for advice and opinions on my research. I would like to thank also Monica Giomo, my supervisor at the University of Padua, for her precious support and the energy spent for correcting this study. My gratitude is also extended to all the people I encountered in Belgium and in the Netherlands for their great hospitality. A special thank goes to Paolo Rizzato, for being the wise and real friend that I needed. I can only say I'm thankful to my mom, dad, and sister for their incessant comfort and affection. Finally, I would like to express my deep gratitude to all the friends that I've met during these magnificent years in University. Every day, they show me a safe road to go through.

Davide Andriollo
Padua, October 2014

Contents

Introduction

Water is a shrinking resource in the world. Aqueous-based industrial processes usually generate highstreams in organic and inorganic components. These components can have a negative impact on the overall process sustainability. Therefore, wastewater reuse efficiency and reclaimed water quality are highly requested in industries.

Electrodialysis (ED) is an electrochemical separation process in which charged membranes areapplied to separate ionic species from one solution to another under an electric field. Recently, this process has been widely used for production of drinking and process water from brackish water and seawater, treatment of industrial effluents, organic acids production, recovery of useful materials from effluents and salt production (Strathmann, 2004).

When the polarity of the electrodes is reversed, the system is called Electrodialysis Reversal (EDR). The main benefit of this procedure, compared to the conventional ED, is the self-cleaning of the membranes over the long-term operation (Chao and Liang, 2008).

Continuous Electrodeionization (CEDI) is an innovative separation process that incorporates ion-exchange resin beads within an ED stack. The CEDI gained increasing attention for high efficiency in ions' removal from water (Ganzi, 1988).

The study presented in this Thesis aims to investigate on the desalination process of salt solution and wastewater, comparing the conventional ED operation with EDR and CEDI. The activity was specifically developed during a stage at VITO.

VITO, Flemish Institute for Scientific Research, is an independent and customer-oriented research organisation which develops technological innovations in sustainable chemistry, energy, health, materials and land use. Research at VITO aims to stimulate development and reinforce the economic and the social fabric Flanders. This specific study was supported by the business unit Separation and Conversion Technology which focuses on the integration of (biological) conversion and separation technologies. VITO made available to this research a pilot scale ED/EDR installation, an industrial regenerate wastewater sample and resin beads.

Batch experiments were carried out to study the effects of different operating conditions on global process efficiency. Experimental results were then compared with the output of a simulation model, developed and solved using COMSOL Multiphysics software.

This Thesis consist of four chapters: a theoretical review of the ED process, an experimental verification of Lee - Strathmann model, proposed in Lee *et al.* (2001) to determine the limiting current density, a critical process design parameter, a case study of an EDR plant and an investigation on CEDI process.

In the first chapter, the theoretic principles of ED, including the issue of concentration polarisation and limiting current density, are reviewed. Problems related to the membranes, such as fouling and solvent flux through membranes, are pointed out. The discussion also relates design aspects, operating modes, energy requirements, applications and limitations of ED process and its variants.

Chapter 2 presents the experimental verification of the Lee - Strathmann model for the empirical determination of the limiting current density. In this section, some modifications and improvements to the model are discussed.

In the third chapter, the calculation of an industrial EDR plant treating regenerate wastewater and its economical evaluation are presented. In particular, the relevance of different aspects such as organic and inorganic substances separation rate, water transport and membrane fouling are investigated. An economical evaluation of the industrial plant is proposed.

Chapter 4, the last chapter, analyses the results obtained by CEDI and ED operations, using the same lab-scale stack geometry. The comparison between the two processes is focused on several parameters, such as: limiting resistance, limiting current density, current efficiency, energy consumption and removal of NOM.

Chapter 1
The principle of Electrodialysis

In this chapter, the membrane process ED is reviewed. The theoretic principles of ED including ionic transport in solutions and through ion-exchange membranes and the issue of concentration polarisation and limiting current density are outlined. Problems related to the membranes, such as fouling and solvent flux through membranes, has serious implications on ED process, thus physiochemical properties influencing these aspects are investigated. A general description of design techniques, operating modes and energy requirements is given in this chapter. Finally, the basic concept of CEDI is reviewed and most important applications, design aspects and limitations are briefly discussed.

1.1 Introduction to Electrodialysis process

ED is an electrochemical separation process which allows to transfer ions through ion-conductive membranes and to convert a salt solution feed into a concentrated solution (concentrate) and a diluted solution (diluate). If ions have to be removed below a specific concentration level, the diluate is the product of the process (e.g. production of potable water). Whereas, if ions have to be concentrated above a specific level, the concentrate is the product (e.g. reclamation of valuable solutions in metallurgy).

First commercial equipment based on ED technology was developed in the 1950s (Juda and McRae, 1950). Since then ED has been applied to many applications, including brackish water desalination, treatment of industrials wastewaters, separation processes in the food, biotechnology and pharmaceutical industry.

In the 1960s, EDR was introduced, to avoid fouling problems (Mihara and Kato, 1969). Today this technique is extensively applied in industry and allows to automatically clean membrane on surface.

Nowadays, as the growth of chemical industries increases rapidly, the demand of ultrapure water for industrial processes becomes more important. CEDI, a process combining ion exchange and Electrodialysis process, is a novel technology for producing ultrapure water that emerges as an alternative solution for producing ultrapure water with high quality. CEDI is widely used today in the electronic industry, in analytical laboratories and for the production of boiler feed water used in power generation plants.

1.2 Principles of conventional Electrodialysis

The principle of ED is illustrated in Figure 1.1 which shows a schematic diagram of an Electrodialysis cell arrangement consisting of a series of anion- and cation- exchange membranes (AEMs and CEMs, respectively) arranged in an alternating pattern between an anode and a cathode. The driving force for the ion transport in ED is an applied electrical potential between the anode and the cathode. CEMs allows the passage of cations but reject anions, while AEMs allow the passage of anions but not cations. As a result, ions accumulate in concentrate compartments and are depleted in the channels of diluate.

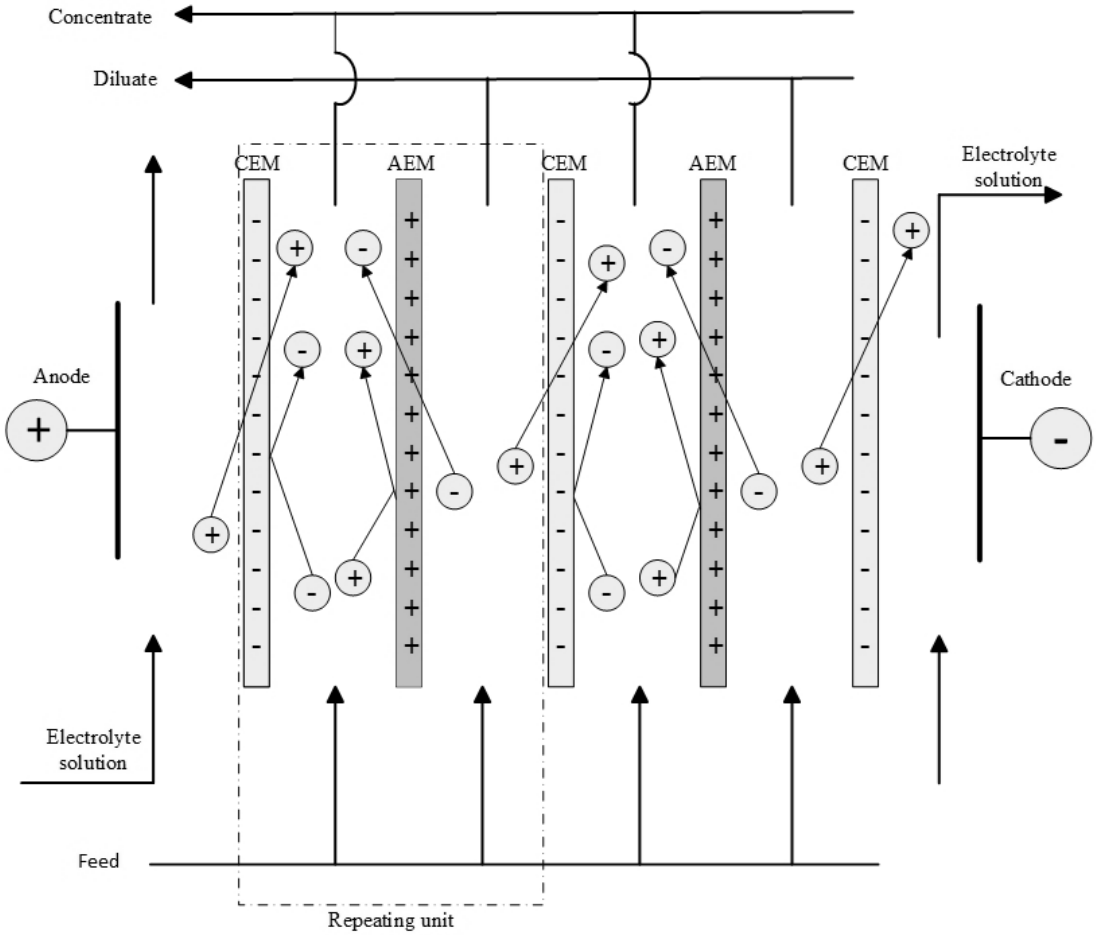

Figure 1.1. *Schematic illustration of the principle of desalination by ED in a stack with AEMs and CEMs in alternating series between two electrodes.*

To protect the electrodes from the processed fluid, they are placed in a separate compartment, which contains electrolyte fluid. Only small amounts of electrolyte solution has to be added once in a while to replenish losses of the system, e.g. leakages or evaporations.

A unit composed of a CEM, a compartment with the diluate, an AEM and the concentrated compartment is referred to as a cell pair. An ED stack is a device composed of individual cells in alternating series with electrodes on both ends. In industry, a stack contains typically up to

200 cell pairs between two electrodes. To achieve a higher degree of desalination more stacks can be placed in series.

In the ED stack the overall ion transport is proportional to the current passing through a cell pair multiplied by the number of cell pairs in the stack. The total power required for a certain degree of desalination is given by the area of one cell pair multiplied by the current density and the voltage drops between the two electrodes. The total voltage drop across the stack is that of one cell pair multiplied by the number of cell pairs.

1.2.1 Mass transport and balance in a Electrodialysis system

The mass transport that occurs during ED in a stack is illustrated in Figure 1.2 which shows a cross-section through a cell pair containing a diluate and a concentrate compartments separated by two membranes (a CEM and an AEM) between two electrodes.

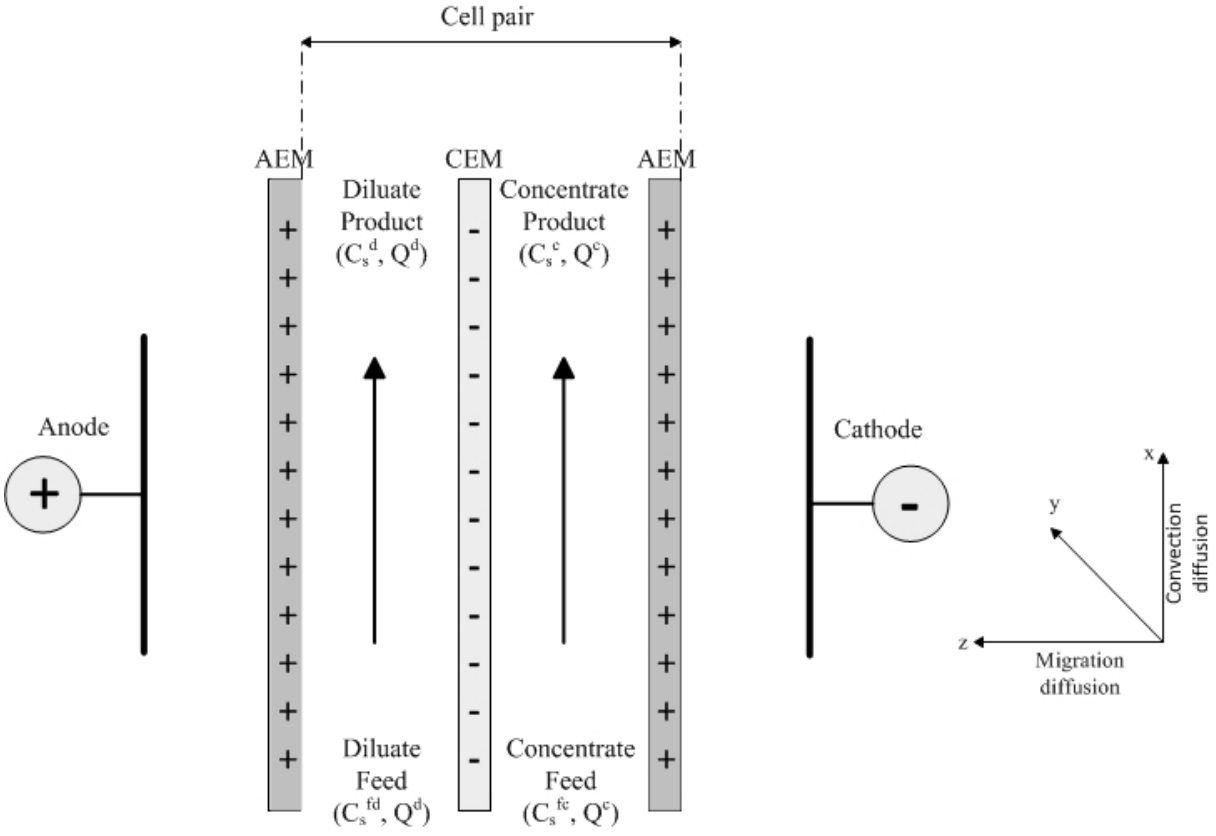

Figure 1.2. *Schematic illustration of the ionic transfer in an ED cell pair due to migration and diffusion in z-direction and convection and diffusion in x-direction.*

For simplicity reasons it is assumed that the diluate and concentrate compartments have identical geometries and hydrodynamic conditions so to avoid the build-up of pressure differences between the concentrate and diluate solutions.

The mass transport in the cell pair is the result of fluxes caused by migration and diffusion of cations and anions due to an electrical potential gradient and concentration differences between the diluate and concentrate solution in z-direction and by convection of the solutions in x-direction from the entrance to exit of the cells. The diffusive salt flux in x-direction is negligibly small compared to the convective flux in this direction (Strathmann, 2004).
The migration of ions through the membranes due to the electrical potential difference is proportional to the electrical current passing through the cell pair. The ionic fluxes from diluate to concentrate solutions leads to differences in concentration between the feed and the exit of both channels.
A material balance of mass transport within an ED stack is given in the following equation:

$$\left(C_s^{fd} - C_s^{d}\right)Q^{d} = \left(C_s^{c} - C_s^{fc}\right)Q^{c} = \frac{\xi I}{\sum_c \nu_c F} \quad ; \tag{1.1}$$

where C is the salt concentration (keq/m^3), I is the total passing current trough a cell pair (A), ξ is the current utilization, F the Faraday constant (96485337 C/keq), Q^d and Q^c are the flow rates of diluate and concentrate solutions in the cells parallel to the membrane surface (m^3/s). The superscripts *fd* and *fc* refer to the diluate and concentrate cell inlets, the superscripts *d* and *c* refer to diluate and concentrate and the subscripts *s* and *c* refer to salt solution and to cation.
The current utilization, ξ, is a measure for the amount of total current through an ED stack that can be utilised for the removal of the ions from feed. The current utilization is always <1 because of inevitable energy losses. Several factors may contribute the incomplete current utilization, such as not entirely selective membranes and water transport across the ion-exchange membranes due to osmosis and electro-osmosis.

1.2.2 Transport of ions in solution and through ion-exchange membranes

To describe ionic flux in solution and in ion-exchange membranes two principles are widely used: the Nernst-Plank equation and Donnan exclusion (Banasiak, 2004).
The extended Nernst-Plank flux equation is given by:

$$J_i = -D_i \frac{dC_i}{dz} - D_i \frac{C_i F}{\dot{R}\,\dot{T}} \frac{d\varphi}{dz} + u_i C_i \quad . \tag{1.2}$$

Here J is the ionic flux (keq/m^3 s), D is the diffusion coefficient (m^2/s), $\dot{R}$ is the gas constant (8314 J/keq K), $\dot{T}$ is the absolute temperature (K), φ is the electrical potential (V), u is the linear velocity (m/s), z is the directional coordinate and the subscript i represents individual components.

Looking at the right side of Eq. (1.2), the first term represents the diffusion, the second term represents the migration, and the third term represents the convection along z-direction. This last term can be neglected because in ion-exchange membrane separation processes pressure differences between two solutions separated by a membrane are kept as low as possible.
The simplified Nernst-Plank equation can be adapted to both solution and membrane phase, as show in the following two equations:

$$\text{Solution: } J_i = -D_i \left(\frac{dC_i}{dz} - \frac{C_i F}{\dot{R}\,\dot{T}} \frac{d\varphi}{dz} \right) \quad ; \tag{1.3}$$

$$\text{Membrane: } J_i^m = -D_i^m \left(\frac{dC_i^m}{dz} - \frac{C_i^m F}{\dot{R}\,\dot{T}} \frac{d\varphi}{dz} \right) \quad ; \tag{1.4}$$

where the superscript *m* refers to the membrane phase.
An ion-exchange membrane is composed by a polymer matrix with fixed ions. The CEMs contain negative fixed ions, whereas the groups fixed to polymer matrix of AEMs are positively charged. Mobile ions can move through the membranes, they are called co-ions if their electrical charge is identical to that of fixed ions or counter-ions if they have opposite charge.
To obtain a completely permselective membrane the co-ions should be completely excluded from the membrane phase. This exclusion is referred to as Donnan exclusion.
However, in real membranes, co-ions can be found within the membrane, thus decreasing membrane permselectivity. The membrane permselectivity depends on the concentration of the fixed ions, the valence of the co-ions and counter-ions and the affinity of the membrane with respect to the counter-ions (Nagarale *et al.*, 2006).
In ED it is assumed that total current through the membrane is carried by counter-ions only, thus is:

$$i = \frac{I}{A} = F \sum_i J_i \quad . \tag{1.5}$$

Here i is the current density (A/m^2), A is the membrane surface (m^2) and the subscripts i refer to cations if the membrane is cation-exchange or to anions if an AEM is considered.

1.2.3 Concentration polarization and limiting current density

In the ion-exchange membranes the current is assumed to be carried by counter-ions. The electric current passing through an ED cell pair is carried in the solution by both cations and anions, according with their transport numbers, which are the number of moles of the ionic species transported by 1 Faraday of electricity. However, the transport numbers in aqueous solutions are not very different for cations and anions.

A rigorous treatment of ionic fluxes in the ED process is quite complex, but the so-called Nernst film model can be applied. It assumes that the solution in a cell between two membranes can be divided into a bulk phase between two laminar boundary layers at the membrane surfaces. The bulk solution is well-mixed and has uniform concentration, whereas the concentration in the boundary layers changes over the thickness.

The transport of charged species in presence of an electrical potential difference in an ED stack leads to a concentration decrease of counter-ions in the boundary layer at the membrane surface facing the diluate and an increase at the surface facing the concentrate. The depletion and accumulation of ions at the membrane surfaces in ED is referred to as concentration polarisation and is illustrated in Figure 1.3.

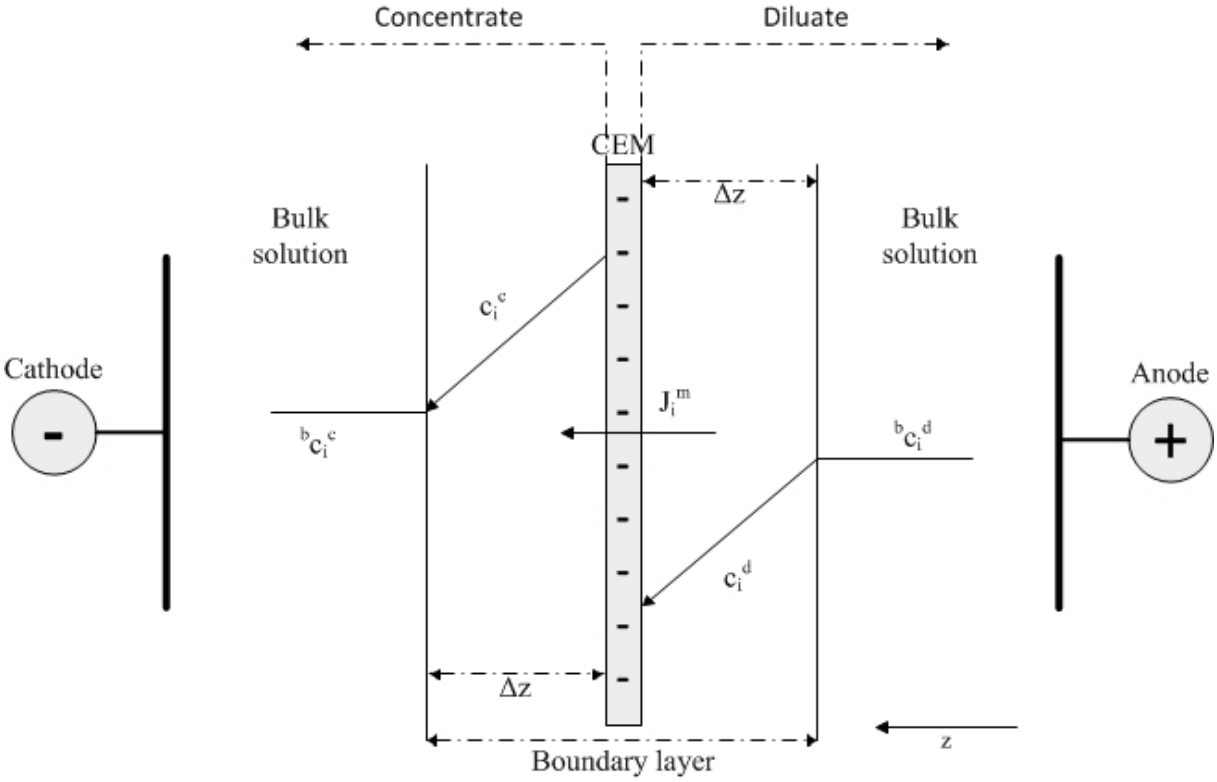

Figure 1.3. *Concentration polarization.Concentration profiles of ion iin the boundary layer on both sides of a CEM.*

The schematic drawing illustrates concentration profiles of a salt in the boundary layer on both sides of a CEM and the fluxes of cations in the membrane due to the migration. In the boundary layers the concentration and the electrical potential gradients perpendicular to the membrane surfaces cause the mass transport as the sum of a migration flux and a diffusive flux. It is assumed that the transport of cations through a highly permselectivity CEM is caused only by migration due to an electrical potential gradient within the membrane. In steady state, $J_i = J_i^m$.

The total flux of counter-ions through the boundary layer and membrane can be obtained by the following equations:

$$\text{Boundary layer: } J_i = -D_i \frac{dC_i^d}{dz} + T_i \frac{i}{F} \quad ; \tag{1.6}$$

$$\text{Membrane: } J_i^m = T_i^m \frac{i}{F} \quad ; \tag{1.7}$$

where T_i is the transport number of the counter-ion within the boundary layer and T_i^m is the transport number of the counter-ion within the membrane.
Combining Eqs. (1.6) and (1.7) gives the current density carried by an ion *i* from the diluate to the concentrate compartment through the membrane:

$$i = \frac{F\, D_i}{(T_i^m - T_i)} \frac{dC_i^d}{dz} \quad . \tag{1.8}$$

When, due to concentration polarization, in the diluate solution the salt concentration at membrane surface is reduced to 0 there are no more salt ions available to carry the electric current. Thus, the voltage drop across the boundary layer increases drastically resulting in water dissociation. The correspondent phenomenon is known as limiting current density (LCD). When exceeding this current density, there is a loss of energy utilization and drastic pH-values shifts. Therefore, ED system needs to be operated below LCD.
LCD can be calculated by integrating Eq. (1.8) with the boundary conditions that at the membrane surface $C_i^d = 0$and $z = 0$, and in bulk solution $C_i^d = {}^bC_i^d$ and $z = \Delta z$.

$$i_{lim} = \frac{F\, D_i}{(T_i^m - T_i)} \left(\frac{{}^bC_i^d}{\Delta z} \right) \quad . \tag{1.9}$$

Here i_{lim} the limiting current density, ${}^bC_i^d$ is the concentration of diluate in the bulk solution and Δz is the thickness of the laminar boundary layer.
It's important to observe that this current is a function of the transport number of ion *i* in the membrane and in solution, its diffusion coefficient, its concentration of the well mixed solution and the thickness of the boundary layer.

1.3 Membrane characterization

In the last 50 years, a significant effort has been made in academic institutions and in industry to develop efficient membranes for ED and others ion-exchange membrane processes: a great number of publications appeared on different aspects of membranes and many patents described preparation procedures.

The two type of ion-exchange membranes used in ED are:

- Cation-exchange membranes which are electrically conductive membranes that allow only positively charged ions to pass through;
- Anion-exchange membranes which have a selective permeability for anions.

CEMs contain fixed negatively charge ions, whereas AEMs contain cations as fixed ions. The co-ions are more or less completely excluded from the polymer matrix, because of their electrical charge which is identical to that of the fixed ions.

The most desired properties required for the successful ion-exchange membranes are:

- high permselectivity: a permselective membrane combines a high permeability for counter-ions and impermeability for co-ions;
- low electrical resistance: the required voltage to transfer ions through the membrane should be as low as possible;
- good chemical and form stability: membrane should be mechanically strong and should have a low degree of swelling;
- high chemical stability: membrane should be stable over a wide pH-range and in the presence of oxidizing agents.

It's often difficult to optimize the properties of ion-exchange membranes because the parameters determining some properties, often have the opposite effect on others. For instance, a high concentration of fixed ions in the membrane matrix leads to a low electrical resistance, but also causes a high degree of swelling combined with poor mechanical stability (M.Y. Kariduraganavar *et. al.*, 2006). Thus, it's necessary to find a compromise between these properties to develop good ion-exchange membranes.

1.3.1 The structure of ion-exchange membranes

According to their structure and preparation procedure, ion-exchange membranes can be classified in two big categories:

- homogeneous ion-exchange membranes in which the fixed groups are evenly distributed over the entire matrix polymer;
- heterogeneous ion-exchange membranes which have distinct macroscopic domains of ion-exchange resins in the matrix of an uncharged polymer.

Commercial membranes used in ED processes have usually a heterogeneous structure, therefore this paragraph focuses mainly on their structure and characteristics.

Heterogeneous ion-exchange membranes can be produced by melting and pressing of a dry ion-exchange resin with a granulated polymer, or by dispersion of the ion exchange resin in polymer solution. Most commercial membranes contain strong acidic or basic fixed ions, such as quaternary ammonium ($R\text{-}(CH_3)_3N^+$) in AEMs and sulfite ($R\text{-}SO_3^-$) in CEMs. The inert matrix is usually constituted by commercial polymers, such us polyethylene, phenolic resins or polyvinylchloride.

These membranes have a heterogeneous two phase structure composed of a crystalline phase and an amorphous phase, which contains the fixed ions. The amorphous region contains many clusters of fixed charges which are spherical regions connected by *bottle necks* between crystalline regions. So, the transport of counter-ions from one cluster to the next is restricted by these narrow channels.

Generally, the heterogeneous membranes show a good dimensional and mechanical stability compared to the homogeneous membranes; but the last ones allow better electrochemical performances. However, in the Literature there are numerous methods reported for the preparation of ion-exchange membranes with electrochemical properties and mechanical strength to be used in ED.

The diffusion of water into the membrane causes swelling phenomenon in the membranes.The membrane water content depends on the properties of the membrane, such as the nature and the cross-linking density of polymer matrix, the nature and concentration of fixed charges, and the homogeneity of the membrane. The swelling is also influenced by the composition of the solution with which the membrane is in contact, because of osmotic effects.

The swelling of a membrane can be obtain in weight percent (wt% swelling) by:

$$wt\%\ swelling = \frac{W_{wet} - W_{dry}}{W_{wet}} \times 100 \ ; \tag{1.10}$$

where W_{wet} and W_{dry} are the weight of a membrane sample in the wet and dry state.

Although the most practical applications of ED operate with low pressure gradient across the membrane, it's important to consider the hydraulic permeability of the membranes. This measure provides information on the diffusive or convective transport of solvent through a membrane under a hydrostatic pressure driving force.

Another important property of ion-exchange membranes is their long-term chemical stability under process conditions. Some phenomena, such as degradation and re-crystallization of basic polymer, loss of water and plasticizing agents can affect the structure and the mechanical and electrochemical properties. Particular attention has been paid to the use of oxidizing agents, bases and acids, high or low pH values and elevated temperatures.

1.3.2 Electrochemical properties of membranes

The main electrochemical properties of membranes influencing a typical ED process are ion-exchange capacity, electrical resistance and permselectivity.

The ion-exchange capacity of charged membranes is a measure of the number of fixed charges per unit weight of dry polymer; it's usually expressed in milli-equivalents per gram dry membranes.

The electrical resistance is a crucial parameter which effects the energy requirements of ED process. It is directly linked with the ion-exchange capacity and ion mobility within the membrane. The membrane area resistance, in unit of Ωcm^2, is generally determined by direct current measurements.

The mobility of different ions in the membrane in an aqueous solution do not differ very much from each other, while the ionic mobility in membrane depends mainly on the radius of hydrated ions and the membrane structure. A typical counter-ion exchange sequence of a cation-exchange membrane containing a SO_3^- group as fixed charge is:

$$Pb^{2+} > Ca^{2+} > Mg^{2+} > K^+ > NH^{4+} > Na^+ \quad . \tag{1.11}$$

A correspondent sequence is obtained for ions in an anion-exchange membrane containing quaternary ammonium groups as fixed charges:

$$NO_3^- > Br^- > Cl^- > SO_4^{2-} > F^- \quad . \tag{1.12}$$

Both sequences are shown in Strathmann (2004).

The permselectivity of a membrane refers to its ability to discriminate between positive and negative ions to allow passage through the membrane. This parameter is determined by concentration and mobility of co- and counter- ions in the membrane, which depend mainly on the ion-exchange capacity of the membrane and the ion concentration in the outside solution. The membrane permselectivity decreases with increasing salt concentration of outside solution because co-ions transport becomes considerable.

The permselectivity can be calculated using transport numbers by the following equation:

$$\psi^m = \frac{T_{cou}^m - T_{cou}}{T_{co}} \quad ; \tag{1.13}$$

where ψ is the permselectivity, T_{cou}^m is the transport number of counter-ions in the membrane, T_{cou} and T_{co} are respectively the transport number of outside solutions of counter- and co-ions. An ideal permselective membrane has a permselectivity coefficient equal to 1.

1.3.3 The flux of solvent through ion-exchange membranes

The solvent transported through an ion-exchange membrane can be due to osmosis or electro-osmosis. The osmotic solvent transport is caused by a chemical potential gradient in the membrane; whereas electro-osmosis refers to the solvent flux coupled to the flux of ions in the hydration shell and due to coupling to an electrical current. Both terms can be dominant in an ED process, depending on operative conditions: electro-osmotic solvent flux can be much higher than the osmotic flux in presence of highly permselective membranes and moderate differences in the salt concentration in diluate and concentrate solution; osmosis becomes relevant with a high concentration gradient.

In most practical applications of ion-exchange membrane separation processes the solvent is water, and water flux can be expressed to a first approximation by the water transport number. The water transport number, T_w^m, refers to the number of water molecules transported by ions through a given membrane, and can be expressed as function of the current density:

$$T_w^m = \frac{J_w}{\sum_i J_i} = \frac{F\,J_w}{i} \quad ; \tag{1.14}$$

where J_w is the water flux expressed in moles per unit area and time.

Considering aqueous solutions and typical commercial ion-exchange membranes, the water transport number is in the order of 4 to 8, i.e. one mole of ions transport ca. 4 to 8 moles of water through the membrane.

The water transport number is decreasing with increasing salt concentration because of a decrease of the membrane permselectivity.

1.3.4 Membrane fouling and poisoning

A possible important problem that can be encountered in a common ED application is the fouling of the membrane. Accumulation of suspended and colloidal matter, organic compounds and multivalent salts near to saturation level that adhere to the membrane surface causes an increase of the electrical resistance and a decrease in the selectivity of the membrane. Generally, the AEM is more sensitive to organic fouling than CEM due to electrostatic attraction between negative charged organics and the positively charged AEM (Kim *et. al.*, 2002).

The most severe of the membrane obstructions is poisoning by organic ions that are small enough to penetrate the membrane but whose mobility is so low that they virtually remain inside the membrane causing a drastic decrease in ionic transport through the membrane (Lee *et. al.*, 2002).

Membrane fouling can be avoided by a proper pre-treatment of the feed solution, such as precipitation, flocculation, microfiltration, ultrafiltration or ion-exchange to remove contaminants. Obviously the use of a pre-treatment will represent an extra operating cost to the

process. Mechanical cleaning and chemical treatment with dilute acids can generally restore the original properties of the membranes, but they have just a temporary impact on membrane resistance.
EDR operating mode is a very effective technique against membrane fouling which adds almost no additional costs; it will be discussed later in §1.4.3.

1.4 Process and equipment design

An ED plant consists of several components, such as a stack, a power source, pumps process monitoring and control devices. The technical feasibility and the economics of an ED process are determined by several process and equipment design parameters, such as cell geometry and spacer configuration of the stack, flow velocities and mode of operation, i.e. batch or continuous operation.
In systems where high capacities are required, two or more stacks can be placed in series or part of concentrate solution may be recycled.

1.4.1 The Electrodialysis stack design

A section of an ED stack is shown schematically in Figure 1.4. In a commercial stack rectangular membranes are separated from each other by spacer gaskets; AEMs and CEMs are arranged alternately. Holes in the spacer gaskets are aligned with holes in the membrane to form manifold channels that distribute the process fluids in the different compartments.

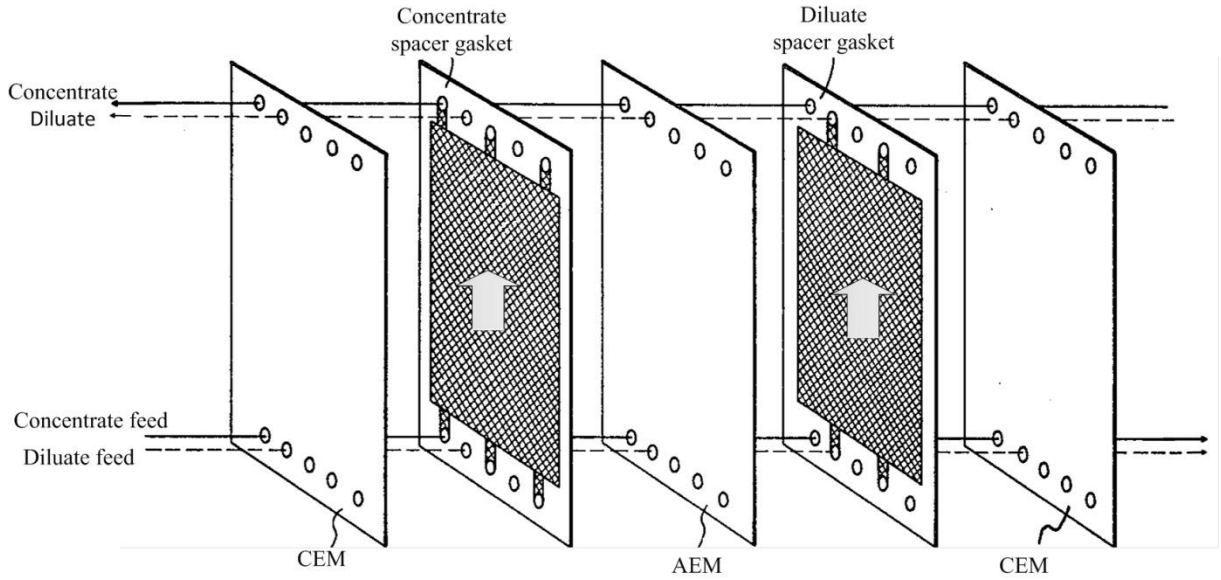

Figure 1.4. *Schematic illustration of a sheet-flow ED stack in which flow streams are co-current.*

The membrane are separated by a spacer screen which supports the membranes and also provides turbulent mixing in the cell compartments. In general the increase of turbulence decreases the thickness of boundary layer in the cells and promotes the use of the membrane area and the transfer of ions.
The resistance of the solutions in the cells compartments increases with the increasing of distance; therefore the cell thickness is as short as possible to guarantee a low energy consumption. In industrial ED stack, membrane distances are between 0.3 and 2 mm, whereas solution flow velocities are typically 3 to 10 cm/s.
Electrode compartments are placed at both ends of the stack; they consists of an electrode and a spacer gasket which adheres to a membrane. To avoid corrosive phenomena, electrode are usually made of titanium and plated in platinum. The assembly of membrane spacers and electrodes is held in compression by a pair of end plates.
The figure 1.4 shows a co-current flow streams design, but the diluate and the concentrate flows can move also in opposite directions (counter-current flow).
Two different spacer gasket designs are available on large scale. One is the sheet flow, and the other is the tortuous path-flow stack. In a sheet-flow ED stack the solutions flow is approximately in a straight path from the entrance to the exit, which is located in opposite side of the stack. In a tortuous path-flow stack the spacers are folded back upon their self and the solution flow path is much longer than the linear dimension of the stack.

1.4.2 Continuous and Batch type operation in Electrodialysis

ED can be applied in batch or continuous production processes. During batch mode, the diluate, the concentrate and the electrolyte solution are recirculated in the system until the required product qualities are reached. In contrast, in a continuous ED process, only the electrolyte solution is recycled and it allows to meet the required product qualities in a single run. A pure batch operation is hardly used in industry, but it's commonly used in laboratory experiments to verify modelling results and optimize operational parameters.
It is possible to distinguish the continuous mode in a single-stage or a multi-stage process, depending by the number of installed stack in series; each stack has its own set of electrodes, power supply and feed pump.
If a high recovery rate is required, the process must be operated in a feed and a bleed mode, i.e. with partial recycling of the diluate and/or the concentrate solutions.

1.4.3 Unidirectional Electrodialysis and Electrodialysis Reversal operating mode

In an unidirectional ED system the electric field is permanently applied in one direction over the period of operation. This operating mode is rather sensitive to membrane fouling and a substantial feed solution pre-treatment or adding of an acid solution to the concentrated stream is required.

EDR is a variation on the ED process, which helps to prevent membrane fouling problems. EDR operating mode is been developed by Ionics Incorporated; it works the same way as ED, except the polarity of the electric field applied to the stack is reversed every 30 to 60 minutes. Simultaneously the diluate and concentrate streams are reversed, with the result that the matter that has been precipitated at the membrane surface will be re-dissolved in the original solution. The EDR process requires a more sophisticated flow control and some loss of product is unavoidable. During the reversal of polarity and flow streams, there is a period of a few seconds when the concentration of diluate product exceeds the quality specification due to a partial mixing between diluate and concentrate solutions. An additional three-way valve controlled by a concentration sensor diverts the diluate solution to the product outlet or to the waste, according to the actual concentration value (Ionics Inc., 1984).

In certain applications in the food and drug industry, where high value-added products are processed, the product lost to waste stream might be not acceptable and the unidirectional operating mode is used. This is usually no problem in almost all ED water desalination systems, where EDR is commonly applied.

1.4.4 Practically used relations for the Design of an Electrodialysis plant

The performance of an ED process is determined by a set of fixed and variable parameters that can be optimized in terms of overall costs. Typically, the capacity of the plant, the composition of the feed and the desired product diluate concentration are fixed. The stack dimensions, i.e. the number of cells and the width of membranes, are given by the manufacturer. The total current, the applied voltage to achieve this current, the required membrane area, and the required process path length must be determined.

The main mathematical and design relations for the desalination process presented in this paragraph and in §1.4.5 are been adapted from Lee *et al.* (2001). It's assumed that the stack is operated in a co-current flow, the concentrate and diluate cells have identical geometry and flow conditions. Furthermore, the back-diffusion of ions is neglected and the only driving force for the transport is the electrical potential gradient which is constant over the entire cell length. These relations might not be appropriate when multi-component solutions are considered, because here the activity coefficients of solution are assumed to be equal to 1.

Appling the mass balance (1.1) to the salt, the concentration difference, C_s^{Δ} (keq/m^3), between a feed and a concentrate and diluate solution achieved during the desalination process is given by:

$$C_s^c - C_s^{fc} = C_s^{fd} - C_s^d = C_s^{\Delta} \quad . \tag{1.15}$$

when the flow rates of concentrate and diluate solutions are assumed identical and equal to the production rate Q (m^3/s). For constant production rate, current density and number of cells (N), the degree of desalination as a function of the membrane area of a cell is given by:

$$dC_s^{\Delta} = \frac{i\,\xi\,N}{F\,Q} dA_{cell} \quad ; \tag{1.16}$$

where A_{cell} is the membrane area surface of a cell expressed in m^2.
The current density is related to the applied voltage U by the following equation:

$$i = \frac{\sigma_{av}\,U}{2\,\Delta\,N} \quad . \tag{1.17}$$

Here Δ is the thickness of a cell (m) and σ_{av} is the average electrical conductivity (1/Ωm). The latter can be obtained by:

$$\sigma_{av} = \frac{2\Delta}{\frac{\Delta}{\Lambda_s C_s^d} + \frac{\Delta}{\Lambda_s C_s^c} + r^{am} + r^{cm}} \quad ; \tag{1.18}$$

where Λ_s is the equivalent conductivity of the solution (S m^2/keq), r^{am} and r^{mc} are the resistances (Ωm^2) of AEMs and CEMs, respectively.
Introducing Eqs. (1.17) and (1.18) in Eq. (1.16) and rearranging leads to:

$$\left(\frac{C_s^d + C_s^c}{\Lambda_s\, C_s^d\, C_s^c} + \frac{r^{am} + r^{cm}}{\Delta}\right) dC_s^{\Delta} = \frac{U\,\xi}{F\,Q\,\Delta} dA_{cell} \quad . \tag{1.19}$$

The introduction of (1.15) and integration with the boundary condition $C_s^{\Delta} = 0,\ A_{cell} = 0$ and $C_s^{\Delta} = C_s^{\Delta}, \mathrm{A}_{cell} = A_{cell}$ results in:

$$ln\frac{C_s^c C_s^{fd}}{C_s^d C_s^{fc}} + \frac{\Lambda_s (r^{am} + r^{cm})\left(C_s^{fd} - C_s^d\right)}{\Delta} = \frac{\Lambda_s\,\xi\,U\,A_{cell}}{F\,Q\,\Delta} \quad . \tag{1.20}$$

Rearranging Eq. (1.20) gives the required membrane area per cell:

$$A_{cell} = \left[\frac{\Delta}{\Lambda_s}\, ln\frac{C_s^c\, C_s^{fd}}{C_s^d\, C_s^{fc}} + (r^{am} + r^{cm})\left(C_s^{fd} - C_s^d\right)\right]\frac{F\, Q}{U\, \xi} \quad . \tag{1.21}$$

The effect of spacer is considered introducing two correction factors α and β, both ≤1. α is a correction factor taking the effect of spacer on the volume flow rate into account, whereas β accounts for the shadow effect, i.e. the fact that part of membrane is not accessible to the current. Thus, Eq. (1.21) becomes:

$$A_{cell} = \left[\frac{\Delta}{\Lambda_s}\, ln\frac{C_s^c\, C_s^{fd}}{C_s^d\, C_s^{fc}} + (r^{am} + r^{cm})\left(C_s^{fd} - C_s^d\right)\right]\frac{F\, Q\, \alpha}{U\, \xi\, \beta} \quad . \tag{1.22}$$

The limiting current density expressed by (1.9) it's difficult to calculate, therefore is usually determined experimentally as a function of flow velocities and concentration:

$$i_{lim} = a u^b (C_s^d)^n \quad . \tag{1.23}$$

Here *a*, *b* and *n* are characteristic constant for a given stack design, and *u* is the linear flow velocity of solution through the cells. Therefore, the flow rate *Q* can be written as:

$$Q = N\, Y\, \Delta\, u \quad ; \tag{1.24}$$

where *Y* is the cell width.
The current density used in praxis is given by:

$$i = s\, i_{lim} = s\, a\, u^b (C_s^d)^n \quad ; \tag{1.25}$$

where *s* is safety factor which always is <1.
The total current required to transfer ions, *I*, expressed in Ampere, is given multiplying the current density by the membrane area surface:

$$I = i\, A_{cell} \quad . \tag{1.26}$$

Introducing Eqs. (1.25) and (1.18) in Eq. (1.17) and rearranging gives the applied voltage across the stack:

$$U = \frac{s\, a\, u^b (C_s^d)^{n-1}\, N\, \Delta}{\Lambda_s}\left[\frac{C_s^d}{C_s^c} + 1 + \frac{\Lambda_s\, C_s^{fd}}{\Delta}(r^{am} + r^{cm})\right] \quad . \tag{1.27}$$

The total membrane area, A (m^2) required for the entire stack is given by:

$$A = N\, A_{cell} \quad . \tag{1.28}$$

The introduction of Eqs. (1.22), (1.24) and (1.27) in Eq. (1.28) results in:

$$A = N \frac{\left[ln\frac{C_s^c\, c_s^{fd}}{c_s^d\, c_s^{fc}} + \frac{\Lambda_s}{\Delta}(r^{am}+r^{cm})\left(c_s^{fd}-c_s^d\right)\right]}{\left[\frac{c_s^d}{c_s^c}+1+\frac{\Lambda_s\, c_s^{fd}}{\Delta}(r^{am}+r^{cm})\right]} \frac{F\,\Delta\, u^{1-b}\, Y\, (c_s^d)^{1-n}\,\alpha}{\beta\,\xi\, a\, s} \quad . \tag{1.29}$$

The process path length in a cell, L_{pp}, can be expressed by the relationship between the cell area A_{cell} and the cell width Y:

$$L_{pp} = \frac{A_{cell}}{Y} \quad . \tag{1.30}$$

Therefore, L_{pp} is given by:

$$L_{pp} = \frac{\left[ln\frac{C_s^c\, c_s^{fd}}{c_s^d\, c_s^{fc}} + \frac{\Lambda_s}{\Delta}(r^{am}+r^{cm})\left(c_s^{fd}-c_s^d\right)\right]}{\left[\frac{c_s^d}{c_s^c}+1+\frac{\Lambda_s\, c_s^{fd}}{\Delta}(r^{am}+r^{cm})\right]} \frac{F\,\Delta\, u^{1-b}\, (c_c^d)^{1-n}\,\alpha}{\beta\,\xi\, a\, s} \quad . \tag{1.31}$$

(All the symbols have been presented before and it's possible recover them in the section Nomenclature).

1.4.5 Energy requirements in a Electrodialysis desalination process

The total energy requirements in a practical ED process are mainly due to the ionic transfer from a feed to a concentrated solution. In addition, energy is required to pump the solutions through the stack and it is also consumed by the electrode reaction. However, the energy consumed by the electrode reaction are generally neglected or taken as a fixed item which is between 1 and 3% of the energy used for ion transfer and pumping the solution.

The electric power, P (W), required for a plant with a product capacity Q for the transfer of ions in an ED process is given by the current passing through the stack multiplied with the total voltage drop encountered between the electrodes:

$$P = I\, U \quad . \tag{1.32}$$

The specific energy consumption E_{spec} (J/m^3), i.e. the energy consumption per unit product volume, is given by:

$$E_{spec} = \frac{P}{Q} = \frac{I\, U}{Q} \quad . \tag{1.33}$$

Equation (1.33) shows that the energy dissipation in an ED processes is proportional to the square of the current (*U* is proportional to *I*), so the higher the current density the more energy is needed to maintain a given production rate. However, the higher the current density the lower is the required membrane area. Thus, for a certain ED plant there is an optimum in the current density and in the total membrane area which must be determined. The limiting current density represents the upper limit for the current density which should not be exceeded.
Substituting the expressions of *I*, *U* and *Q*, before obtained in Eqs. (1.24) - (1.27) in Eq. (1.33) and rearranging results in:

$$E_{spec} = \left[ln \frac{C_s^c \, C_s^{fd}}{C_s^d \, C_s^{fc}} + \frac{\Lambda_s}{\Delta} (r^{am} + r^{cm}) \left(C_s^{fd} - C_s^d \right) \right] \frac{s \, a \, u^b (C_s^d)^n \, N \, F \, \Delta}{\Lambda_s \, \beta \, \xi} \quad . \tag{1.34}$$

The energy required for circulate solutions through the stack for a given production capacity of the plant can be determined by the following expression:

$$E_{pump,\ spec} = \frac{(\Delta p^d + \Delta p^c)}{\eta} \quad ; \tag{1.35}$$

where $E_{pump,\ spec}$ (J/m^3) is the total energy for pumping the solutions in a ED plant per unit product volume, η is the pump efficiency, Δp^d and Δp^c are the pressure drops for diluate and concentrate loops, respectively.
The energy consumption due to pressure loss in the electrolyte solution is neglected because generally the volume of the electrolyte solution is very small compared to the volume of the diluate and concentrate.

1.5 The principle of Continuous Electrodeionization

CEDI is a relatively new process for removing ions from watery feed, become very popular nowadays. It combines ion-exchange and ED processes and emerges today as an alternative solution for producing high-purity water.
The process is similar to the conventional ED, but the diluate compartments are filled with a mixed bed ion-exchange resin. In some stack arrangements, the concentrate compartments are also filled with resin beads. The mechanism for the removal of ions in a CEDI stack is shown in Figure 1.5.
Anion- and cation-exchange resins (AERs and CERs, respectively) facilitate ion transfer in low concentration solutions, increasing the conductivity in the diluate cell substantially.

1.5.1 Mass transport and energy requirements in Continuous Electrodeionization

Ganzi *et al.* (1992) proposed a theoretical model based on two stages to explain the removal of ions in the diluate channel. In the first stage the ions are transferred from the solution to the ion-exchange resin particles, whereas in the second stage the ions are transported along the chain of ion-exchange beads. In praxis, the ion-exchange resins act as an *ionic bridge* to speed the passage of ions from the diluate to the concentrate compartment.

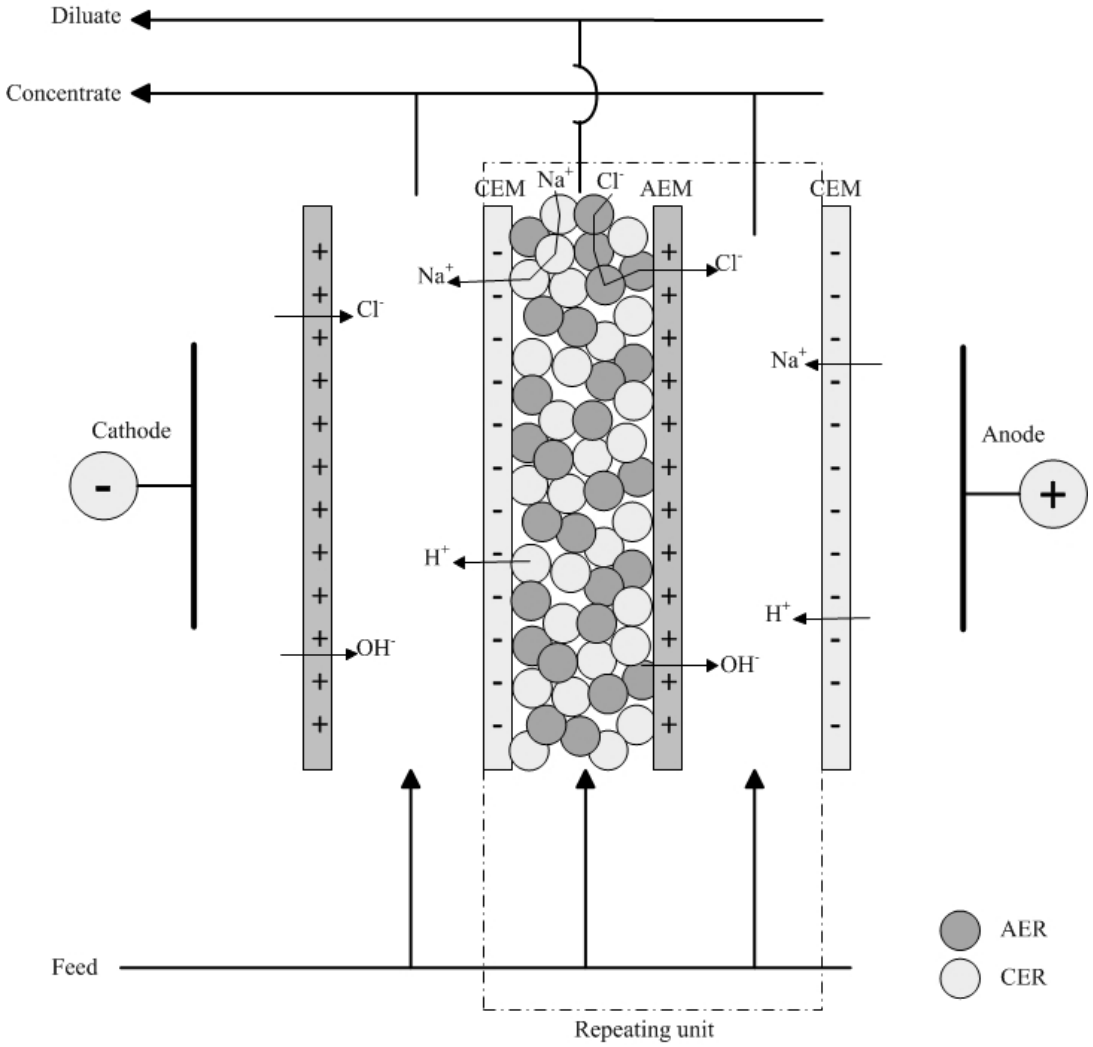

Figure 1.5. *CEDI process. Schematic diagram illustrating the ion transport in the ion-exchange resins filled diluate cell. . AER = anion-exchange resin; CER= catio-exchange resin.*

Furthermore, resins allow to minimize the concentration polarization phenomena. As the concentration of strongly ionized substances in the bulk solution is depleted, at cation/anion (resin/resin and resin/membrane) interfaces water splitting can occurs. The resulting H^+ and OH^- ions regenerate the resins continually without any addition of chemical reagents. Water

splitting leads to local pH-value changes in the solution which effect the degree of dissociation of weak acids and bases that can become ionized and be moved into the concentrate stream (Ganzi, 1988).
The current utilization in CEDI is generally lower than in conventional ED because of energy consumed in water dissociation and a substantial back diffusion of the ions from the concentrate to the diluate solution through the ion-exchange membranes. This back diffusion is proportional to the concentration difference between the concentrate and the diluate solution which in a CEDI practical application can be very high. If CEDI is operated at too high gradient concentration, the ionic migration from diluate to concentration is no longer capable to balance the back diffusion of ions (Ervan and Wenten, 2002).
However, a comprehensive mathematical or experimental model which explains the relation between process parameters and their performance in CEDI must still be developed.

1.5.2 Applications in water purification

CEDI systems are now operating in a variety of industries, from microelectronics and pharmaceuticals to power generation and biotechnologies. A recent application is in the ultrapure water production as an alternative technology of the mixed bed ion-exchanger. The most important advantages of this technology are the continuity of the process, no need of regeneration chemicals, less raw water consumption, and a substantial reduction in costs.
Of particular importance on the electronics and optical glass applications is the demonstrated ability of CEDI in reduction of total organic carbon (TOC) (Wilinks and McConnelee, 1988).

1.5.3 Design aspects of Continuous Electrodeionization process

In the most common stack arrangement in CEDI, AERs and CERs are placed in a mixed bed in the diluate channels. Nevertheless several modifications of this disposition, including the use of bipolar membranes for the regeneration of ion-exchange resins are described in literature.
The bed of ion-exchange resin beads in the cells effects the flow distribution and the pressure drops of the solution drastically. This fact is generally solved adopting different dimensions of the diluate and concentrate cells.
In CEDI systems CERs and AERs are not always equally distributed; the resins are often placed with a volume ration of 30:70, even though the influence of volume resin composition on performance of process is not clear in literature.

1.6 Modelling desalination process in an Electrodialysis cell

This section describes an ED desalination process, modelled using the software COMSOL Multiphysics 4.4. The model geometry is 2-dimensional. *Electrochemistry* and *Fluid Flow* modules are used, particularly the following physics: *Secondary Current Distribution*, *Tertiary Current Distribution, Nernst-Plank* and *Laminar Flow*. This study considers only the stationary state.

1.6.1 Model geometry

The model geometry for this study is based on a cell pair, i.e. the repetitive unit within an ED stack. The dimensions of a real lab-scale stack are reproduced in this model: the thickness of compartments (Δ) is 2 mm, the thickness of membranes is 0.7 mm and the length of cells is 10 cm.

The geometry contains three free flowing electrolyte domains and two ion-exchange membrane domains, as shown in Figure 1.6.

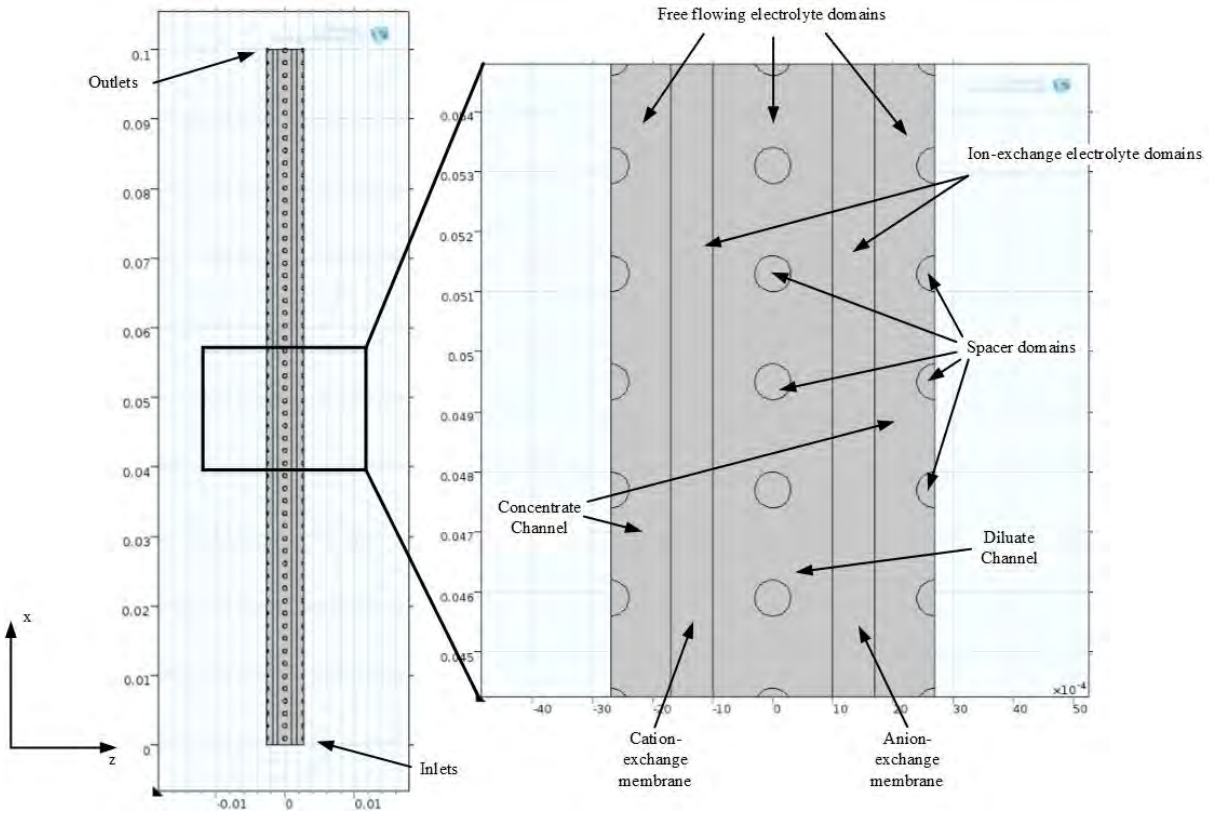

Figure 1.6. *Illustration of the model geometry; on the enlargement the position of the various domains is shown.*

Considering the electrolyte domains, the middle domain represents the diluate compartment, while the rightmost and the leftmost domains are fed with the concentrate solution. The cathode and the anode are hypothetically on the left-hand and on the right-hand respectively. During

cell operation, the ion concentration will increase in the concentrate and the salt will be removed in the diluate domain.
The electrolyte solutions flow from the bottom to the top of their respective cells, but the inlet and outlet flow regions are excluded from this model geometry. Both the diluate and concentrate cells are fed with a 0.2 M NaCl aqueous solution; the diffusivity coefficients of Cl^- and Na^+ ions are taken from literature (respectively 2.0×10^{-9} and 2.5×10^{-9} m^2/s).
The left and right membrane domains represent a CEM and an AEM, respectively. The membranes are assumed to be permeable to counter-ions only. The counter-ions concentrations contained in the membranes are obtained from ion-exchange capacity value of Ralex® membranes, reported in Table 2.1. Hence, the concentration of Na^+ in the CEM and the concentration of Cl^- in the AEM are imposed to be 1.92 and 1.57 keq/m^3, respectively.
During lab experiments a plastic net was placed in each compartment. This net is represented in this model as a series of circular elements, which diameter is 0.6 mm. This domain is here indicated as spacer domain.

1.6.2 Building of the mesh

An unstructured mesh can be generated quickly, automatically and for complicated geometry. In particular, a triangular cells based mesh is entirely applied to membrane and spacers domains. Since only the gradients in electrolyte potential are relevant in such domains, the mesh is relatively coarse.
The physics in the free flowing electrolyte domains is strongly isotropic: the boundaries with the membranes creates vertical boundary layers for the ionic concentration and the tight curvature of spacer domains modifies the flow direction. Therefore, a structured mesh is built in the boundaries of the diluate and concentrate compartments, excluding the inlet, outlet, leftmost and rightmost boundaries. The resulted mesh is shown in Figure 1.7.
In the structured mesh, the cells are quadrilateral and the thickness of the first element layer, i.e. the layer adjacent to the corresponding boundary, is set to 1/20 of the local domain element height. The selection of the *Splitting* option (the default) introduces layer splits at sharp corners. The *boundary layer stretching factor* specifies the increase in thickness between two consecutive boundary layers as a scaling factor. The default value equal to 1.2 is used, i.e. the thickness increases by 20% from one layer to the next.
The option *Smooth transition to interior mesh* is selected in order to smooth the transition in element size from the boundary layer mesh to the interior mesh.

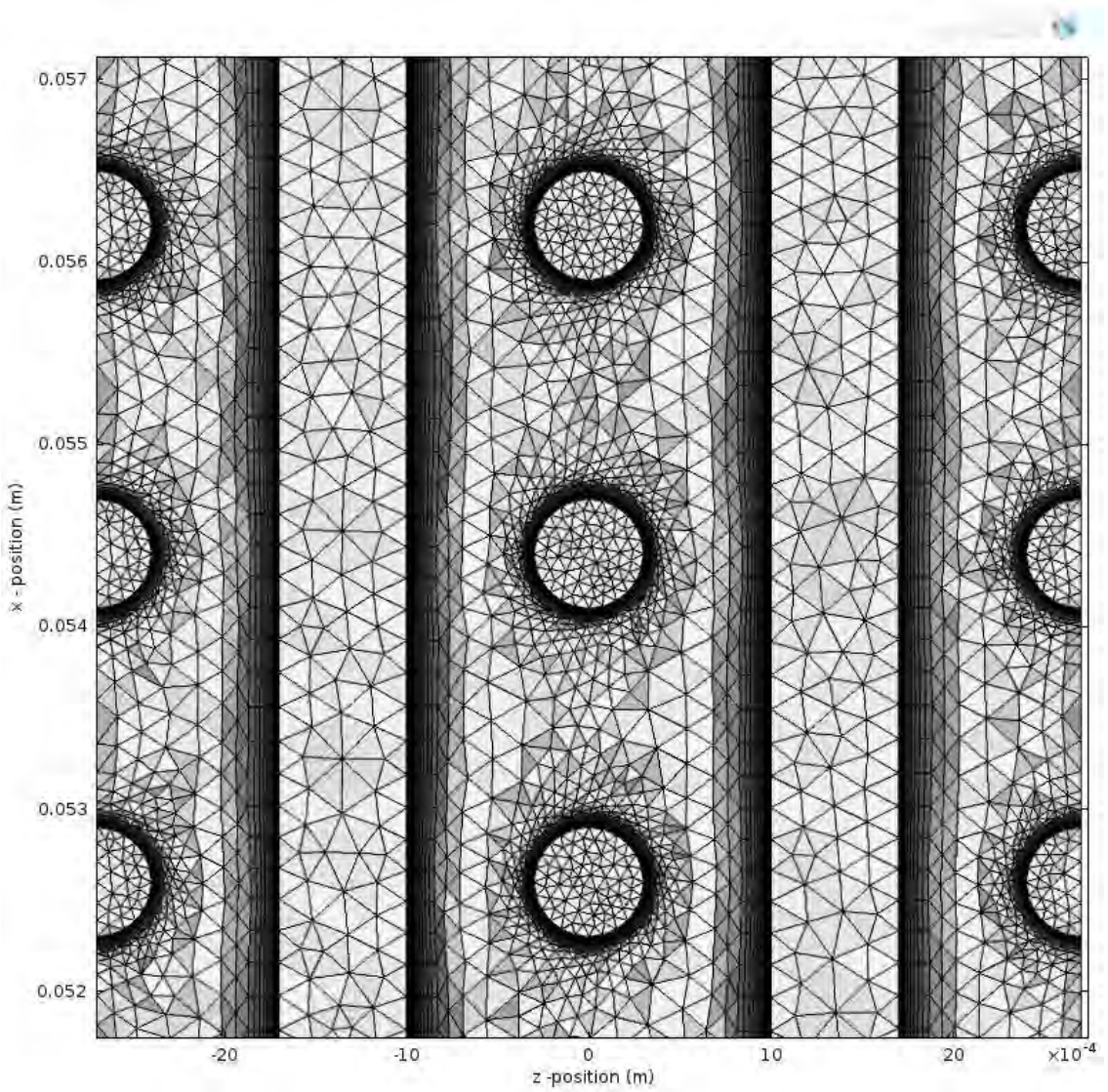

Figure 1.7. *A particular of the hybrid mesh applied on the model geometry.*

1.6.3 Tertiary and Secondary Current Distribution interface

In this model the ionic flux and the charge transport are described applying extended Nernst-Plank flux equation given by Eq. (1.2). COMSOL requires that the concentrations are expressed in moles and the fluxes in kmol/(m^{3}s); therefore Eq. (1.3) is rewritten as:

$$J_i = -D_i \nabla C_i - z_i D_i \frac{C_i F}{\dot{R}\,\dot{T}} \nabla \varphi + u\, C_i \quad ; \tag{1.36}$$

where z is the species charge number and it is equal to +1 for sodium ion and -1 for chloride ion. The temperature is here imposed to be equal to 298.15 K.

The Eq. (1.5) has to be rewritten taking in account the charge number. Thus, the electrolyte current density is given by:

$$i = F \sum_i z_i J_i \quad . \tag{1.37}$$

The introduction of Eq. (1.36) in Eq. (1.37) leads to:

$$i = F \sum_i z_i \left(-D_i \nabla C_i - z_i D_i \frac{C_i F}{\dot{R}\,\dot{T}} \nabla \varphi + u\, C_i \right) \quad . \tag{1.38}$$

The general electrolyte current conservation is expressed by:

$$\nabla \cdot i = \dot{Q} \quad ; \tag{1.39}$$

where $\dot{Q}$ is the general electrolyte current source term and it is expressed in A/m^3.
This model uses the *Tertiary Current* Distribution, Ne*rnst-Plank* interface when solving for the electrolyte potential in the free electrolyte domains. The Tertiary Current Distribution (TCD) accounts for the effect of variations in electrolyte composition, as well as solution resistance. To achieve this, the Nernst-Plank equation is solved explicitly for each chemical species to describe its mass transport through diffusion, migration and convection. In fact, in the diluate and the concentrate domains, the gradients of Na^+ and Cl^- concentration are not negligible.
In TCD the electrolyte is subject to the electroneutrality approximation, which is expressed by:

$$\sum_i z_i C_i = 0 \quad . \tag{1.40}$$

The imposition of electroneutrality means that convective flux does not contribute to the current density, as expressed by:

$$i = F \sum_i z_i \left(-D_i \nabla C_i - z_i D_i \frac{C_i F}{\dot{R}\,\dot{T}} \nabla \varphi \right) \quad . \tag{1.41}$$

This expression of the current density and the general electrolyte current conservation expressed by Eq. (1.39) describe the TCD physics.
Since in the ion-exchange membranes there are no significant gradients of concentration in fixed charges, the concentration of the counter-ions can be considered constant, as well. This is the main simplifying hypothesis of the Secondary Current Distribution (SCD), applied to the ion-exchange membrane domains. Consequently, Eq. (1.41) reduces to (here written for Na^+ in the CEM):

$$i = -\frac{D_{Na+}}{\dot{R}\dot{T}} F^2 C_{Na+} \nabla \varphi = -\sigma_m \nabla \varphi \quad ; \tag{1.42}$$

where σ_m is the membrane conductivity which is assumed to be 0.833 S/m.
A SCD interface is used to describe the physics in the spacer domain, as well. Since the plastic net can be considered an electric insulator, the conductivity in the spacer domain is imposed to be arbitrarily very low (8.33×10^{-4} S/m).

1.6.4 Membrane and electrolyte boundary conditions

At the boundaries between the membrane and the free electrolyte, the normal electrolyte current density is imposed to be equal to the current density in the membrane:

$$F \sum_i z_i \left(-D_i \nabla C_i - z_i D_i \frac{C_i F}{\dot{R}\dot{T}} \nabla \varphi\right) = \pm \sigma_m \nabla \varphi \quad ; \tag{1.43}$$

where the left-side term is positive for AEM boundaries, vice versa when the CEM is considered.

Since the membranes are considered completely permselective, the co-ions flux is fixed to 0. Additionally, at the boundaries between the TCD and SCD interfaces, the relation between the potentials and the concentrations is given by the following expression:

$$\varphi_m = \varphi_e + \frac{\dot{R}\dot{T}}{F} \ln\left(\frac{\dot{a}_{i,m}}{\dot{a}_{i,e}}\right) \quad ; \tag{1.44}$$

where $\dot{a}$ is the counter-ion activity, the subscripts *m* and *e* refer to the membrane and the electrolyte solution, respectively. In this model the activities are equal to the respective concentrations divided by 1000 mol/m^3. The potential shift caused by Eq. (1.44) is called Donnan potential.

These boundary conditions are defined in the model using a point wise constraint with a user-defined reaction force.

At the inlet of the free flowing electrolyte an user-defined *inward flux* is inserted. It is expressed multiplying the inlet concentration by the fluid velocity in the normal direction to the boundary. The boundary condition at the outlet of the free electrolyte domain excludes any concentration gradients. Thus, the diffusive flux is considered negligible compared to the convective flux.

Furthermore, a *linear extrusion* operator is used to set the concentration on the rightmost boundary to equal that of the leftmost boundary.

1.6.5 Laminar flow interface and boundary conditions

The single-phase laminar flow interfaceis used to compute the velocity and the pressure fields under the flow of a single-phase fluid in the laminar flow regime. The equation solved by the laminar flow interface are the Navier-Stokes equations for the conservation of momentum and the continuity equation for the mass conservation. The stationary hypothesis is here included.

The density in liquids under normal conditions can be assumed constant or nearly constant, i.e. the fluid is incompressible. For a steady flow of a Newtonian and incompressible fluid, the Navier-Stokes equations solved on the vertical direction (z) in laminar flow interfaces apply the incompressible formulation of the continuity equation:

$$\rho \frac{\mathrm{d}u_z}{\mathrm{dz}} = 0 \ ; \tag{1.45}$$

and the momentum equation:

$$\rho \left(\frac{\mathrm{d}u_z}{\mathrm{dz}}\right) u_z = -\frac{d\dot{p}}{dz} + \mu \frac{d^2 u_z}{dz^2} + \dot{F}_z \tag{1.46}$$

Here $\dot{F}$ is the volume force vector (N/m^3), $\dot{p}$ is the pressure term (Pa) and μ is the dynamic viscosity (Pa s). Default dynamic viscosity and density values of water are considered.
The default wall boundary condition for laminar flow is named *no slip* and prescribes that the fluid at the wall is not moving ($u = 0$). In the model, this condition is applied to the boundaries between the electrolyte solution and the membrane and between the electrolyte domain and the spacer domain.

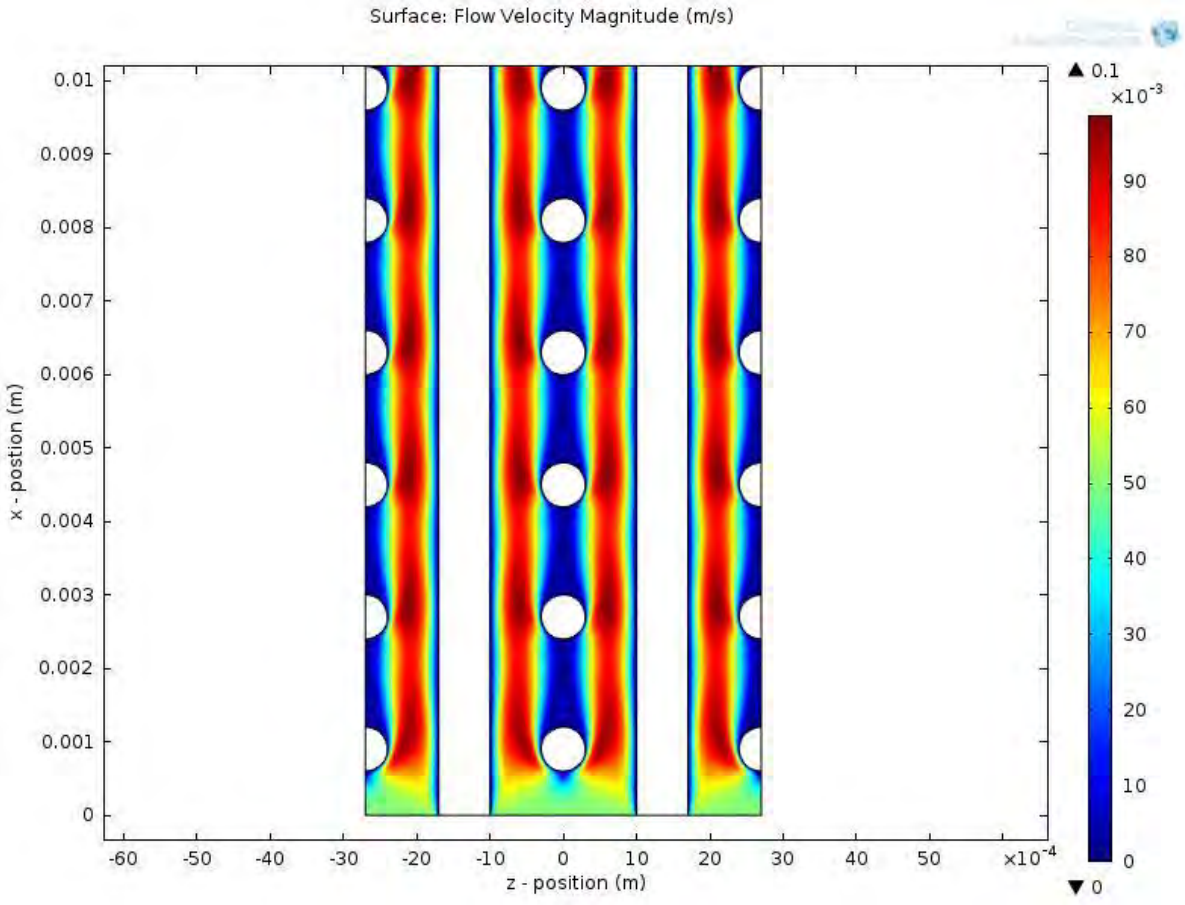

Figure 1.8. *Flow velocity distribution along the diluate and concentrate channels. The bottom of the cell pair is shown.*

At the rightmost and leftmost boundaries there is a *slip* boundary condition which assumes a no-penetration condition. It implicitly assumes there are no viscous effects at the slip wall and hence, no boundary layer develops.

While the inlet boundary condition imposes a normal inflow velocity equals to 5 cm/s, the outlet boundary condition is based on the pressure. The pressure at the top of the model geometry is set to 0 Pa. The *Supress backflow* option is active, in order to prevent fluid from entering the domain through the boundary.

Setting the linear solver *PARDISO*, a stationary study solves the laminar flow settings. Figure 1.8 shows the distribution of the flow velocity within free flowing electrolyte domains under the boundary conditions previously discussed.

The effect of mixing due to the spacers turns out to be good and permits a strong reduction of the thickness of the boundary layer in proximity of the membranes. On the other hand, a dangerous *dead zone* takes place between a spacer and the next.

1.6.6 Current distribution study

From the previous study, the continuity and momentum balances are solved and the velocity field is fixed. A new stationary study in now carries out considering the TCD in the free flowing electrolyte domains and the SCD in the membrane domains.

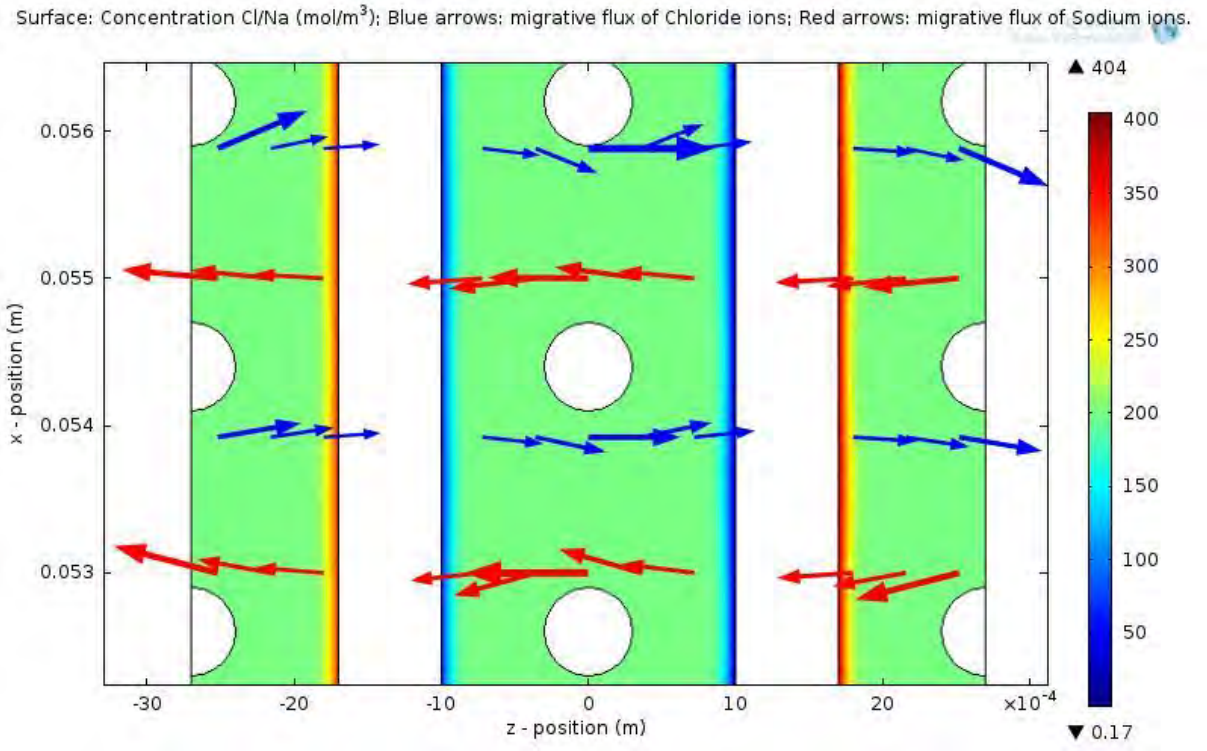

Figure 1.9. *Concentration distribution in the diluate and concentrate compartments. Blue arrows refer to the migration flux of Cl^- ions and red arrows refer to the migration flux of Na^+ ions. This Figure shows a central section of the cell pair.*

The *Auxiliary parameter sweep* permits to solve for a given combinations of values of a certain parameter. This study is conducted for the following values of global cell electrolyte potential: 0.2 V, 0.7 V, 1.2 V, 1.7 V and 2.2 V. Each step uses the converged solution from the previous step to reach the convergence in the iterative procedure. The *MUMPS Solver* is set for this study and the relative tolerance is set to 10^{-5}.

Figure 1.9 shows, in a central section of the cell pair, the concentration distribution in the free flowing electrolyte domains when the global potential is set to 2.2 V. The ionic concentration increases at the concentrate boundaries, and decreases at the diluate boundaries, as expected. On the rest of the domain, the concentration is homogeneously distributed. The thickness of the boundary layers increases from the bottom to the top of the geometry because the concentration increases along the concentrate channel and deceases along the diluate channel. Red and blue arrows shown in the picture refer to the migration flux of the Na^+ and Cl^- ions, respectively.

Although, the spacers cause a change of direction in the migration of ions, they don't affect concentration profiles in their proximity.

1.6.7 Mesh refinement approach

In computational fluid dynamic simulations, it's usually important to refine the mesh in order to capture gradients of velocity and concentration. The refinement method can be applied only to an unstructured mesh. Hence, a new completely unstructured mesh is built (see Figure 1.10*a*). The adaptive solver searches a solution on the existing mesh and estimates the residuals on all mesh elements. Successively, the solver refines a subset of the elements based on the sizes of the local error indicators. This procedure is repeated for two times and the result is shown in Figure 1.10*b*.

Both laminar flow and current distribution study were performed with the new mesh obtaining the same results achieved using the hybrid mesh. That confirms the effectiveness of the hybrid mesh, which makes the mesh refinement approach unnecessary.

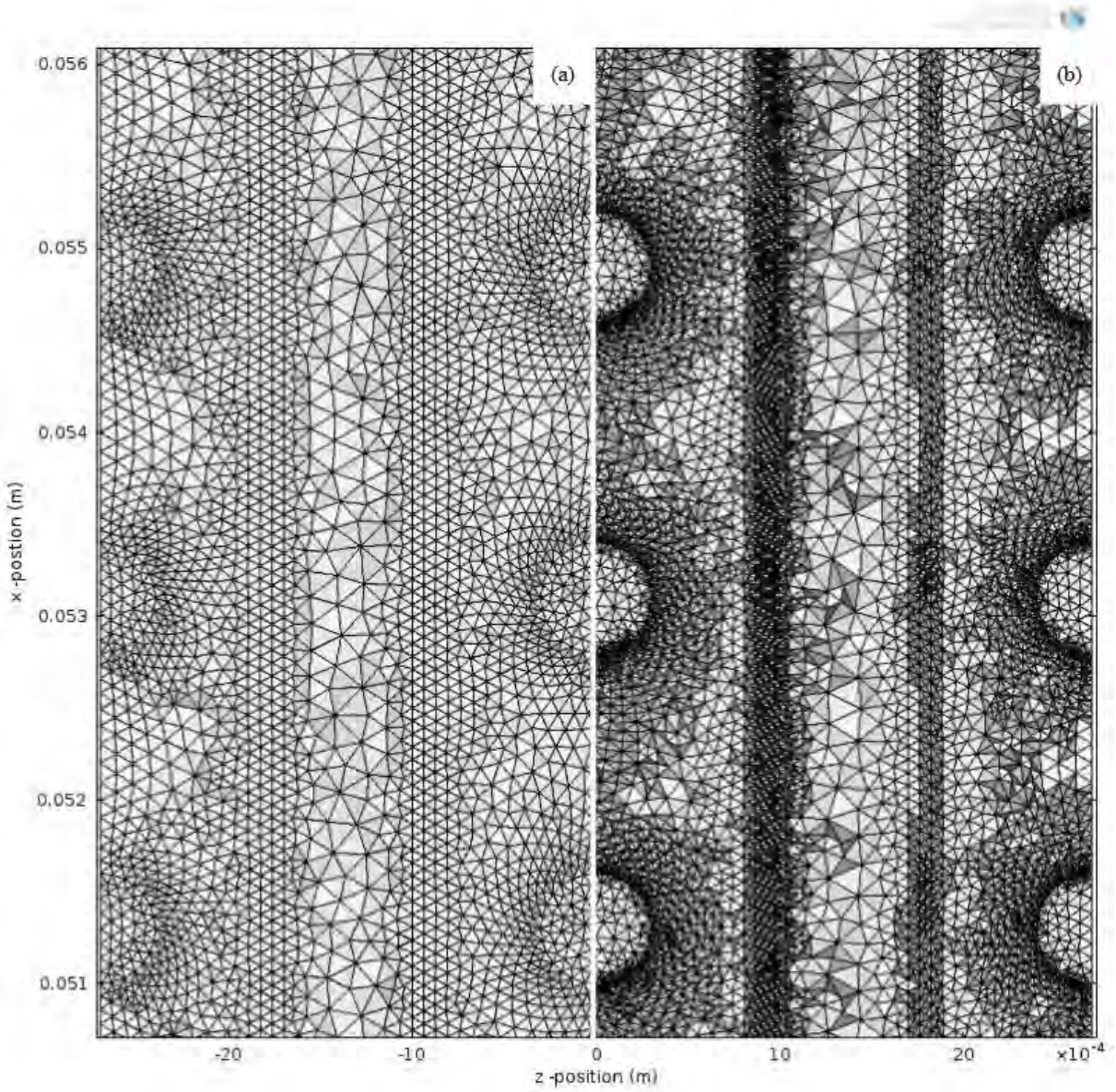

Figure 1.10. *Figure (a) shows the initial unstructured mesh and Figure (b) shows the mesh after the refinement procedure.*

1.6.8 Electrolyte potential and limiting current density

Figure 1.11 shows the profiles of five different electrolyte potentials along a horizontal line placed at the half of cell pair. The main part of the potential losses occurs in the membranes. The discontinuity at the boundaries between the free electrolyte and membrane domains is due to Donnan potential.

The profile of the current density along the boundaries between the diluate domain and the AEM is shown in Figure 1.12.

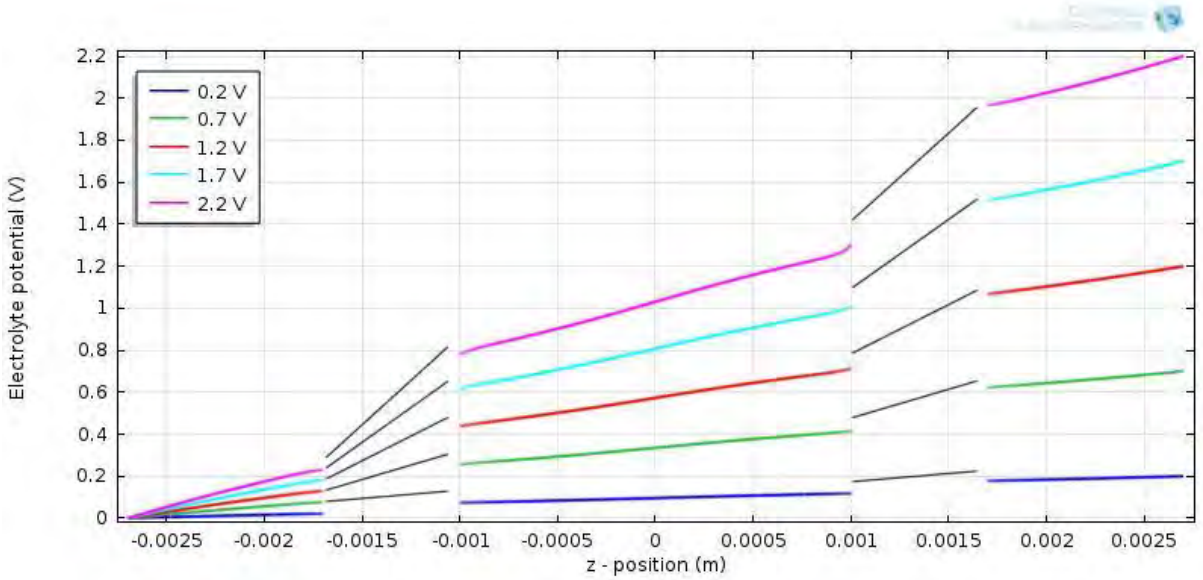

Figure 1.11. *The plot shows different electrolyte potentials along a horizontal line placed at half the cell height. The colored lines refer to the potential in the free flowing electrolyte domain and the black lines refer to the potential in the ion-exchange membrane domains*

Each line refers to a different global voltage drop imposed to the model. The wave trend is due to the presence of the spacers and becomes more relevant at high values of potential. Depletion of chloride ions gets more pronounced towards the top of the diluate cell, resulting in a higher Donnan potential shift and a lower current density. Therefore, the LCD is reached at the 2.2 V voltage drop. For higher values of electrolyte potential the calculation time significantly increases, leading to convergence problems.

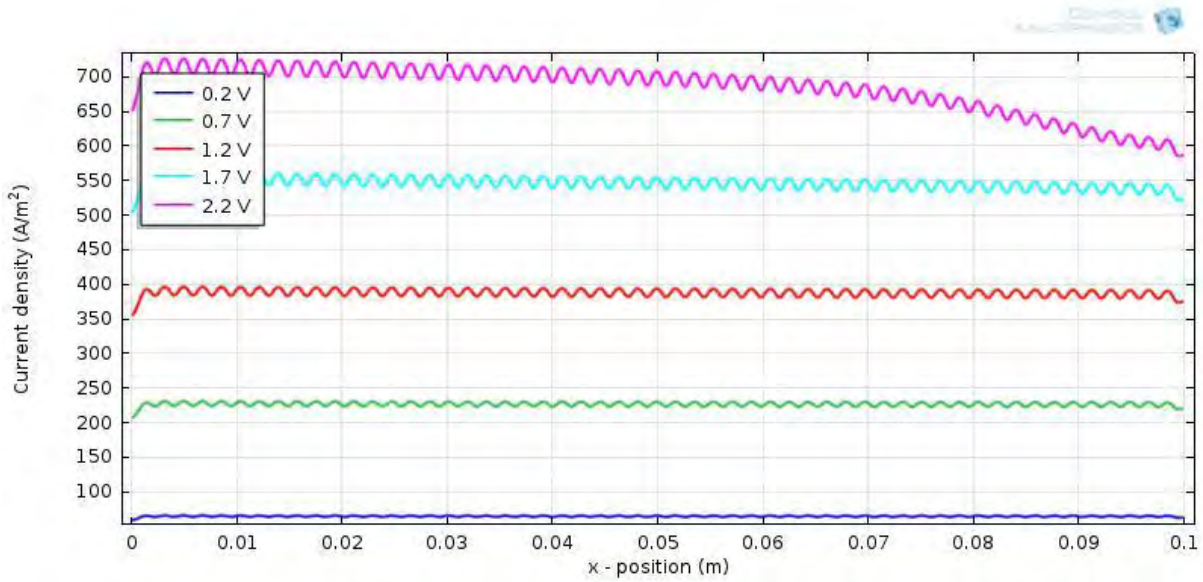

Figure 1.12. *Current density along the boundaries between the diluate domain and the anion-exchange membrane versus the x- position for different cell voltages*

1.6.9 Comparison between experimental data and simulation

Main graphic techniques to detect the LCD are widely discussed in §2.2. Cowan plot shows the reciprocal of the current on the x-axe and the resistance on the y-axe. The curve shows a sharp change in the resistance once the LCD has been reached. The resistance of the cell pair is calculated as the ratio between the imposed electrolyte potential and the average current passing across the system. The average current is calculated with a 4^{th} order integration at the boundary between the diluate compartment and the AEM. The model simulation gives the profile represented in Figure 1.13.

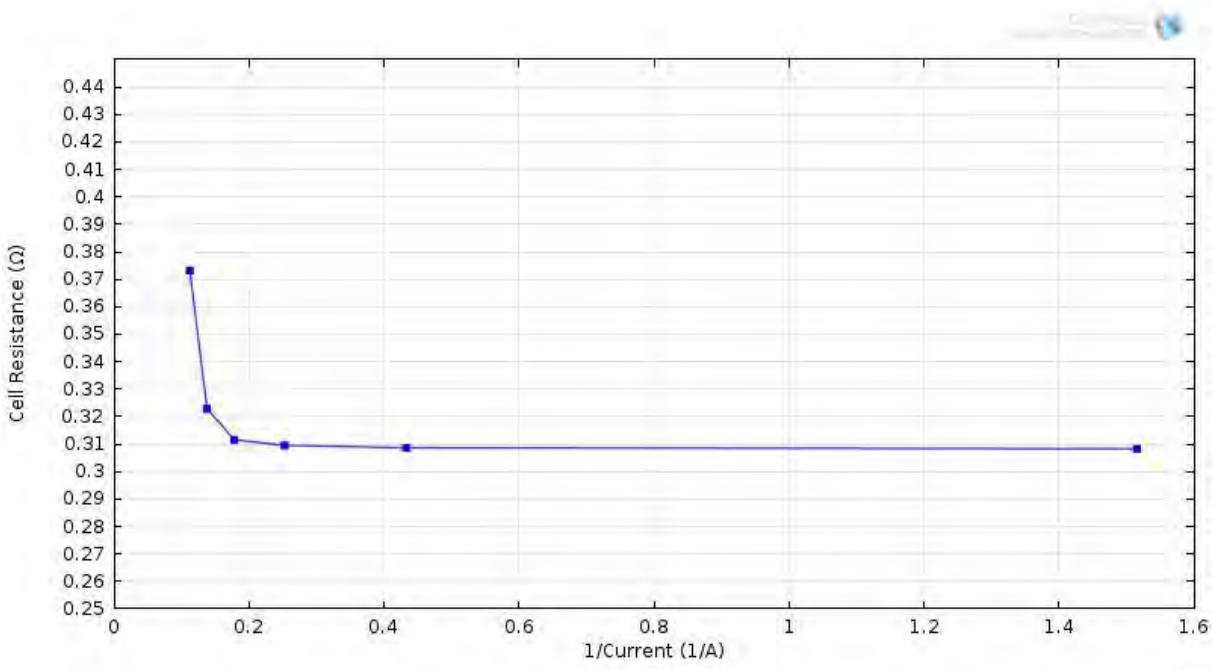

Figure 1.13. *Cell resistance versus reciprocal current at linear flow velocity 5 cm/s and 0.2M NaCl concentration*

The obtained Cowan plot can be compared with the experimental graph, considering the same stack geometry and operative conditions (linear flow velocity and bulk concentration). In reality, the experimental stack consists of three cell pairs and platinum wires were placed in two consecutive concentrate compartments. The wires are connected to a voltmeter to measure the voltage variations during the operation. The cell pair voltage is recorded by a computer at regular intervals of 10 s. The current passing across the stack is increased stepwise. A time interval of 10 s between two voltage-current measurements is chosen in order to consider steady-state conditions. Figure 1.14 shows the Cowan plot obtained with three cell pairs stack in laboratory. The profile of the resistance is similar to that shown in Figure 1.13, and in both cases the slope change is evident. Nevertheless, the limiting current obtained by the experimental graph (≈ 3 A) is slightly lower than that resulted by the simulation study (≈ 5 A).

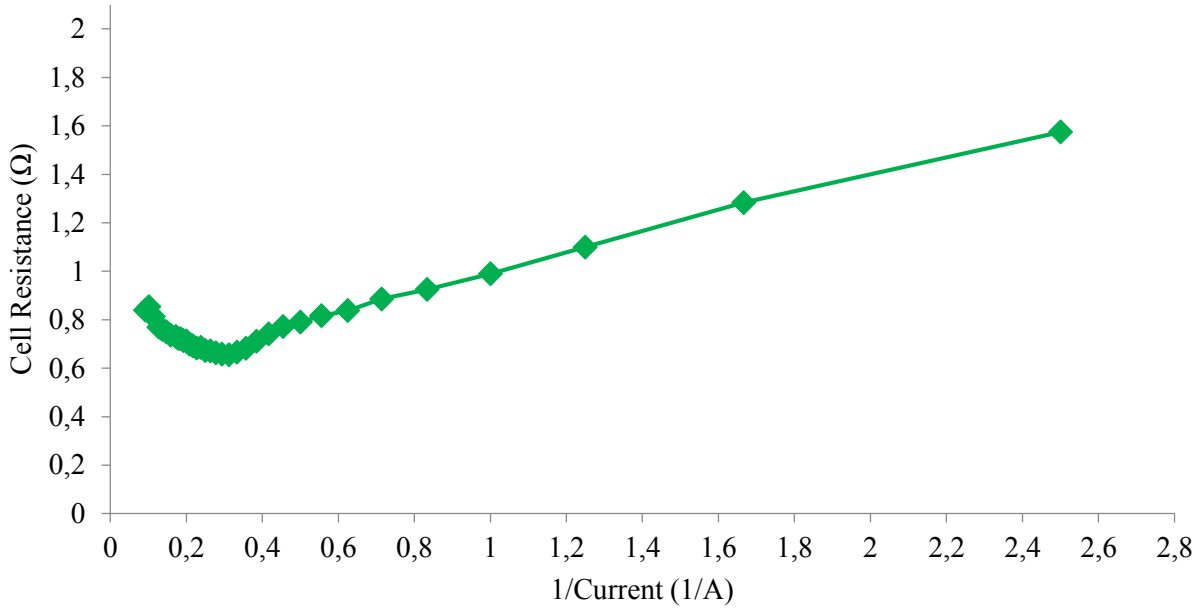

Figure 1.14. *Lab experiment using a three cell pairs stack. Cell resistance versus reciprocal current at linear flow velocity 5 cm/s and 0.2 M NaCl concentration.*

1.6.10 Recommendations for the future

By comparing the ED experiments to the simulations, it is shown that the model is well suited to describe the actual desalination process. In particular, the model designed by COMSOL can reliably predict the LCD. The limitations are that the concentration of ions within the membranes is considered exactly constant and the solvent flux across the membranes is neglected.

On the other hand, the lab experiment is not completely controlled by the user. The effective position and the consequent effect of the plastic net during the experiment is little known; e.g. it can adheres to the membranes. Moreover, the bulk concentration in the both concentrate and diluate compartments can change during the experiment time. To avoid this inconvenience, the solution flowing in the diluate and concentrate cells is continuously mixed. Nonetheless, some variations in concentration of ionic species are inevitable.

Therefore, the model can be improved by introducing a TCD in the ion-exchange membrane domains, as well. A new boundary condition that takes in account the electro-osmotic flux of water through the membranes can be added. Moreover, the reliability of the results can increased executing a fully coupled study that includes both the laminar flow physics and the current distribution physics. Obviously, this strategy can lead to convergence problems or to extremely slow calculations.

Once these improvements are been introduced, a CEDI process can be modelled introducing a domain representing the ion-exchange resins within the diluate compartment.

Chapter 2
Experimental verification of Lee - Strathmann model

This chapter starts considering the Lee - Strathmann model, proposed in literature for the empirical determination of the LCD. In particular the physical meaning of the parameters is pointed out. Based on these considerations some modifications are conducted on this model. The modified model is experimentally verified.
The graphic determination of the LCD and a statistical approach for the evaluations of results are presented, and the pilot equipment is described in detail.

2.1 Lee - Strathmann model

As previously discussed, LCD is considered as one of the most relevant design parameters because it influences the efficiency as well as the cost of an ED desalination process. Lee *et. al.* (2005) proposed an empirically derived expression in which i_{lim} is a function of the feed flow velocity in the stack and the concentration of diluate solution. The correspondent equation, which refers to Lee-Strathmann model, is:

$$i_{lim} = a'\,{}^{b}C^{d}\,(u)^{b'} \quad ; \tag{2.1}$$

where the coefficients *a'* and *b'* are constant; *a'* is expressed in $As^{b'}m^{1-b'}/keq$ and *b'* is dimensionless. These coefficients are estimated by the measurements of the respective i_{lim} with different flow velocities, a defined diluate concentration and for a specific cell design. Basically, the membrane type, the thickness of a cell and the geometry of the spacer screen must be known and chosen before, as well as the concentration of diluate solution. Specifically, *a'* and *b'* are estimated from a double logarithmic plot showing i_{lim} divided by the diluate concentration as a function of the linear flow velocity. Indeed, the Eq. (2.1) can be rewritten as follows:

$$\ln\left(\frac{i_{lim}}{{}^{b}C^{d}}\right) = \ln(a') + b'\,\ln u \quad . \tag{2.2}$$

In the mentioned study, the coefficients were estimated in the linear velocity range between 0.022 and 0.044 m/s and a NaCl solution flowed in diluate cells. It was considered diluate concentrations in the range 0.008 - 0.1 keq/m^3. Different ion-exchange membranes (from

NEOSEPTA®, Japan) with effective area of 25 cm^2 were used, the cell thickness was equal to 6 mm.
It was found that the coefficient *a'*, being affected by the transport numbers in the membrane and in the solution, changed significantly in the range of concentration which was investigated. On the other hand *b'* was affected by hydrodynamic conditions including the linear flow velocity.

2.2 Empirical determination of limiting current density

The i_{lim} needs to be experimentally determined for a specific ED stack, for a certain diluate concentration and for given flow rates. The i_{lim} value and the correspondent value of the stack voltage (limiting voltage (V), U_{lim}) can be extracted from the data using two different approaches.
A current-voltage graph can be obtained plotting the measured current as a function of the applied voltage across the stack. In theory, the $I(U)$ graph should show a linear behaviour up to a certain voltage drop; from that point onwards the current profile should be flat. This is the region of the LCD when the complete depletion of ions at the membrane surface facing the diluate solution occurs.
The proportionality between current and voltage in the first part of the graph is due to Ohm's law, expressed by:

$$U = I\,R \quad ; \tag{2.3}$$

where R (Ω) is the global resistance of the stack (calculated as U/I).
In practice, the $I(U)$ graph exhibits a more or less linear behaviour in the ohmic region, and it's not so simple to obtain a horizontal behaviour in the following part of the $I(U)$ graph, usually the slope of the curve decreases slightly, i.e. the current increases marginally with the increasing voltage drop. Therefore, the first approach detecting i_{lim} consists in locating the change in slope in the graph. This is possible by performing a linear regression on the data in the ohmic region and in the LCD region. The intersection point of the two lines identifies I_{lim} (on the y-axe) and U_{lim} (on the x-axe), although the smoothness of the curves causes difficulties in accurately differentiating slopes of the curves. The Figure 2.1 shows a typical current-voltage graph obtained under specific conditions, in which the i_{lim} is identified.

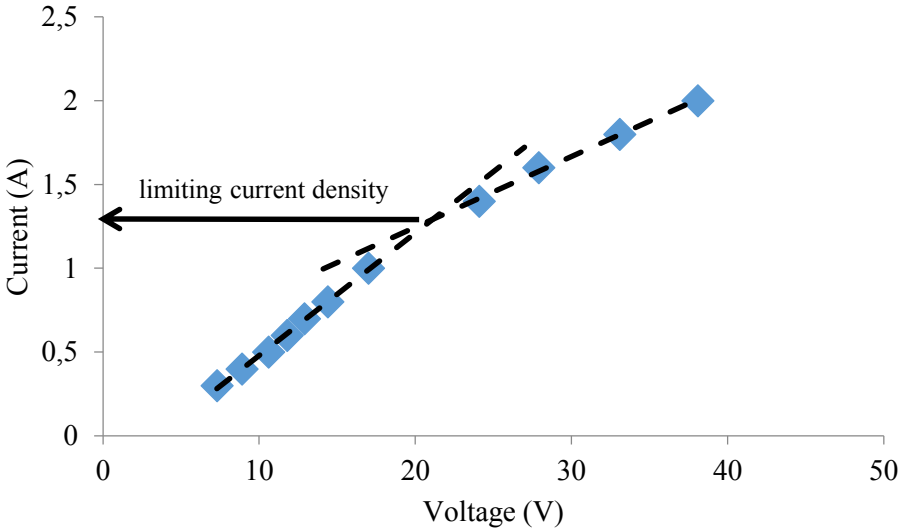

Figure 2.1. *Typical current-voltage graph for a lab-scale stack (10 cell pairs, cell length and width: 10cm, cell thickness: 2mm) at concentration at flow rates 0.015 m/s and NaCl concentration 0.1 M.*

The second approach is commonly known as the method of Cowan and Brown (1959). Cowan plot shows the reciprocal of the current on the x-axe and the stack resistance on the y-axe, as presented in Figure 2.2. The curve shows a sharp change in the resistance once the LCD has been reached. Also this second method is characterized by uncertainty, but it's usually more advisable than the first one. In this study i_{lim} values are obtained using Cowan and Brown method and the first approach was used only as comparison.

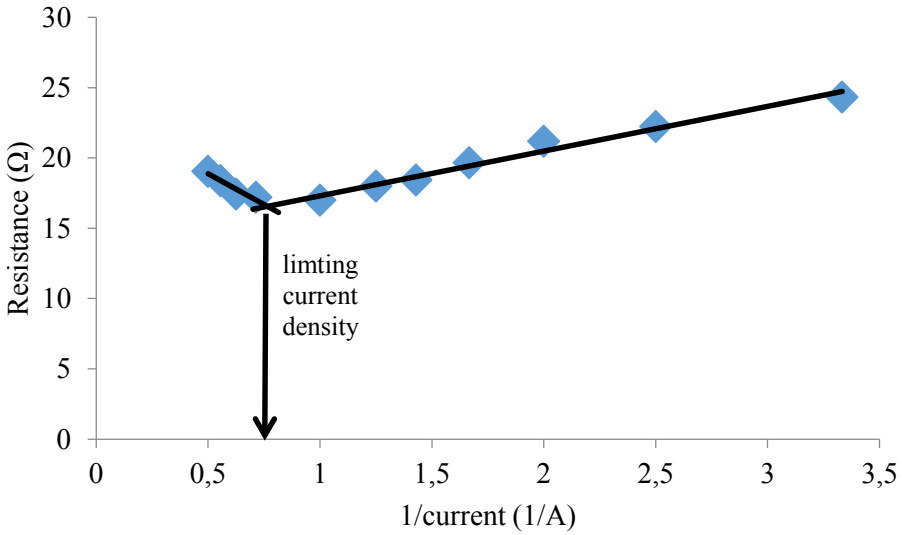

Figure 2.2. *Reciprocal current vs. stack resistance at flow rates 0.015 m/s and NaCl concentration 0.1 M (10 cell pairs, cell length and width: 10cm, cell thickness: 2mm).*

By measuring i_{lim} in a given stack design and for a specific diluate concentration the coefficients *ln(a')* and *b'* of Eq (2.2) represent respectively the y-intercept and the slope of the line which is obtained by plotting $ln(i_{lim}/C)$ versus the logarithm of the linear velocity, *ln(u)*.

2.2.1 Influence of concentrations and the linear velocity on limiting current density

The limiting current density is directly proportional to the concentration of the well mixed solution in diluate channels, as shown in Eq. (1.9). As predictable, the higher the concentration of ions the higher the ionic flux across the membrane. Consequently, the transport of electric current without incurring in concentration polarization is increased, as well as the value of i_{lim}. According with Lee e. al. (2005) the Eq. (1.9) can be rewritten as follows:

$$i_{lim} = \tilde{k} \frac{F \, {}^{b}C_i^d}{(T_i^m - T_i)} \quad ; \tag{2.4}$$

where $\tilde{k}$ (m/s), representing the mass transfer coefficient, can be expressed by:

$$\tilde{k} = u^{b'} \quad . \tag{2.5}$$

Consequently the coefficient *a* from Eq. (2.1) can be considered as a function of the transport numbers in the membrane and in the solution which are influenced by the mobility of ions and their concentration. Within a membrane in presence of an electric potential gradient, generally the counter-ions with the higher charge number and the smaller hydrated radius have a higher mobility than ions with lower charge number and larger hydrated radius.
In the equation (2.4) ${}^{b}C_i^d$ is expressed in keq/m^3, therefore the concentration value contains the charge number and differently charged ions need be compared taking in account their charge. For instance, a bicharged ion allows a double i_{lim} respect to a monocharged ion considering equal molar concentrations and equal operative conditions.
The coefficient *b'* is related to the hydrodynamic condition and defines the nonlinear correlation between i_{lim} and u. The concentration polarization is avoided if a higher linear flow velocity is used on equal bulk salt concentration of the diluate.
The higher the linear flow velocity within the diluate compartments the thinner the boundary layer. In proximity of the membranes surface, along the length of the diluate cell, the concentration of solution decreases in the direction of the flow. The effects of LCD, including the increasing of the cell resistance, appear only if the cell length allows the depletion of ions close to the membranes surface. In the case of an industrial stack, in which the path length can be as long as 1 m, there is much more concentration decline along the flow path, when compared to a small laboratory stack. However, it is assumed here that the LCD occurs at the same diluate concentration and at the same flow velocity independently from the cell path.

2.2.2 Enhancements to the model

The principal drawback of Lee - Strathmann model is that the coefficients of the empirical formulation of i_{lim} expressed in Eq. (2.1) are obtained maintaining the value of concentration of diluate constant. In fact, a typical industrial plant for the desalination by ED generally consists of two or more stacks: their structure and operative conditions are the same, except the solutions concentration. For each stack the i_{lim} needs be determined to calculate the total current, the voltage drop across the stack and the energy consumption, as described in §1.4.4 and §1.4.5. Clearly, it's advantageous to have available unique coefficients, which accounts for the variation of concentration from a stack and the following one.
Moreover, a single stack can work with different concentrations of diluate, especially in batch systems, in which the characteristics of solutions are time-dependent. Appling an adequate model, if the profile of diluate concentration over the time is known, also the optimum profile of the imposed current over the time can be estimated.
In addition, Lee e. al. (2005) considered only the case of monocharged ions (NaCl solution). In view of the fact that wastewaters often contain a variety of salts, an advanced model which considers also ions with a higher number of charge is here discussed.
In order to do this a new equation is used (Brauns *et al.*, 2009):

$$i_{lim} = a\,({}^{b}C^{d})^{n}\,(u)^{b} \quad ; \tag{2.6}$$

where the parameters *a*, *b* and *n* haven't any specific physical meaning and must be considered as pure mathematical modelling parameters. The measurement units of i_{lim}, ${}^{b}C^{d}$, and u are respectively A/m^2, keq/m^3, and m/s, consequently the coefficient a is expressed in $A\,s^{b}/(keq^{n}m^{2+b-3n})$ and b, n are dimensionless.

These parameters are estimated by a nonlinear regression technique, discussed in the paragraph §2.2.3, from a set of experimental data. Limiting current density value is calculated for different combinations of diluate concentrations and linear velocity using two different aqueous solutions: NaCl and Na_2SO_4 solutions.

2.2.3 Statistical approach on results evaluation

In this paragraph, most important concepts about nonlinear regression are presented; all the following definitions are traceable in Graybill and Iyer (1994). In particular the estimation for the unknown parameters in a nonlinear regression function using the method of least squares is discussed briefly. The computation required for nonlinear regression analyses are not feasible without the use of a computer, and most major statistical packages have routines for nonlinear regression.

A nonlinear function of the unknown parameters is a nonlinear function in which its form $\mu_Y(x_1, \dots, x_k)$ is known but it contains unknown parameters $\tilde{\beta}_1, \dots, \tilde{\beta}_P$.In this study, based on previous assumptions, the form of the function μ_Y is $\tilde{\beta}_1 \cdot x_1^{\tilde{\beta}_2} \cdot x_2^{\tilde{\beta}_3}$ and we may not know the values of $\tilde{\beta}_1, \tilde{\beta}_2$and $\tilde{\beta}_3$.

According with the method of least squares, the estimates of $\tilde{\beta}_1, \dots, \tilde{\beta}_P$ are obtained by minimizing the quantity $\sum_{i=1}^{\tilde{n}} e_i^2$, the sum of squares of errors of prediction, where the residual e_i is given by:

$$e_i = y_i - \mu_Y(x_{i,1}, \dots, x_{i,k}) \quad ; \tag{2.7}$$

where y_i refers to experimental value of μ_Y and $\tilde{n}$ is the total number of set of measured variables $y_i, x_{i,1}, \dots, x_{i,k}$.

Thus, the sum of squares of errors, denoted by the abbreviation SSE is expressed by:

$$SSE = \sum_{i=1}^{\tilde{n}} \left[y_i - \mu_Y(x_{i,1}, \dots, x_{i,k})\right]^2 \quad . \tag{2.8}$$

The quantity MSE which is an abbreviation for the mean squared error, and it's an unbiased estimate of variance $\tilde{\sigma}^2$. The corresponding estimated standard error $\tilde{\sigma}$ is given by:

$$\tilde{\sigma} = \sqrt{\frac{SSE}{\tilde{n}-p}} = \sqrt{MSE} \quad . \tag{2.9}$$

Another useful information is the confidence interval. A two-sided confidence interval for a parameter $\tilde{\beta}$is an interval in which the probability of the resulting interval actually containing $\tilde{\beta}$ is a prescribed value 1-$\tilde{\alpha}$. Values of $\tilde{\alpha}$ that are typically used are 0.01, 0.05, and 0.10, with corresponding confidence levels 1-$\tilde{\alpha}$ of 0.99, 0.95, and 0.9. In this study it was considered appropriate a confidence level of 0.95.

Finally, the p-value of an estimated parameter is a decreasing index of reliability of that value. Precisely, the p-value represents the probability of error that is involved in accepting the parameter as valid, i.e. a reliable indicator of the relation between the respective experimental variables. If the considered confidence level of a parameter $\tilde{\beta}$ is 0.95, the p-value of 0.05 can be considered as a *border-line acceptable* error level.

Both calculations of the p-value and the confidence interval are rather complex and will be not discussed here. Generally, the estimation of parameters in nonlinear regression models requires the use of iterative methods on digital computers, and explicit formulas for the estimates are generally not available. Specifically, in this study STATISTCA 12, a statistics and analytics software developed by StatSoft, was used.

2.3 Materials and methods

2.3.1 Electrodialysis pilot equipment

Experimental tests were carried out in the ED pilot installation, shown in Figure 2.3a. The pilot plant consists mainly of three loops (concentrate, diluate, electrolyte solution) and a stack. Each loop has a storage tank, as shown in Figure 2.3b. The volume of each tank is about 25 l.

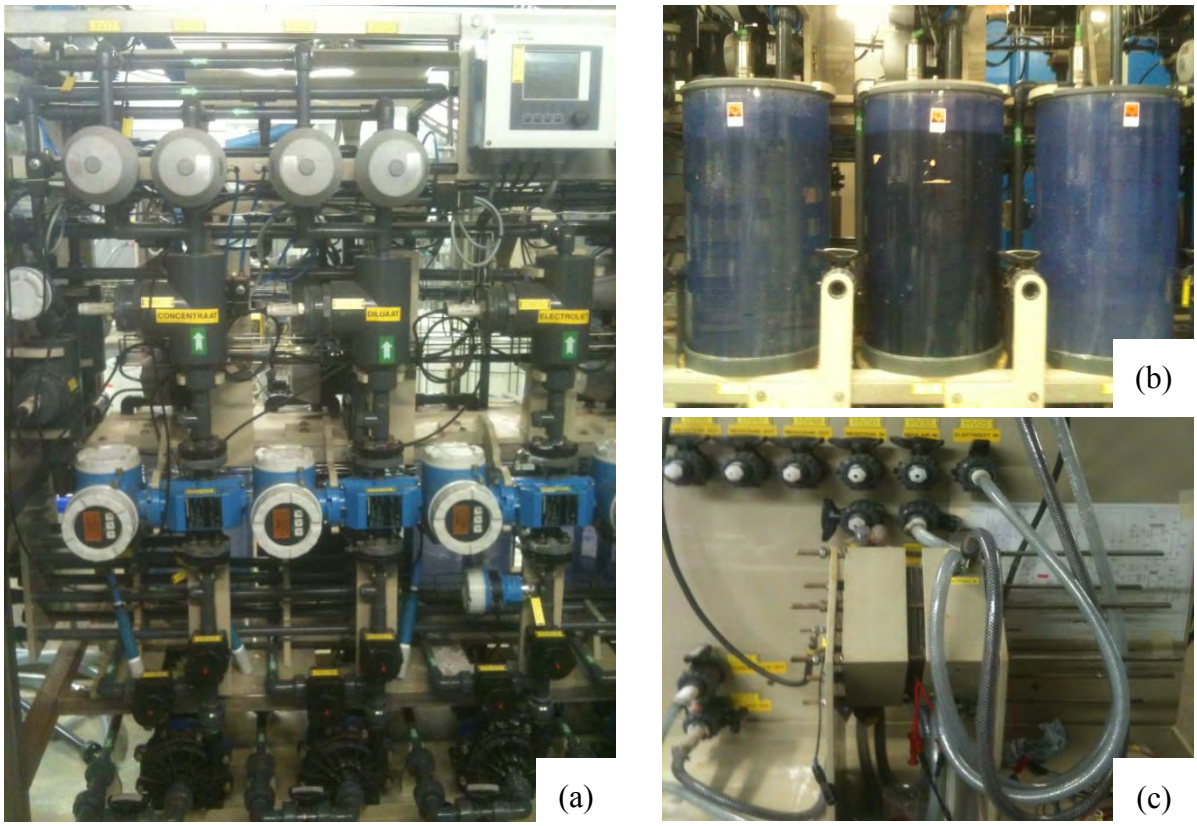

Figure 2.3. *ED pilot at VITO: (a) front-section of (height of installation is about 2 m); (b) storage tanks; (c) lab-scale stack.*

Two recirculating pumps are connected to the concentrate and diluate compartments of the stack and to their tanks, respectively. The ED stack (shown in Figure 2.3c) operates in batch mode, i.e. the solutions in diluate and concentrate compartments are continuously recirculated. A third pump is used to recirculate an aqueous solution of Na_2SO_4 (1.12 M) through both anode and cathode compartments. Conductivity, temperature and pH are measured in the connection between the vessel and the stack for every loop.

The voltage across and the current in the stack are controlled by a direct current power supply. Both current and stack voltage drop are recorded by a computer, as well as the flow rates and the pressure in the bottom of concentrate, diluate and electrolyte solution. The pressure measurement can be easily converted in a volume measurement if the value of the density of liquid is known.

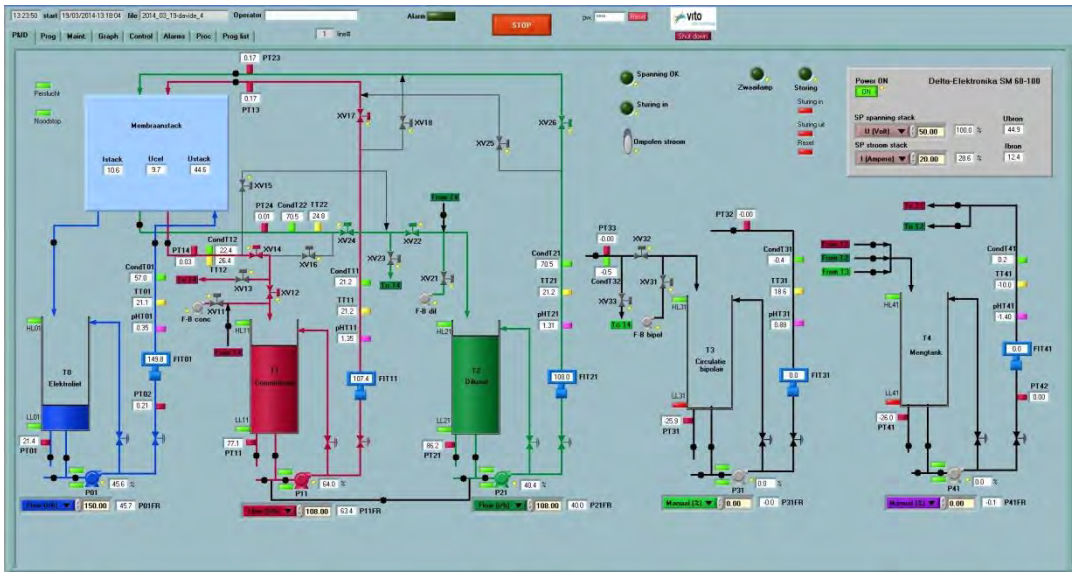

Figure 2.4. *Labview based ED control software.*

The experiments can be fully and automatically controlled by a specific Labview based software (see Figure 2.4) developed at VITO.

2.3.2 Lab-scale stack structure

The ED stack used in this section contains 10 cell pairs, the active surface of membranes is (0.1×0.1) m^2 and the spacers have a thickness (Δ) equal to 2 mm. A plastic net is placed in each compartments, including electrolyte solution compartments, to guarantee good mixing.
AEMs and CEMs Ralex® are purchased from MEGA (Czech Republic) and their main properties are reported in Table 2.1.

Table 2.1. *Properties of heterogeneous ion-exchange membrane Ralex® produced by MEGA (Czech Republic).*

Property	Unit of measurement	CEM	AEM
Ion-exchange group		$R\text{-}SO_3^-$	$R\text{-}(CH_3)_3N^+$
Swelling	wt%	<55	<65
Hydrodynamic permeability (ΔP=1bar)	ml/h m^2	0	0
Area resistance in 0.5 M NaCl (measured under direct current)	Ωcm^2	<10	<7.5
Ion-exchange capacity	meq/g	2.2	1.8
Transfer number of the counter ion (0.5/0.1M KCl)		>0.95	>0.95

Membranes Ralex® are heterogeneous membranes composed of fine polymer particles with ion-exchange groups anchored by polyethylene matrix and reinforced by fitted fabrics in polyester which improves the mechanical properties. CEM transmits cations and AEM transmits anions, while both type of membranes prevent to hydrodynamic flow of solvent. These membranes have a long life cycle (up to 10 years, based on the environment) in both laboratory and industrial scales. Specifically, the membrane Ralex® can work in a wide pH range (0-10), in temperatures from 10 °C to 50 °C, and it's possible perform an alkaline treatment (pH up to 12) for a short time.
The relation between the flow linear velocity in the diluate or concentrate compartments of the stack and the flow rate of the centrifugal pump is expressed by:

$$Q = u\, N\, A_{cross} \quad ; \tag{2.10}$$

where A_{cross} (m^2) is the cross-sectional area of a compartment, which is given by:

$$A_{cross} = \Delta\, Y \quad . \tag{2.11}$$

In this particular stack, A_{cross} is equal to $2 \cdot 10^{-4}$ m^2.

2.3.3 Mixing operating mode

Each LCD determination experiment is performed with a prescribed linear flow velocity and a specific concentration solution in both diluate and concentrate compartments. Two different salts are considered: NaCl and Na_2SO_4; identical molar concentration of the solutions are compared. The investigated velocities and concentrations of NaCl and Na_2SO_4 solutions are reported in Table 2.2.

Table 2.2. *Linear flow velocities values and concentrations of NaCl and Na_2SO_4 aqueous solutions used in the experimental investigation.*

Linear flow velocity	**m/s**	**Concentration of NaCl aqueous solution**	**keq/m³**	**Concentration of Na_2SO_4 aqueous solution**	**keq/m³**
u_1	0.015	C_1	0.01	C_5	0.02
u_2	0.03	C_2	0.02	C_6	0.04
u_3	0.05	C_3	0.1	C_7	0.2
u_4	0.07	C_4	0.2	C_8	0.4

Initially the vessels are filled up with the respective solutions reaching a volume of 20 l. While the flow rate of the electrolyte solution is still 100 l/h, the flow rates of diluate and concentrate solutions are adjusted to the linear flow velocities u_1-u_4 given in Table 2.2.
Cowan plot is drawn increasing stepwise the voltage drop and recording the correspondent current passing across the stack. This operation requires about 10 s for each voltage-current measurement, in order that the system reaches the stationary state.
The value of i_{lim} is obtained for a specific value of the diluate bulk solution. If a certain voltage drop across the stack is applied, obviously in this batch system the diluate concentration decreases with time. In order to avoid this inconvenience the diluate and concentrate tanks contain the same solution and the two streams are shifted at the exits from the stack, i.e. diluate solution moves toward the concentrate vessel and vice versa. This operation is called "mixing operating mode" and it allows to maintain the same concentration of the solutions during the experiment.

2.4 Results and discussion

Using a test salt solution, 32 combinations of concentrations and velocities were investigated. Only in 4 cases, it was not possible to determine the value of LCD, as no change in slope have been detected either in $I(U)$ or in Cowan graphs. However, the remaining data-points were sufficiently reliable for estimating the parameters of a model relating the limiting current density with the concentration of diluate and the velocity in diluate channels.
Data referring NaCl and Na_2SO_4 solutions are compared in Figure 2.5: the experimental i_{lim} is plotted versus the linear flow velocity u for each concentration value of NaCl and Na_2SO_4 solutions. This plot clearly shows that increasing linear flow velocity increase LCD more at relatively high concentrations. In contrast, using a concentration up to 0.02 keq/m^3, independently of the dissolved salt, the profile of the i_{lim} with u is more or less flat. This result implies that when few ions are available in the solution to transfer the electric current the effect of increased mixing on the LCD is neglectable.
The models for the empirical determination of i_{lim} expressed by Eqs. (2.1) and (2.6) are compared and can be applied to a specific salt solution or to both solutions.
The principal and immediate instrument for this comparison is the standard error $\tilde{\sigma}$ of the entire model. The coefficients a' and b' are estimated by a linear regression, whereas a nonlinear regression is applied for the estimation of a, b and n. The model with three parameters was not linearized because the correspondent $\tilde{\sigma}$ was higher than that relevant to the three parameters non-linearized model. Table 2.3 reports the estimated standards errors of the models for each case. Generally, it's observed that the model with three parameters guarantees a lower $\tilde{\sigma}$ than a linear regression with two parameters.

The three parameters nonlinear regression concerning the Na_2SO_4 solution presents a quite high standard error (28.13). This fact can be due to an uncertainty of i_{lim} identification or to the uncertainty in the analytical determination of the bulk salt concentration, especially with the lowest values.

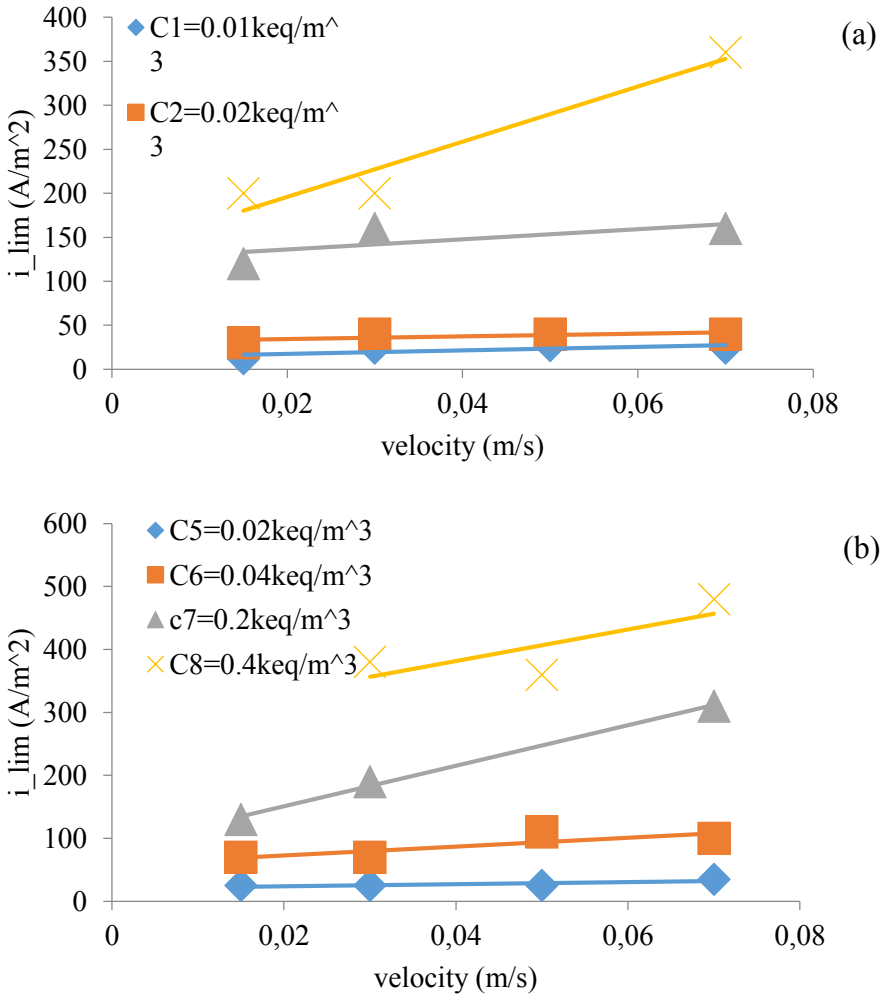

Figure 2.5. *Experimental i_{lim} as a function of linear flow velocity (u_1-u_4) determined at different diluate concentration of (a) NaCl aqueous solutions (C_1-C_4) and (b) Na_2SO_4 aqueous solutions (C_5-C_8).*

Table 2.3. *Standard errors of the models with two parameters (linear regression) and with three parameters (nonlinear regression) considering NaCl solution, Na_2SO_4 solution and both solutions.*

	NaCl solution	**Na_2SO_4 solution**	**Both solutions**
2 parameters model	22.42	43.22	42.42
3 parameters model	19.92	28.13	26.49

However the standard error decreases if both solutions are considered, (the total number of variables sets, $\tilde{n}$, is duplicated). This confirms that the model works properly also considering different salt solutions, in particular the parameters are not excessively affected by different ionic charge numbers.

When different models are investigated, it's essential also assess standard error, p-value and confidence interval of the estimated parameters. These indexes are shown in Table 2.4, which refers to nonlinear regression of coefficients *a*, *b* and *n* in the case of NaCl solution, Na_2SO_4 solution and both solutions.

Table 2.4. *Estimated parameters a, b and n using model with 3 parameters expressed by Eq. (2.6) in the case of NaCl solution, Na_2SO_4 solution and both solutions. A confidence level of 0.95 is considered (α=0.05). For each parameter standard error, p-value and confidence level are reported.*

Solution	Parameter name	Estimated parameter	Standard error	p-value	Lower confidence limit	Upper confidence limit
NaCl	*a*	3354	895	0.0022	1583	5524
	b	0.37	0.064	0.00011	0.23	0.51
	n	0.85	0.079	0	0.68	1.02
Na_2SO_4	*a*	2690	683	0.0023	1186	4193
	b	0.41	0.084	0.00045	0.23	0.60
	n	0.71	0.061	0	0.57	0.84
both	*a*	2485	448	0.000009	1561	3408
	b	0.38	0.058	0.000001	0.26	0.50
	n	0.70	0.04	0	0.61	0.78

Applying the model to both solutions allows to reduce standard error and p-values and to limit the 95% confidence interval for each parameters. Therefore, the effectiveness of the model expressed in Eq. (2.6) is further confirmed. A three-dimensional representation of this model applied to both NaCl and Na_2SO_4 solution is shown in Figure 2.6.

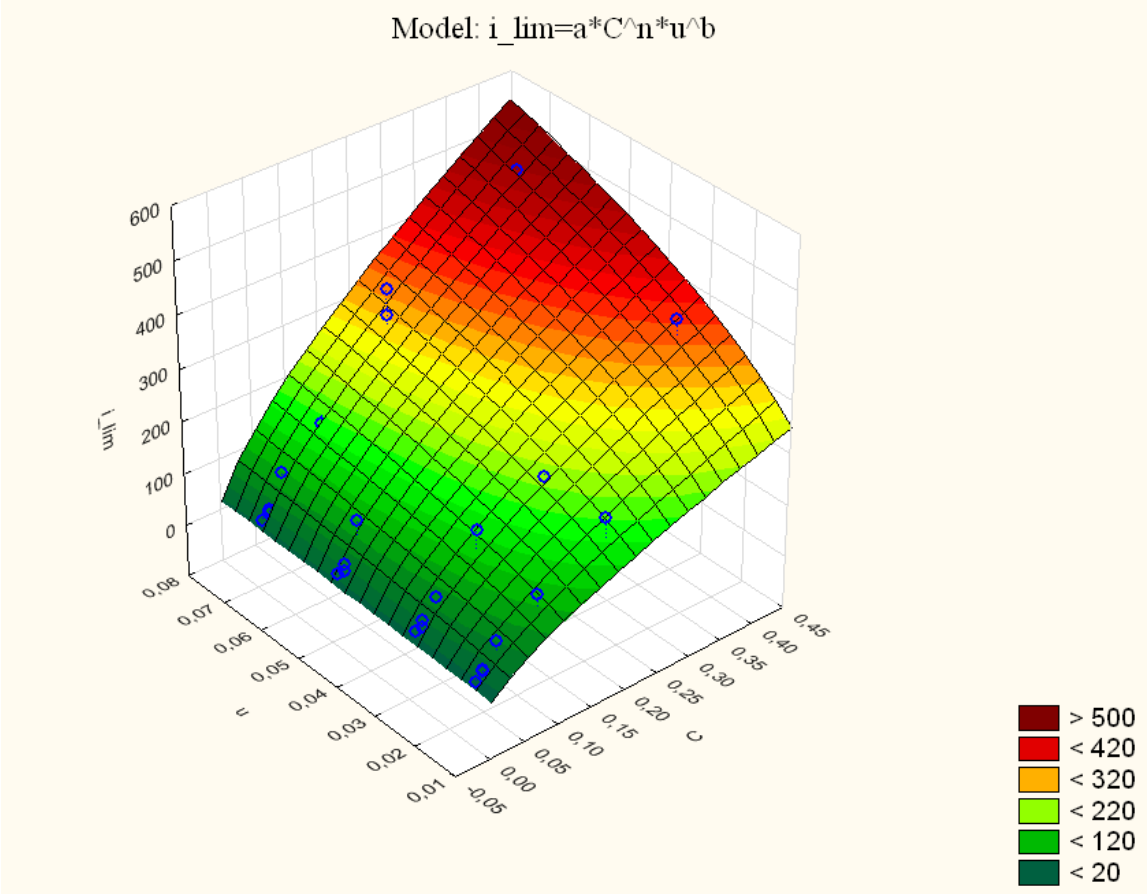

Figure 2.6. *Three-dimensional graph representing the 3 parameters model considering both NaCl and Na_2SO_4 solutions . a=2485 $As^b/(keq^n m^{2+b-3n})$; b=0.38; c=0.70.*

In this way, depending on the equivalent concentration of salt solution and the linear flow velocity for a given stack design, i_{lim} can be adequately estimated.

2.5 Conclusions

An ED system needs to operate near the limiting current density without exceed this boundary to avoid drastic energy losses and pH variations. Thus, a careful prediction of the value of the limiting current density is essential for designing and operation of an ED industrial plant.

Two different empirical expressions for the empirical determination of the LCD were compared following a statistical approach. The Lee - Strathmann model is discussed, in particular the physical meaning of the parameters are pointed out. Subsequently, a mathematical curve-fitting equation is studied, verifying its adequacy when differently charged ions in diluate solution are considered.

The second model, describing the LCD as a function of the linear flow velocity and the diluate equivalent concentration, allows to foresee the LCD deviations, when the operative conditions change, for a given stack.

It is notable that it's necessary to execute a multi-variables nonlinear regression for each specific stack because the parameters estimated in this section are dependent on the structure of the stack, especially the type of membranes, channel width and spacer geometry. However, the obtained model is independent of the equivalent concentration of the diluate and the presence of dissolved bicharged ions is contemplated. This is very convenient when series of stacks for the treatment of wastewaters or batch systems are considered.

Chapter 3
Case study: Electrodialysis plant for desalination of regenerate wastewater

The aim of this investigation is to study the efficiency of the ED process in separating salts from a highly concentrated wastewater and evaluate process limitations, such as water transport and membrane fouling. In particular, reference experiments are applied to evaluate the increasing of the membrane's resistance due to fouling phenomena. Moreover, the efficiency of EDR is studied through a long exposure experiment. Starting from these results a calculation of an industrial plant and its economical evaluation were carried out.

3.1 Introduction

3.1.1 Wastewater treatment by Elelctrodialysis

ED process is widely employed in industry for wastewater treatment, especially as an alternative to Reverse Osmosis. ED is mainly used in plants with capacities up to 20000 m^3/d, and brackish water salinity of 1 to 5 g/l total dissolved solids. ED is generally believed to be advantageous when high water recovery rates of the feed are expected, even for raw water with high sulphate content (Strathmann, 2004).

The fouling of ionic-exchange membranes is one of the most significant considerations in the operation of the ED process. Fouling of ion-exchange membranes during ED occurs mostly due to deposition of organic colloids on the membrane surface, which is dependent on the electrochemical interaction between the surface and the particles. Some organic ions, having low mobility, can penetrate into the pores of the membranes and remain there owing to an electrostatic interaction with the functional groups of the membrane matrix. A hydrophobic interaction with non-charged sections of the membrane is also possible (Grebenyuk *et al.*, 1998).

Membrane fouling results in an increase of membrane resistance which consequently causes a decrease of counter-ions flux through a membrane and increased energy consumption. Also a reduction of selectivity with respect to counter-ion transfer can occur (Lindstrand *et al*., 2000). It is known that most organic foulants in many effluent streams are negatively charged. Therefore AEMs are more susceptible to fouling by organic compounds than CEMs because of positively charged functional groups (Lee *et. al.*, 2002).

Generally, fouling phenomena can be classified as reversible and irreversible fouling in membrane processes, depending on the recovery of the process performances. The cleaning of fouled membranes can be carried out with a chemical treatment, by adding of dilute acid or base, or introducing EDR process. EDR permits the self-cleaning of reversible fouled membranes over the long-term operation (Chao and Liang, 2008). This technique will be reviewed in details in §3.2.3, showing benefits and drawbacks.

3.1.2 Description of the industrial plant

In the context of water purification, deionization by ion-exchange resins is a common and reversible process in which impurity ions present in the water are replaced by ions released by resins. This process continues until the resin is saturated with impurity ions.

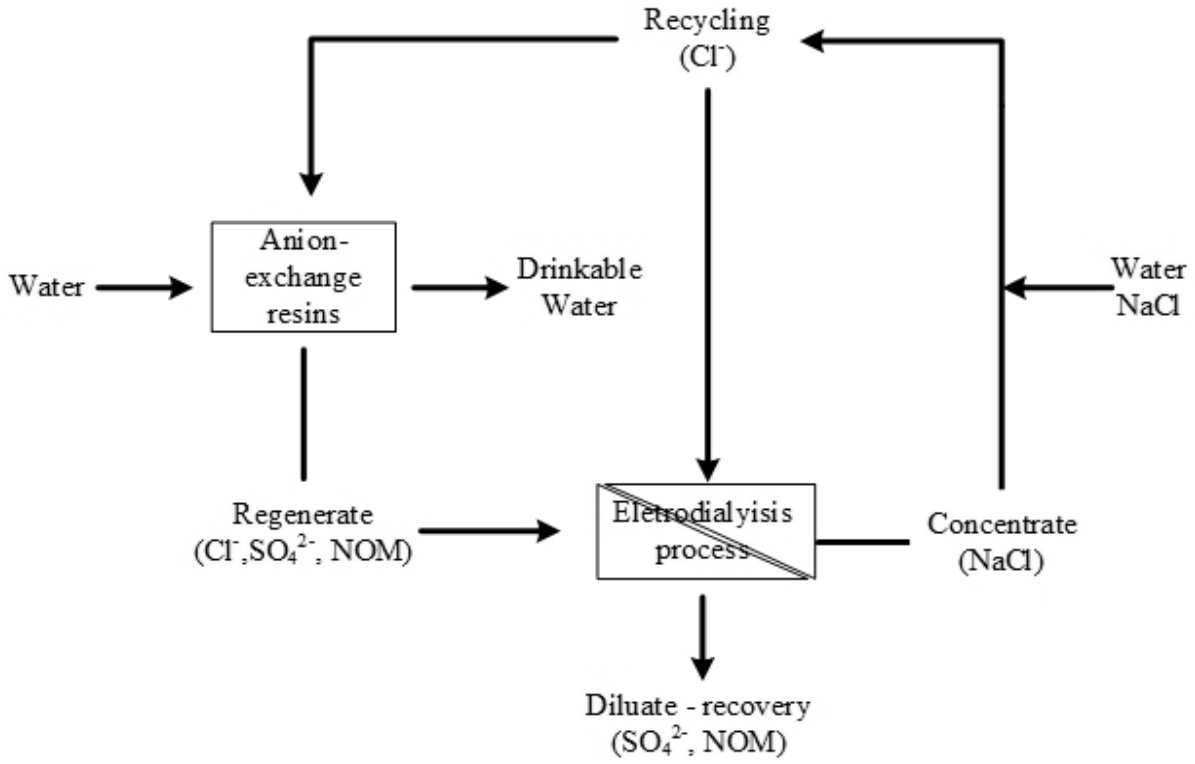

Figure 3.1. *Schematic illustration of an industrial plant in which deionization by ion-exchange resins and ED are coupled for the production of drinkable water.*

In this particular case study, AERs are used to remove negatively charged organic contaminants from groundwater. Upon saturation, the resin is regenerated by washing with a highly concentrated NaCl solution. The chloride ions replace the organic ions on the resins due to chemical equilibrium, (i.e. high concentration of chlorides in solution). The outlet stream of the regeneration process of the resins contains high concentrations of mainly sulphate, sodium, chloride and NOM which is problematic in view of discharge.

An alternative process scheme combines deionization by ion-exchange resins and ED for the recovery of the chloride ions (Figure 3.1).
The outlet stream of the regeneration process of the resins contains mainly sulphate, sodium, chloride and natural organic matter (NOM). This regenerate wastewater forms the initial diluate solution for the ED process, whereas the final concentrate solution will be the inlet stream of the regeneration process. The target of ED process is to recycle as much NaCl as possible and retain as much NOM in the diluate as possible. In this way, NaCl can be completely recycled instead of being discharged, and NOM can be sold as a soil enhancer.

3.2 Materials and method

3.2.1 Regenerate wastewater characteristics

The ED experiments illustrated in this chapter were performed using a specific regenerate wastewater produced from an industrial ion-exchange process for NOM removal.
The regenerate presents a high salinity and contains NOM which gives to the water a black colouring. In average, this water has the following characteristics: pH 8.3, conductivity 77 mS/cm, TOC 6 g/l, Cl^- 22.6 g/l, SO_4^{2-} 23.7 g/l, Na^+ 22.7 g/l.
The NOM has a heterogeneous nature and contains aromatic and aliphatic macromolecules. Cho *et al.* (2000) studied the influence of the molecular weight and the constituents of NOM and the pH value on the adsorption to the membrane surface.

3.2.2 Experimental set-up

The following experiments were performed using the ED pilot installation described in §2.3.1. The experiments were done in batch recirculation mode. The plant works in an automated manner, while the data acquisition concerning pressures, conductivities, pH values, temperatures, flow rates, currents and voltage drops are computerized.
The ED stack consists of three pairs of diluate and concentrate channels arranged alternately, meaning that 3 pieces of AEM and 4 pieces of CEM are used in total. Figure 3.2 shows the arrangements of diluate, concentrate and electrolyte solution compartments in the stack.
The lab-scale stack geometry offers a 0.01 m^2 of active membrane area with a channel thickness (Δ) of 0.002 m in each compartment. Thus, the total anionic membrane surface area in the stack is 0.03 m^2. Ralex® ion-exchange membranes are used and their main properties are mentioned in Table 2.1.
An electrolyte solution (20 l of Na_2SO_4 aqueous solution 1.12 M) is recirculated in a closed cycle between the electrode chambers.

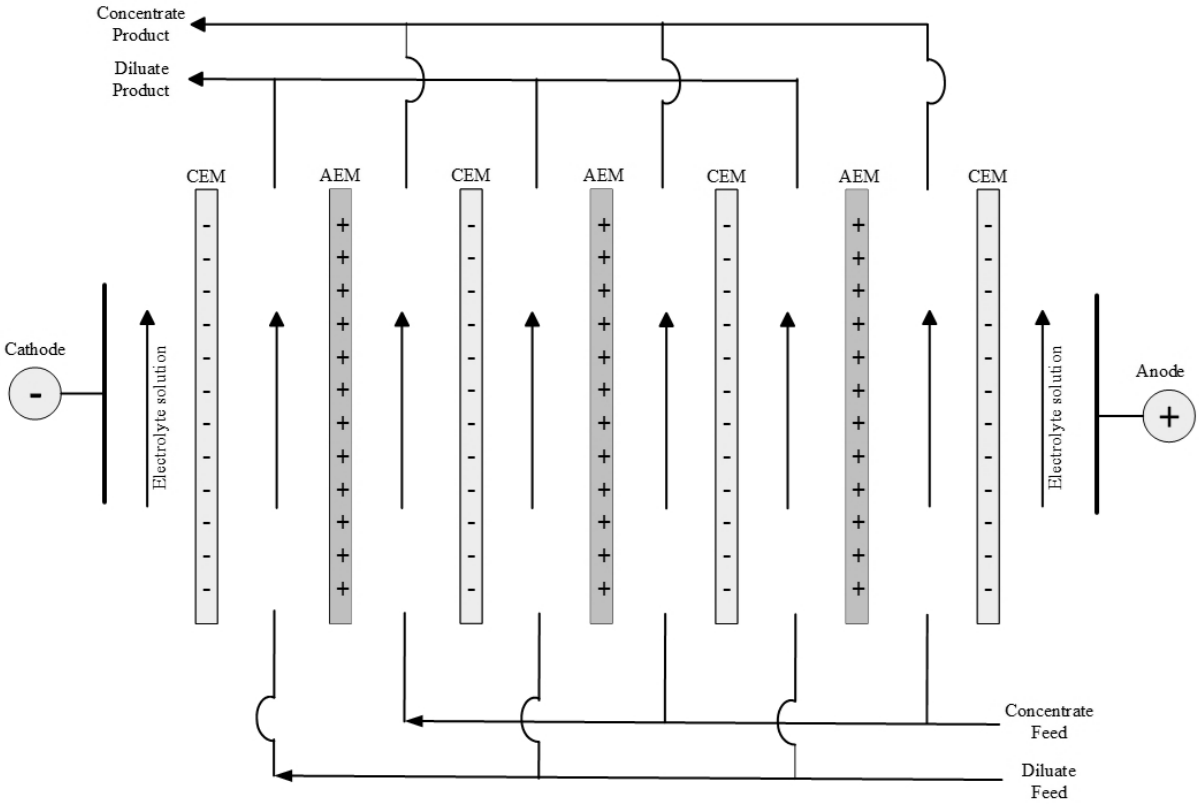

Figure 3.2. *Schematic illustration of the ED lab-scale stack used during batch experiments treating regenerate wastewater.*

In order to obtain information about design and economical aspects of an industrial ED plant the following experiments were carried out:
(1) a desalting experiment of regenerate wastewater using a unidirectional ED operating mode;
(2) a short reversal operation;
(3) a long exposure experiment testing the effectiveness of Reversal EDR operating mode;
(4) a chemical treatment of the fouled membranes.

1- In the first experiment initially the diluate is regenerate wastewater and the concentrate is a 2 M NaCl solution. A desalination of the diluate is carried out using a 108 l/h flow rate for both diluate and concentrate streams (i.e. linear flow velocity in the cells is 5 cm/s) and a current density equal to 80% of i_{lim}.
The desalination rate of the diluate (*DR*) is obtained by the following expression:

$$DR = \left(1 - \frac{m_D^t}{m_D^0}\right) \times 100 \quad ; \tag{3.1}$$

where *m* is the amount of salts in the solution expressed in keq, the superscripts *0* and *t* refer respectively to the initial instant and a specific instant of time, the subscript *D* refers to the diluate solution.

During the experiment the concentration values are not available so a desalination rate (*DR'*) based on the conductivity of the solutions is used.
Thus, *DR'* is expressed by:

$$DR' = \left(1 - \frac{\sigma_D^t}{\sigma_D^0}\right) \times 100 \quad ; \tag{3.2}$$

where σ is the conductivity of solution expressed in 1/Ω m. The measurement of conductivity of diluate, concentrate and electrolyte solutions is continuous and automatic.
In the beginning and at 25%, 50%, 70% of R_D' the limiting current density is obtained from Cowan plots. Subsequently the limiting resistance (R_{lim}) is calculated by the following formula:

$$R_{lim} = \frac{U_{lim}}{I_{lim}} \quad ; \tag{3.3}$$

The total process can be considered as split in three intervals: the first from the beginning to 25% of *RD'*, the second from 25% to 50% of *RD'* and the third interval up to 70% of the desalination rate. At the start and at the end of each interval both I_{lim} and R_{lim} are calculated using two different flow velocities for both diluate and concentrate solutions: 2.5 and 5 cm/s. In addition samples of diluate and concentrate are taken for composition's analysis of Na^+, Cl^-, $SO4^{2-}$, Ca^{2+}, Mg^{2+} and TOC.

2- To restore the original properties of the membranes at the end of the desalination experiment the reverse polarity operating mode is carried out for three times using regenerate wastewater in both diluate and concentrate streams. Therefore, this treatment is here called "short reversal operation".

3- During the long exposure experiment both diluate and concentrate tanks are filled with regenerate wastewater and a constant current is applied (about 80% of I_{lim}). The limiting current density and the limiting resistance are calculated hourly; and every 3 hours the mixing and reverse polarity operating mode are carried out at the same time in order to guarantee the same conditions there were at the start (see §3.2.3). In addition the wastewater in the tanks is replaced daily.
The system operates in this way for 42 hours. Then, the desalination process runs for 25 hours applying 80% of limiting current; i_{lim} and R_{lim} are obtained at the start and at the end. This operation is repeated three times, and every 25h-period is followed by the mixing and reverse polarity operating mode. Finally the system operates for 4 hours and the mixing and reverse polarity operating mode are carried out for the last time.

4 - For the chemical cleaning of fouled membranes, a 0.01M NaOH solution (with pH equal to 12) is used. The caustic solution is circulated in the concentrate and diluate compartments for 15 min.

3.2.3 Mixing and Reversal Polarity operating mode

The periodic reverse polarity provides to EDR process a self-cleaning mechanism to reduce the membrane fouling. EDR operating mode is used nowadays in almost all industrial ED plants. The polarity of the electrodes of EDR system is periodically reversed; the concentrated streams become dilute stream and vice versa. Accordingly, the charged particles divert their movement direction. When the polarity of the electric field is reversed, the charged components migrate away from the membrane back into the feed stream and the membrane properties are restored.
During the reversal of the polarity and the flow streams a partial mixing of the solutions cannot be avoided. Since the volumes of solutions treated in the pilot installation are undersized the mixing effect has a drastic impact on the composition of solutions. For this reason the mixing and reverse polarity operating mode are often coupled in order to guarantee uniform conditions in the solutions. Essentially, the same solution is fed into both concentrate and diluate chambers in the ED cells in order to maintain the same properties in the solution during the test.
This operation can be carried out automatically but it requires about 10 minutes. Practically the diluate and the concentrate are mixed as long as they reach the same conductivity, which can be considered an indirect measurement of the composition.

3.2.4 Reference experiments procedure

Observation of properties for the initially unfouled and fouled membranes is essential since NOM causes the electrochemical and physical properties to change. To compare the effect of fouling during the several experiments, a reference experiment was performed. It consisted in measuring I_{lim} and R_{lim} using a 0.2 M NaCl solution in both diluate and concentrate compartments. The mixing operating mode is used and the linear flow velocity in the channels is equal to 5 cm/s.
In order to maintain the same external conditions in each reference experiment, the stack is not changed or opened until all the experiments are carried out. Before and after the desalination experiment, the short reversal operation, the long exposure experiment and the caustic cleaning, a reference experiment is carried out.

3.2.5 Equivalence of conductance and concentration

Since conductivity of an electrolyte solution is a measure of its ability to conduct electricity, it is directly related to the concentration of salts dissolved in water. The electrical conductivity of the water can be determined in a quick and inexpensive way. Therefore, conductivity

measurements are often used in laboratory and industrial applications as a reliable way of measuring the concentration of salts dissolved in water.
While the electrical conductivity is a good indicator of the amount of salts, it still does not provide any information about the ion composition in the water. Moreover, when the salt concentration reaches a certain level, electrical conductivity is no longer directly related to salts concentration. It's clear that the conductivity of the regenerate wastewater cannot be easily related to its salts concentration also because of the presence of NOM.
Nevertheless, in these experiments the conductivity of solutions is used as an approximate measurement of the trend of desalination process.

3.2.6 Calculation of an Electrodialysis plant

The design procedure of a continuous operated ED plant is now presented. The system treats an industrial wastewater stream and its design is based on the theoretical model above described (…) and lab batch experiments.
A process design for ED plants has been presented by Lee *et al.* (2001) and it has been used and modified by Brauns *et al.* (2009) in order to reduce the amount of uncertain parameters.
The first parameter to determine in the design of a plant is the recovery rate characterizing the process. The recovery rate (Θ) is a value between 0 and 1 and determines which fraction of a feed solution is obtained as product. The recovery rate is given by the following expression:

$$\Theta = \frac{Q^d}{Q^{fd}+Q^{fc}} \quad . \tag{3.4}$$

In this case both diluate and concentrate final solutions can be considered as products, so the product recovery is considered to be 50%. Theoretically, the diluate flow rate is identical to that of the concentrate, since both the diluate and the concentrate cells have identical geometries. Diluate and concentrate flow rates are different for a recovery rate different from 0.5, and one flow stream must be operated in a feed and bleed mode to obtain identical linear flow velocities in the cells
The water capacity Q of the plant for the treatment of the regenerate wastewater with an initial concentration of 2.24 keq/m^3 is supposed be equal to 100 m^3/day. So both flow rates of concentrate and diluate products are 11.57×10^{-4} m^3/s.
The dimensions of the stack are given by the manufacturer and in this study the cell width Y, the path length of a cell L_{pp} or the length of a single stack and the cell thickness Δ are respectively 0.42 m, 0.725 m and 0.65 mm.
Choosing the number of cells N in a single stack is an essential decision to make. From Eq. (1.24) it's clear that N influences the linear flow velocity u in the cell compartments and consequently also the current density which must be applied.

As described in §1.4.5, both the required membrane surface, depending on *N*, and the current density influence strongly the energy consumption and the membrane investment of the entire plant. Thus, an optimum in the linear flow velocity and in the number of cells must be determined.

The limiting current density should be determined experimentally for this specific stack construction, for instance applying the Lee - Strathmann model. In this study, the model expressed by Eq. (2.6) is applied to determine the limiting current density. The estimation of parameters is deepened in the following paragraph.

The parameters *a*, *b* and *n* can be considered as constants in a limited range of linear flow velocity between 2 and 7 cm/s. In fact for a lower velocity the limiting current density is immediately reached while a too high velocity impedes a homogenous flux in the cell compartments causing energy losses.

An average value of equivalent conductivity Λ equal to 4 S m^2/keq is considered. The volume factor α, the area factor accounting for shadow factor β and the safety factor *s* are taken from Lee *et al.* (2001). The current utilization ξ and the total area resistance of membranes are adapted from the example of design study given in the above said paper as well.

The input data for the design calculation are summarized in Table 3.1.

Table 3.1. *Input data for the calculation of an in industrial plant treating regenerate wastewater.*

Q	11.57×10^{-4} m^3/s	n	0.46
C_s^{fd}	2.24 keq/m^3	α	0.8
Θ	0.5	β	0.7
Y	0.42 m	s	0.7
L_{pp}	0.725 m	ξ	0.9
Δ	6.5×10^{-4} m	$r^{am} + r^{cm}$	7×10^{-4} Ω m^2
a	2527 $A\,s^b/(keq^n m^{2+b-3n})$	Λ	4 S m^2/keq
b	0.56		

The process path length in a cell L_{pp}, as expressed in Eq. (1.31), is related to the feed and product concentration of diluate and concentrate solutions. Considering a single stack the outlet concentrations must be adjusted to set L_{pp} exactly equal to the length of the stack, i.e. 0.725 m. An iterative calculation in which the outlet stream concentrations become the concentrations of the inlet stream of the following stack must be carried out.

The concentration of diluate and concentrate are related to the recovery rate by a mass balance. The required concentrations of the concentrate feed solution and outlet concentration of the concentrate for a given stack are given by:

$$C_s^c = \frac{C_s^{fd} - \Theta C_s^d}{1-\Theta} \quad ; \tag{3.5}$$

$$C_s^{fc} = \frac{C_s^{fd}(1-\Theta)}{\Theta} + \frac{C_s^c(2\Theta-1)}{\Theta} \quad . \tag{3.6}$$

Each stack will have the same number of cell pairs, consequently the same amount of membrane area. The required number of stacks is given by the number of stacks necessary to reach the expected desalination rate. The total current *I*, the applied voltage *U* to achieve this current, the required membrane area *A* and the specific energy consumption E_{spec} are calculated applying the Eqs. (1.26), (1.27), (1.28), and (1.34), respectively.

3.2.7 Estimation of parameters for limiting current density calculation

In the second chapter the parameters *a*, *b* and *n* considering both monovalent and bivalent ions were estimated as 2485 $A\,s^b/(keq^n m^{2+b-3n})$, 0.38 and 0.70, respectively.

New parameters need to be calculated because this specific plant treats very high salt concentration solutions in comparison with NaCl and Na_2SO_4 solutions previously used. In addition, the ionic transport through the membranes is surely influenced by the presence of NOM and the consequent membrane fouling. On the other hand, carrying out EDR operating mode the fouling of membrane surface is strongly reduced in such a way that the wastewater behaves similar to NaCl and Na_2SO_4 solutions.

Table 3.2. *Bulk concentrations, linear flow velocities and calculated limiting current density for an ED process using Na_2SO_4 aqueous solution and regenerate wastewater.*

Diluate solution	Concentration (keq/m^3)	Linear flow velocity (m/s)	Limiting current density (A/m^2)
Regenerate wastewater	2.24	0.025	750
	2.24	0.05	1000
Na_2SO_4 solution	0.2	0.03	190
	0.2	0.07	310
	0.4	0.05	360
	0.4	0.07	480

According to these considerations the dataset shown in Table 3.2 is utilised to estimate the parameters. Two cases including the regenerate wastewater as diluate are considered. They derive from the LCD determination at the beginning of the desalination experiment when the fouling of membrane hadn't affected the system yet.

The coefficients a, b and n are estimated by a nonlinear regression, as 2527 $A\,s^b/(keq^n m^{2+b-3n})$, 0.46 and 0.56, respectively. These parameters were estimated from 6 data-points only. However, the model was considered reliable since the resulting standard error of the modelled LCD is 27.04 and the parameters' p-values don't exceed the value of 0.012.

3.3 Desalination experiment: results and discussion

A desalination batch experiment was performed according to the procedure described in §3.2.2. The experiment was run until the conductivity on the diluate side was less than 30% of the initial value.On the whole the experiment lasted for 86 hours.

When the conductivity of the diluate reached 23 mS/cm, the process became very slow and the limiting current's value was extremely low; so the experiment was stopped. The analysis' results highlighted that chloride ions were almost depleted (0.67g/l), so the electric current's transition was obstructed. The membrane's fouling played an important role in this phenomenon, too.

3.3.1 Limiting current density and limiting resistance profiles

As shown in Figure 3.3, the limiting current density decreases with desalination rate and the i_{lim} profile is higher when the liner flow velocity is increased, as expected. In addition, it is observed that at low salt concentrations in the diluate the flow velocity becomes less influential.

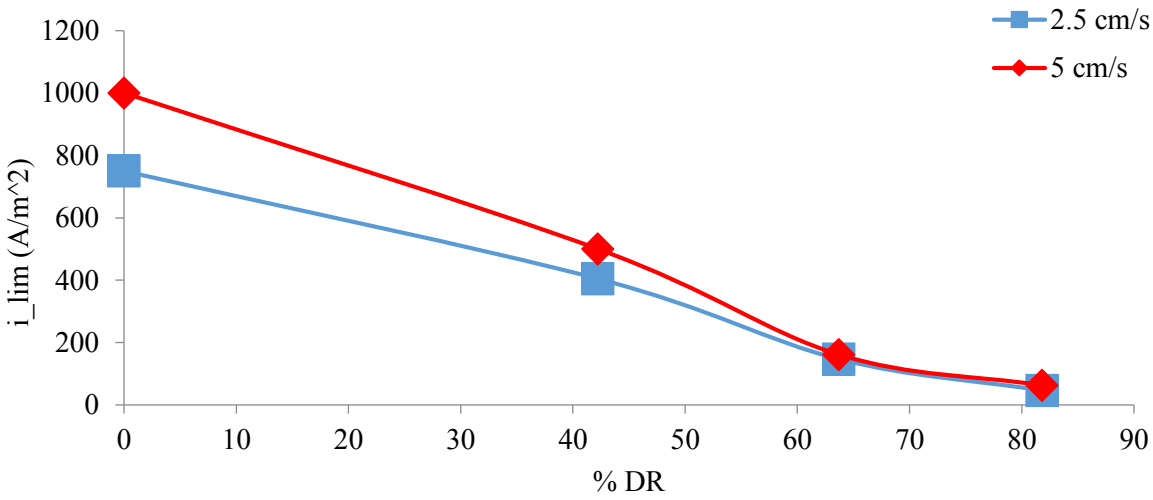

Figure 3.3. *Experimental i_{lim} determined at different linear flow velocities versus the desalination rate during the desalination experiment.*

This confirms our findings on experimental verification of the Lee - Strathmann model as described in Chapter 2. The linear flow velocity was found to influence LCD primarily at relatively high concentrations.

In ED it is assumed that the total current trough the membrane is carried by ions only, as expressed in Eq. (1.5). The contribute $\sum_i z_i J_i$ is equal to 62.8 eq/(s cm^2) in the first interval, 21.3 eq/(s cm^2) in the second interval and 9.9 eq/(s cm^2) in the third interval.

The reduction in ionic transport can be also observed as an increase in the membrane resistance; Figure 3.4 shows the limiting resistance versus the desalination rate at two different linear flow velocities.

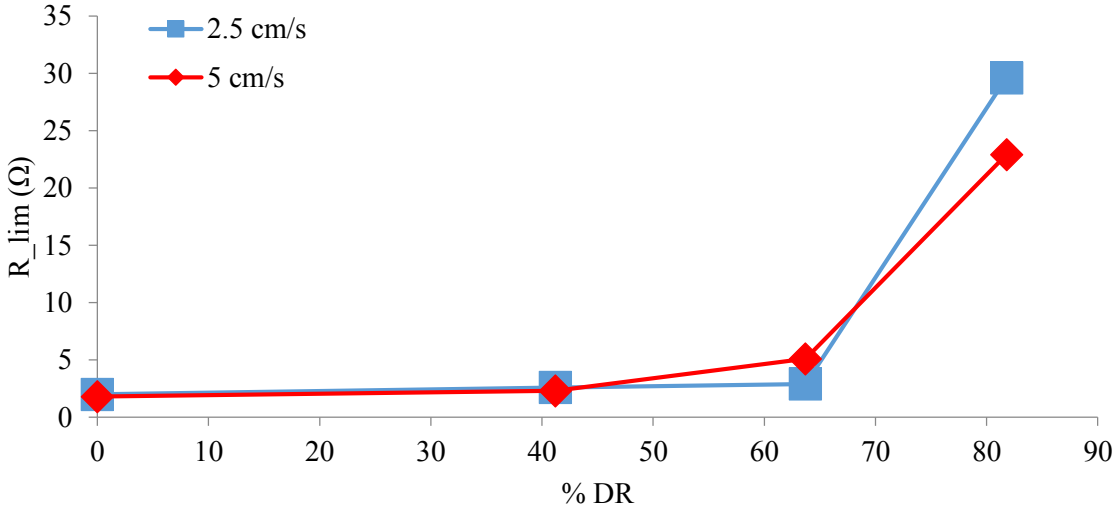

Figure 3.4. *Experimental R_{lim} determined at different linear flow velocities versus the desalination rate during the desalination experiment.*

The most critical phenomenon influencing the desalination of regenerate wastewater is the depletion of chloride ions as identified in paragraph §3.3.2. The extremely high value of limiting resistance reached at the end of the process is also caused by fouling on membrane surface which can be reduced in an EDR industrial plant.

3.3.2 Separation of organic and inorganic substances

The results of concentration analysis show that Cl^-, SO_4^{2-} and Na^+ during the entire process are separated at 97.9, 80.0 and 75.0 %, while the TOC separation is less (13.4 %).

The concentrations of Ca^{2+} and Mg^{2+} in the diluate solution are negligible (<0.004 eq/l).

A comparison of desalination profiles between the different ions and TOC is presented in Figure 3.5. A sharp changing in slope is evident considering the sulphate profile between the first interval and the remaining process. This is probably due to the membrane fouling which obstructs the transport of bigger hydrated ions. In a real industrial process EDR operating mode is applied and the fouling of the membrane is definitely less relevant and the desalination

profiles of ions might be different. The unidirectional ED was used because the mixing effect caused by EDR makes a desalination process in a lab-scale system more difficult.

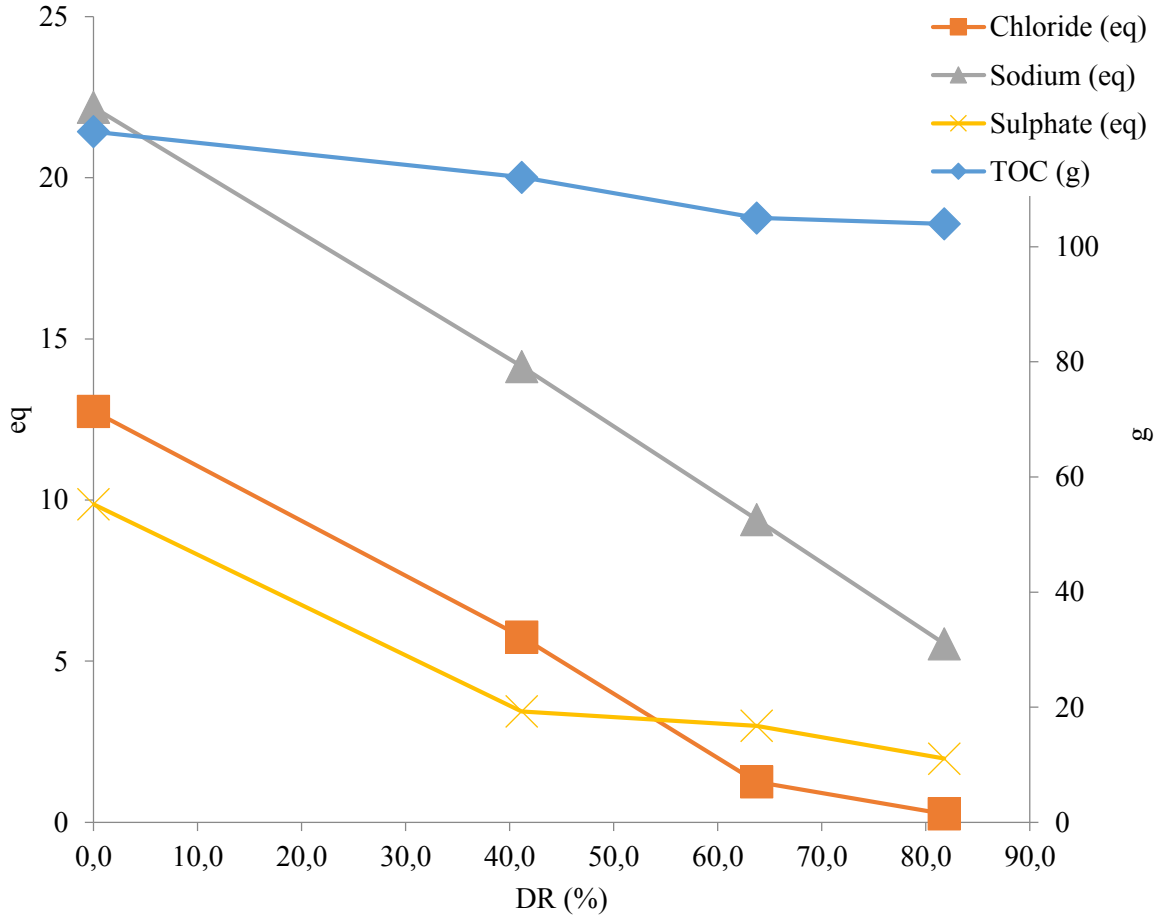

Figure 3.5. *Total equivalents of Cl^-, Na^+, SO_4^{2-} and grams of C (from TOC) contained in the diluate solution versus the desalination rate of the process.*

However, the target of the industrial treatment combining deionization by ion-exchange resins and ED process was reached; in fact it was possible to transfer almost all the chloride ions from diluate to the concentrate solution retaining especially TOC in the diluate.

3.3.3 Water transport due to osmosis and electro-osmosis

The relative desalination rates for each interval are 41.2%, 22.6% and 18.0%; while the corresponding durations are 12.9, 32.4 and 40.7 hours, respectively. The first interval can be considered sufficiently short to neglect the hydraulic permeability of the membranes and therefore the osmotic water flux.

Knowing the variation of volume of diluate solution, the membrane surface area, the duration and the concentrations of salts at the beginning and at the end of the first interval the water transport number of this interval can be calculated. The obtained value (6.1) is applied to

calculate the electro-osmotic flux in the second and third interval, hypothesizing that the water transport number doesn't change during the desalination process. Actually, it's not excluded that the adsorption of organic matter on the membrane surface significantly change the hydraulic permeability of the membranes.

The difference between the total water flux from the diluate to the concentrate and the calculated electro-osmotic flux provides the flux of water due to the osmosis.

Figure 3.6 compares the electro-osmotic and osmotic contributes to the water flux during the desalination process subdivided in the three intervals.

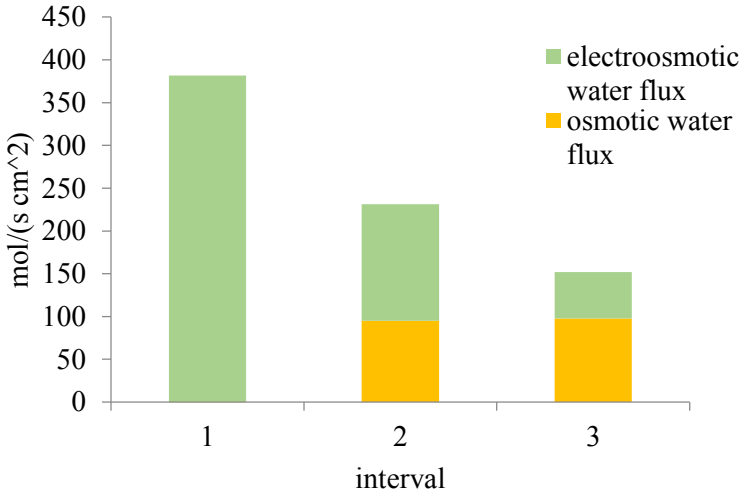

Figure 3.6. *Subdivision of water flux from diluate to the concentrate solution considering electro-osmotic and osmotic fluxes in the 3 intervals of the process.*

Under the hypothesis presented before the contribution due to the osmotic flux becomes very relevant in the second and in the third interval.

3.4 Long exposure experiment: results and discussion

This experiment aims at establishing critical conditions for the membrane's fouling in order to access the reliability of the reverse polarity operating mode.

Figure 3.9 shows the profile of R_{lim} versus the time. The vertical lines represent the reduction in terms of limiting resistance due to simultaneous execution of mixing and reversing polarity. The use of a limited membrane area allows to observe the effects of membrane fouling in a short time; in fact R_{lim} results doubled in few hours.

The EDR operating mode, in this experiment, generally allows to restore the original resistance of the membrane, although at the end R_{lim} is slightly increased and in the last 79 hours it doesn't fall below the value of 2.2 Ω.

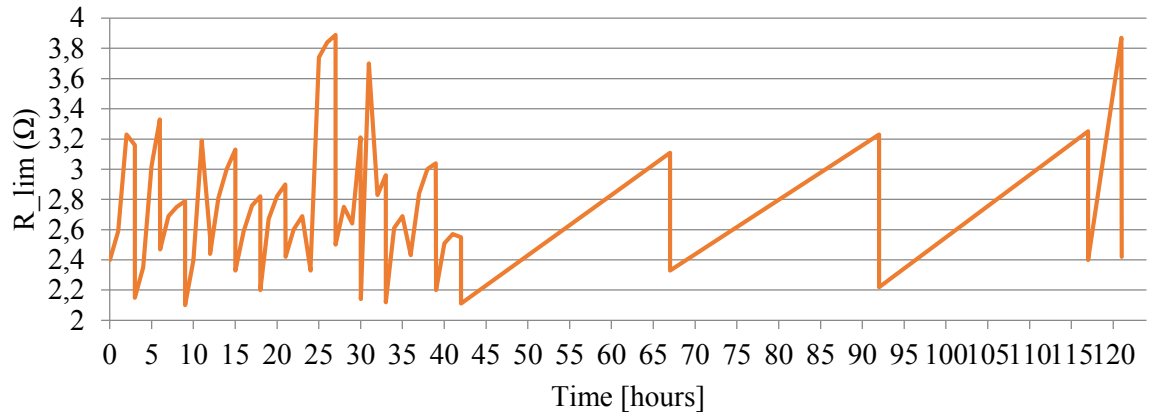

Figure 3.9. *Limiting resistance profile during the long exposure experiment.*

The majority of pollutants in regenerate wastewater are negatively charged and are therefore expected to significantly affect the AEM. The dark coloring of the AEMs at the end of all the experiments confirms the correctness of this assumption. Figure 3.10 shows the different colorations of a CEM and an AEM when all the experiments were completed.

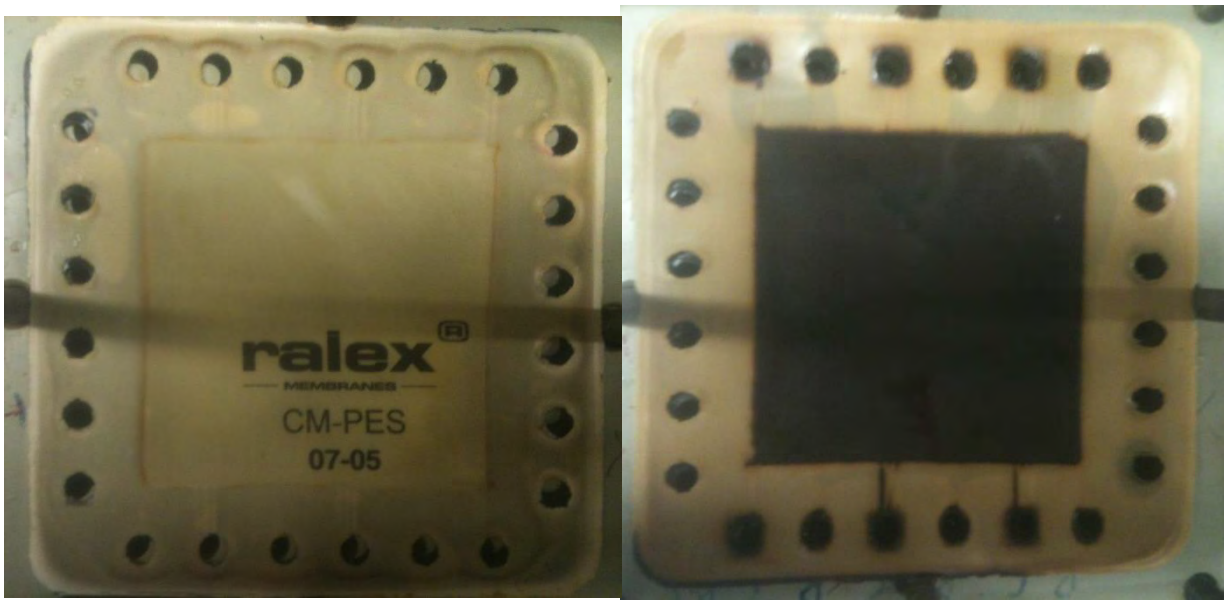

Figure 3.10. *Picture of a CEM (on the left) and an AEM (on the right) at the end of all experiments described in this chapter.*

The final aspect of the CEMs leads to assume a longer life cycle for these membranes than the AEMs. However, inorganic salts deposition must be considered and the erosion of membranes can lead to a hole with drastic consequences to the desalination process.

3.5 Reference experiments: results and discussion

Five reference experiments were performed in order to evaluate the effect of fouling in between several experiments that were carried out with the same stack. Figure 3.11 reports the variation on limiting resistance obtained before and after the desalination experiment, after the short reversal operation, after the long exposure experiment and after the caustic cleaning.
It's noticeable that after a long exposure of the membranes to the fouling the reversal operation mode is not able to restore the original membranes' resistance, in fact, after the long exposure experiment, the limiting resistance (5.6 Ω) is much higher than the R_{lim} after the cleaning of the membranes with diluted NaOH solution (4.1 Ω).

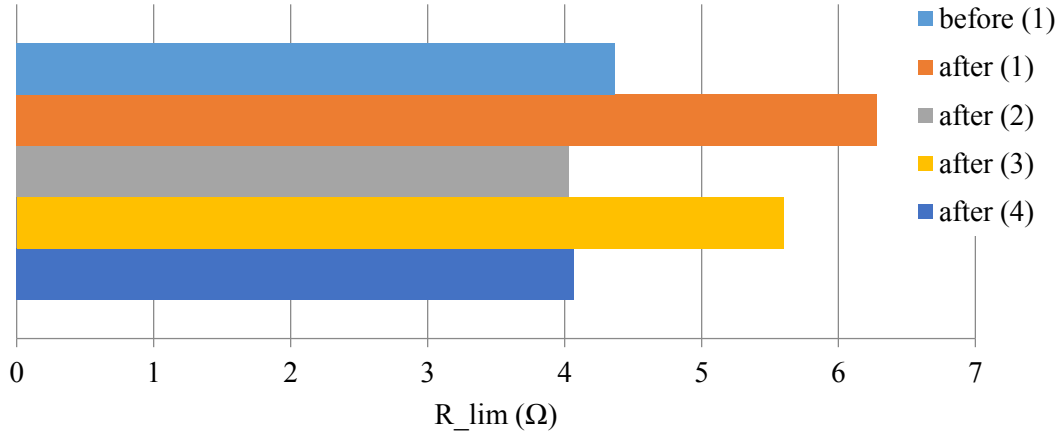

Figure 3.11. *Limiting resistance calculated in reference experiments before and after the desalination experiment (1), after the short reversal operation (2), after the long exposure experiment (3) and after the caustic cleaning (4).*

Reference experiments highlight the increase in membrane resistance much more than the calculation of R_{lim} during the long exposure experiment, meaning that the required voltage drop imposed when LCD occurs is higher when the NaCl aqueous solution is used as diluate, as opposed to the regenerate wastewater. That can be explained considering that the fouling on membrane surface affects much more the ionic transport through the membranes when there are less charged particles to transfer.

3.6 Calculation of an industrial plant and its economical evaluations

From the concentration analysis of the sample, it emerged that at 63% of desalination, 90% of the chloride was separated. According to what above written, this section shows the main results obtained from the calculation of an ED plant suitable to desalt at 63% a regenerate wastewater with a total salinity of 2.24 keq/m^3. The concentration of diluate at the outlet is 0.83 keq/m^3.

To determine an advantageous number of cells to insert in a single stack a desalination rate of 6% is imposed. This value corresponds to a desalination process in a first stack supposing the stack includes 214 cells. In this way the required process path length is exactly equal to the length available in the industrial stack. This condition represents a credible situation to study the profile of global costs on varying of the imposed linear flow velocity. The required low desalination rate avoids an iterative and complex calculation.

Figure 3.7*a* shows the decrease in electrical power consumption and the increase in the required membrane area surface with an increase in the number of cells from 50 to 250. This interval corresponds to the range of linear flow velocity 85 - 17 cm/s.

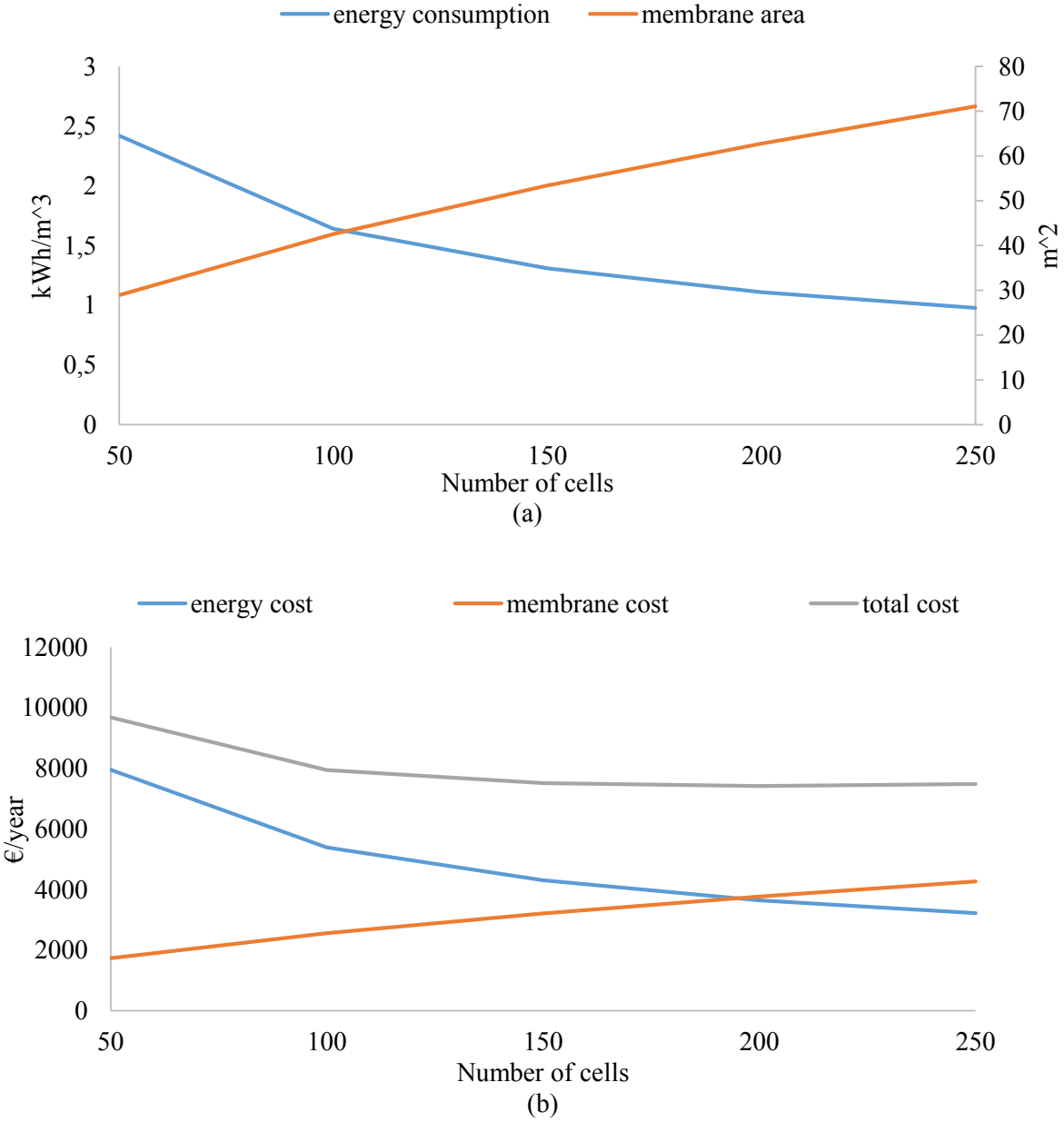

Figure 3.7. *Figure (a) shows the electric energy consumption for desalination and the required membrane area surface versus the number of cells. In figure (b) the annual costs for the membrane replacement and for energy consumption and the global cost are presented*

In Figure 3.7*b* the curves are expressed in economic terms considering as energy price and membrane price 0.09 €/kWh and 60 €/m^2, respectively. To compare these different magnitudes, the annual costs are considered and an annual replacement of the membranes is supposed. The grey curve represents the sum of the membrane and electric energy costs. This presents a minimum in correspondence to a number of cells equals to 200. The following calculations consider 200 as the number of cells for each stack, corresponding to a linear flow velocity of 0.021 m/s.

Each stack will present a total membrane area of 60.9 m^2. The global desalination rate of 63% is reached through the use of 13 consecutive stacks in which the concentrate solution is concentrated from 0.91 to 2.37 keq/m^3.

While in each stack the flows of diluate and concentrate streams are co-current, on the global plant the concentrate stream is set counter-current compared to the diluate. In fact, in order to maintain the same concentration gradient between concentrate and diluate, the concentrate solution moves from the last stack to the first one.

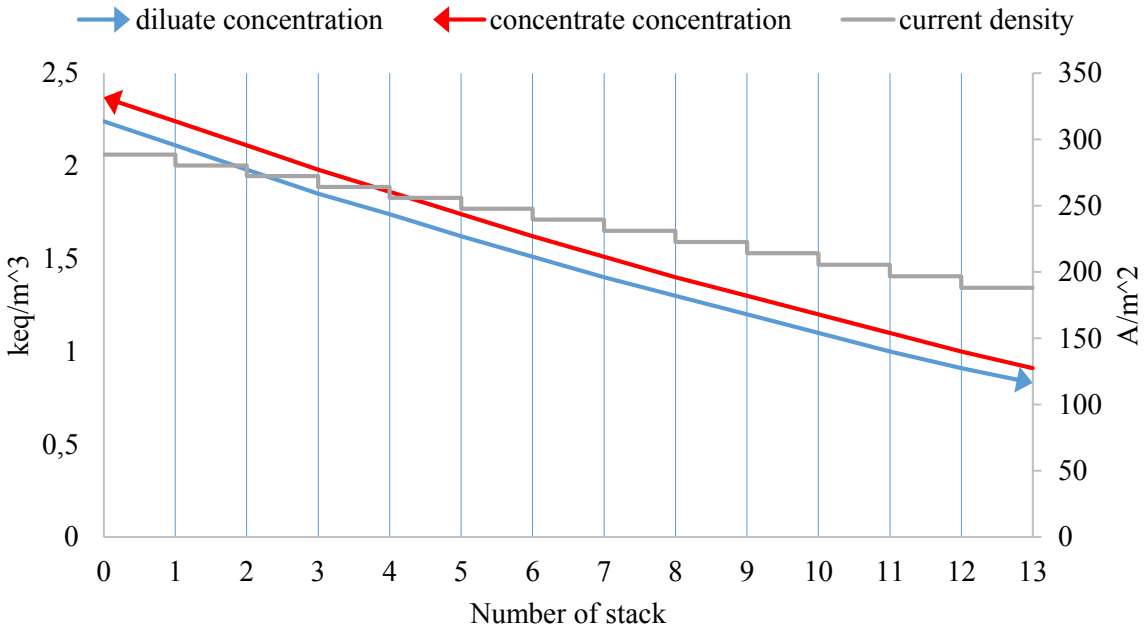

Figure 3.8. *Diluate concentration, concentrate concentration and current density at the inlet and the outlet of each stack.*

The curves in Figure 3.8 represent the profiles of concentration of concentrate and diluate stream versus the number of stacks. The current density applied in each stack is lower compared to the previous one because the imposed current density as expressed in Eq. (1.25) is proportional to the outlet concentration of diluate stream for each stack. Consequently, also the required potential drop and the electrical energy consumption per stack decreases from the first to the 13th stack. The main characteristics of the system for each stack are reported in Table 3.3.

Table 3.3. *Main characteristics regarding each stack calculated using an iterative procedure.*

Number of stack	Concentration diluate outlet, C^d	Total desalination rate	Total current through stack, I	Potential drop per stack, U	Electrical power consumption, E_{spec}
	keq/m^3	%	A	V	kWh/m^3
1	2.24	0.06	87.83	51.27	1.08
2	2.11	0.12	85.38	50.43	1.03
3	1.98	0.17	82.92	49.61	0.99
4	1.85	0.22	80.44	48.80	0.94
5	1.74	0.28	77.94	48.00	0.90
6	1.62	0.33	75.43	47.23	0.85
7	1.51	0.38	72.9	46.47	0.81
8	1.4	0.42	70.35	45.74	0.77
9	1.30	0.46	67.77	45.04	0.73
10	1.20	0.51	65.18	44.37	0.69
11	1.10	0.55	62.57	43.73	0.66
12	1.00	0.59	59.93	43.13	0.62
13	0.91	0.63	57.26	42.61	0.59

Considering a water transport number equal to 6.1, for this specific industrial plant the water passing from the diluate to the concentrate solution due to the water flux in the hydration shell of the ions is estimated to be in the order of 15.49 m^3/day. This unwanted water flux cannot be neglected and a recycling system must be introduced to guarantee identical linear flow velocities in the diluate and concentrate cells. The osmotic water flux from the diluate to the concentration can be omitted because the industrial process is much faster than the batch experiment carried out using the pilot installation.

An approximate economical evaluation for this specific ED plant is shown below. Data on capital and operation costs were collected from various reliable sources.

Table 3.4. *Main prices and cost items used in the economical evaluation of the industrial plan.t*

Energy price	€/kWh	0.09
Membrane price	€/m^2	60
Stack price	€	8000
Pump price	€	4000
Power source price	€	5000
Installation cost (full auto)	€	60000
Electricity for desalination	€/year	35018
Total construction cost	€	281000
Membrane cost	€	47502
Personnel Cost	€/year	25000

The total annual cost of an EDR system is the sum of the following three items: (a) electricity for desalination, (b) total construction costs, (c) membrane cost and (d) personnel cost. Each of these items is estimated as follows:

(a) The evaluated energy cost derives from the sum of the electrical power consumption for each stack previously estimated.

(b) The total construction cost includes the costs for a stack, an energy supply and a pump multiplied by the number of stacks in the plant. The installation cost is considered as well, and it includes the expenses for automation and piping.

For the calculation of annual costs a useful life of 10 years is considered, so total construction costs are depreciated over 10 years.

(c) The cost of membranes is calculated expecting an annual replacement of the membranes.

(d) The annual personnel cost is estimated to be 25000 €.

The main prices and cost items are presented in Table 3.4.

A total annual cost equal to 135620 €/year was obtained. Considering a water capacity of the plant equal to 100 m^3/day the resulting cost for each cubic meter of treated regenerate wastewater is approximately 3.72 €.

3.7 Conclusions

An ED plant to couple to a deionization by ion-exchange resins system for the production of drinkable water is studied. Lab experiments were carried out to elucidate the most relevant design parameters like LCD, membrane resistance, organic and inorganic substances separation rate and water transport number. Particular attention was paid to the effect of membrane fouling caused by NOM and the efficiencies of EDR operating mode and chemical cleaning were compared.

An industrial ED plant was designed following the procedure proposed by Lee. The input parameters consist of the values of current density, potential drop, electrical power consummation and diluate's outlet concentration are fixed in each stack.

A global desalination rate of 63% is reached through the use of 13 consecutive stacks in an EDR system with a water capacity of 100 m^3/day. Various cost items are evaluated in this chapter. The total cost turned out to be 3.72 € per cubic meter of treated water.

Reference experiments revealed that EDR operating mode can't prevent the increase in membrane resistance after a long exposure of NOM. Using this specific wastewater, the reversal operation is a short-term solution for the fouling; only a chemical treatment can restore the original membrane's resistance after a long run fouling process.

In an industrial plant the process of desalination is noticeably fast compared with the lab-scale experiments. Therefore, the water flux from diluate channels to concentrate channels can be entirely considered as electro-osmotic flux which was estimated as 15.5% of the water capacity of the entire plant

.

Chapter 4
Investigation on Continuous Electrodeionization

In this Chapter, CEDI and ED operations are compared using a same lab-scale stack geometry. To achieve this, two different kinds of experiment are carried out. The first procedure consists on calculation of I_{lim} and R_{lim} at different salt concentrations when the mixing operating mode is applied. The second procedure consists on calculation of current efficiency and energy consumption during ED and CEDI desalination experiments. In addition, the removal of NOM during CEDI is reviewed in this study.

4.1 Introduction

The demand for demineralized water will continue to grow with the industrial development. CEDI is a novel hybrid separation process that incorporates ion-exchange resin beads within an ED stack. This process is considered an environment-friendly technology and it's known as an attractive alternative for large scale ultrapure water production. CEDI has also shown great potential to be applied in a number of different applications, such as wastewater treatment, recovery of organic acids and heavy metals and concentration radioactive waste.

In a CEDI stack CEMs and AEMs are placed between the electrodes like in an ED system. Generally, the diluate compartments are filled with ion-exchange resin beads. The packed beads which are immersed in diluted solution reduce the electrical resistance and polarization phenomena. Hence, the ionic transport under an applied electric field is enhanced.

Different configurations in diluate cells are possible, such as intimately mixed AERs and CERs or separate sections of ion exchange resins (Bouhidel and Lakehal, 2006). During CEDI operation, water dissociation reaction occurs on the bead surface producing protons and hydroxide ions. Produced H^+ and OH^- ions continuously replace the adsorbed ions on the beads surface, therefore a chemical regeneration is not required. When only AERs are used the water splitting gets a place between the CEMs and the resins. But if the diluate cells are filled with mixed AERs and CERs, the quantity of regeneration sites are increased, allowing an improved efficiency (Meng *et al.*, 2004).

An excessive production of H^+ and OH^- ions can lead to pH fluctuations and inefficient use of electric current (Ganzi et al., 1987). Water dissociation becomes dominant especially at a higher current density than the LCD. To minimize these disadvantages it is suggested to operate below the LCD.

CEDI system presents other disadvantages such as packing difficulty of the resin beads, reduction of the active surface area due to movement of the resins during operation and decreasing free flow in the cells. Nevertheless, comparing with an ED process, a CEDI plant can generally treat low concentration solution with higher efficiency and higher removal rate.

4.2 Materials and methods

4.2.1 System components and design aspects

The experimental set-up consist of six compartment cell, three separate liquid lines, power supplier and measurement instrumentation similar to that used during experiments described in Chapter 3. The stack has three diluate compartments, three concentrate compartments and two compartments for electrolyte solution, as shown in Figure 4.1.

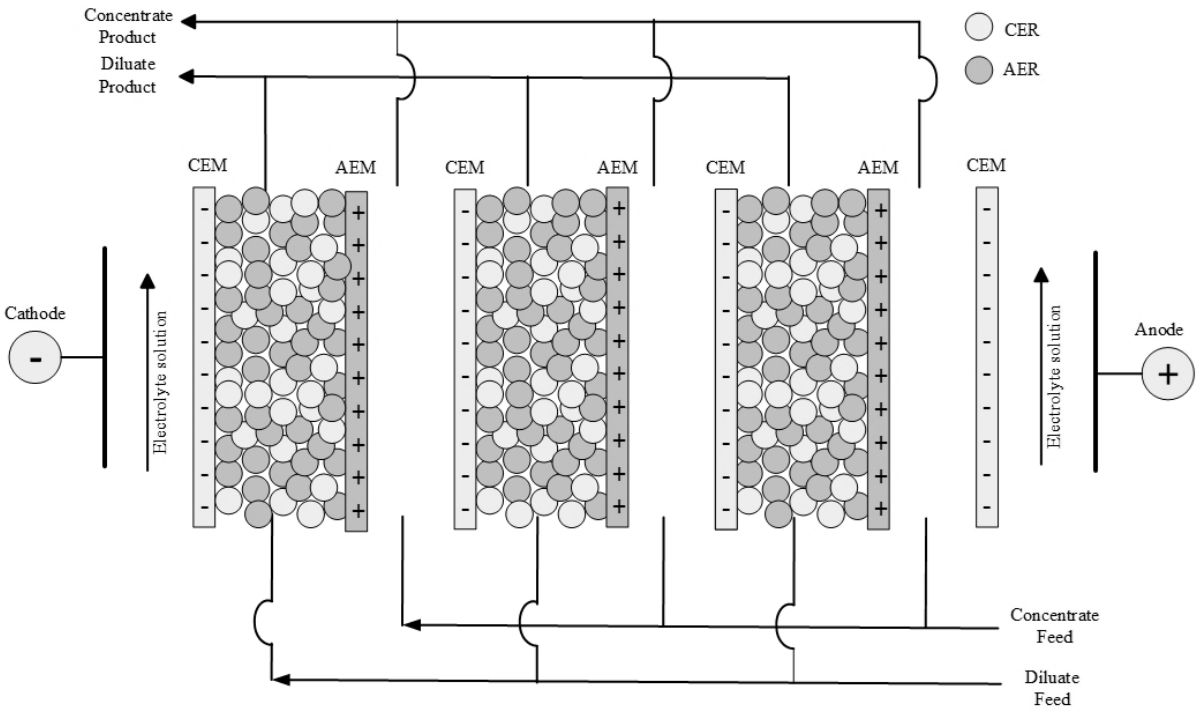

Figure 4.1. *Schematic illustration of the CEDI lab-scale stack. The ED stack does not contain the resin beads but presents the same structure and geometry.*

Heterogeneous CEMs and AEMs Ralex® are used and their properties are listed in Table 2.1. The effective surface area of each membrane was 100 cm^2. The internal spacer was 2 mm and a double pacer is placed in the diluate compartments. Thus, the thickness of diluate cell (4 mm) is two times the concentrate cell thickness. A plastic net is placed in each compartment, including electrolyte solution compartments, to guarantee good mixing. Diluate cells present

also a very fine plastic frame, as shown in Figure 4.2. The net and the frame block the resin beads within the compartments, avoiding their discharge from the stack.

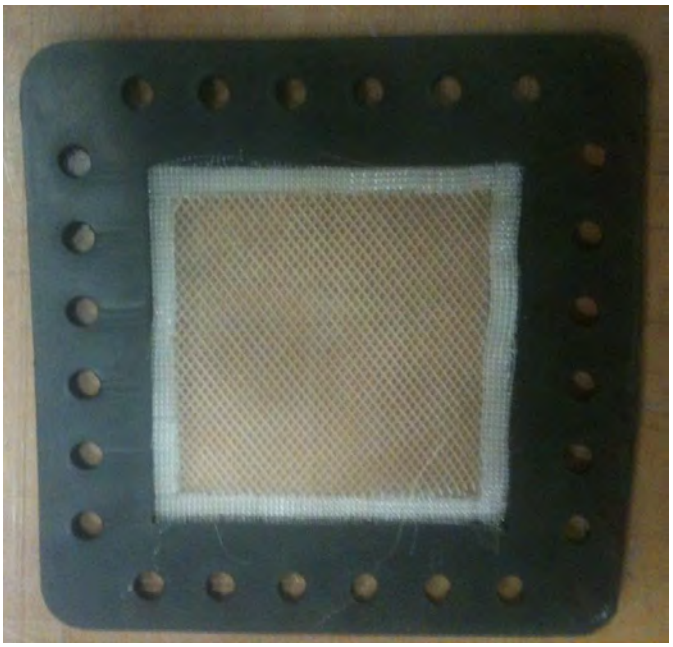

Figure 4.2. *Picture of the spacer, plastic net and fine plastic frame.*

Table 4.1. *Properties of macroporous ion-exchange resins Ralex® produced by Lenntech (Germany).*

Property	**Unit of measurement**	**CER**	**AER**
Ionic form as shipped		H^+	Cl^-
Functional group		sulfonic acid	Quaternary amine, type I
Matrix		crosslinked polystyrene	crosslinked polystyrene
Appearance		grey, opaque	beige, opaque
Uniformity Coefficient		1.1	1.1
Mean bead size	mm	0.67 (+/- 0.05)	0.62 (+/- 0.05)
Density	g/l	1180	1060
Water retention	wt. %	56 - 60	60 - 65
Volume change	max. vol. %	8	22
Operating temperature	max. °C	120	70
Operating pH range		0 - 14	0 - 12
Pressure drop	max. kPa	300	300
Regenerant		HCl, H_2SO_4	NaOH

Diluate compartments can remain empty or be filled with the resin beads. Macroporous ion-exchange resins with beads of uniform size based on a styrene-divinylbenzene copolymer are used. The main properties of Lewatit® MonoPlus MP 500 AERs and Lewatit® MonoPlus SP 112 H CERs are reported in Table 4.1.
The AERs and CERs beads are mixed with a volume ration of 30:70 and a sort of packing bed is formed in diluate cells. The electrolyte solution is a Na_2SO_4 aqueous solution 1.12 M and the volume contained in the respective tank is 12 l.

4.2.2 Ion-exchange resins pre-treatment

Ion-exchange resins that are immersed in a concentrate salt solution give rise to chemical reactions which change electrochemical properties of resins and solution. In order to maintain the same conditions during the CEDI operation, before to insert the beads in the stack a pre-treatment of the resins is required. The AERs and CERs beads are immersed in a 1 M NaCl solution for 30 min. Afterwards the resins are rinsed with deionized water for 5 min and dried. Following this pre-treatment the resins are prepared to be inserted in the diluate compartments.

4.2.3 Determination of correct flow rate of diluate and concentrate solutions

CEDI process guarantees good performance when the concentrate and diluate cells have identical flow conditions. During a CEDI operations resin beads can move because of the gravity and diluate flow effect. Moreover, resin beads' volume depend highly on their degree of wetting. Hence, it is rather complicated to calculate a priori the exact flow rate to apply to the pump to obtain a certain linear velocity in the cells. The correct flow rate of the diluate is obtained applying an empirical procedure.
The diluate compartments are filled with resin beads. A 0.1 M NaCl aqueous solution flows in both diluate and concentrate circuits carrying out the mixing operating mode. The linear flow velocity of concentrate solution within is fixed as 5 cm/s corresponding to 108 l/h flow rate. Different current - voltage curves are obtained changing the flow rate of diluate stream, as shown in Figure 4.3.

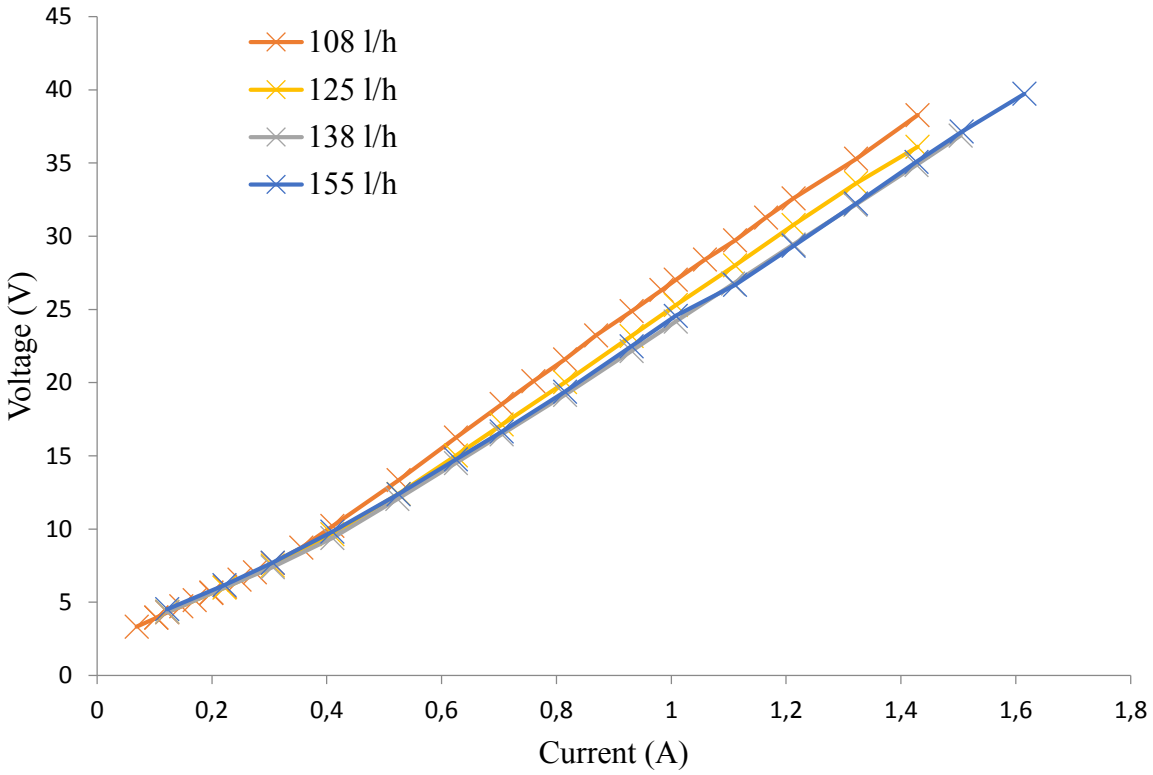

Figure 4.3. *Profiles of voltage versus current at different flow rates for diluate stream in the CEDI stack (3 cell pairs, cell length and width: 10 cm, concentrate cell thickness: 2 mm, diluate cell thickness: 4 mm). Both diluate and concentrate solutions are NaCl solutions 0.1M. The diluate compartments are filled with CERs and AERs with a volume ration of 30:70.*

By increased flow rates the corresponding current-voltage curves decrease down to a level to which an additional increase of flow rate leads to inversion of the trend. The lowest profile identifies the appropriate flow rate of diluate. Thus138 l/h is the flow rate which guarantees the lowest voltage drop on equal applied current between the two electrodes.

When an ED experiment is carried out the diluate chambers are empty and the flow rate of diluate stream is equal to 216 l/h so that the corresponding linear velocity is identical to that of concentrate.

4.2.4 Energy consumption and current efficiency calculations

Electric conductivity σ is a measure of the ability of water to pass the electrical current. Total Dissolved Solids (TDS) is a measure of the total ions in solution. In dilute solution, *TDS* and σ are reasonable comparable. *TDS* is generally expressed in mg/l and can be calculated from conductivity using the following equation (Juhasz and Marsh, 2009):

$$TDS = 5115.3\,\sigma \quad . \tag{4.1}$$

This expression can be used only for salt solutions and it does not apply to wastewater. In this study, a NaCl aqueous solution is used and the *TSD* of diluate compartment is estimated.
Consequently, the mass in kilo-equivalents of ions removed in diluate compartments is given by:

$$\Delta m_D = \frac{(TDS^{fd} - TDS^{d})\,V_D}{MW_{NaCl}}\,10^{-6} \quad ; \tag{4.2}$$

where Δm (keq) represents the total ions removed, V (l) is the volume of the diluate solution and MW_{NaCl} is the molar weight of NaCl (58.44 kg/kmol). The subscript D refers to the diluate compartment.
The energy consumption per unit removed ions $\dot{E}$ is obtained applying the following formula:

$$\dot{E} = \frac{\sum_h V_h I_h \Delta t_h}{\Delta m_D}\,10^{-6} \quad ; \tag{4.3}$$

where $\dot{E}$ is expressed in kJ/eq, Δt_h is the interval of time (10 s) which separates each voltage (V_h) and current (I_h) measurement from the followings; the subscript h identifies the specific interval of time. The sum of all Δt_h gives the total duration of the experiment and will be simply indicated as Δt (s).
The current efficiency is the ratio of the ionic current to the amount of electric current actually consumed. The ionic current is the amount of electric current, in amperes, theoretically required to yield a given quantity of ions in an ED or CEDI process. The percentage value of current efficiency Φ is given by the following expression:

$$\Phi = \frac{IC}{\bar{I}\,N_{cp}} \times 100 \quad ; \tag{4.4}$$

where IC is the ionic current, $\bar{I}$ is the average current of a cell pair; both IC and $\bar{I}$ are expressed in amperes. Finally, the subscript *cp* refers to the cell pair.

4.2.5 Procedure of mixed solutions and desalination experiments

Experiments were carried out using the flow rates of concentrate and diluate defined in §4.2.3, while the flow rate of electrolyte solution is still 100 l/h. . At the start of each experiment, both diluate and concentrate tanks are initially filled up with 12 l of solution.

ED and CEDI processes are compared carrying out two different types of experiments. The first procedure consists on calculation of I_{lim} and R_{lim}at different salt concentrations. The mixing operating mode is applied, i.e. the same solution flows in both diluate and concentrate cells. Different NaCl solutions are prepared at the following salt concentrations: 0.001 M, 0.01 M, 0.1 M and 1 M. Current - voltage graph and Cowan plot are drawn increasing stepwise the voltage drop and recording the correspondent current passing across the stack. I_{lim} and R_{lim} are identified using the 4 NaCl solutions in presence of resin beads (CEDI operation), and without the resins (ED operation).

The second procedure consists on calculation of current efficiency and energy consumption of ED and CEDI operations. The desalination experiments are carried out using two different NaCl solutions: the initial concentrations of diluate and concentrate are listed in Table 4.2.

Table 4.2. *NaCl concentrations of initial diluate and concentrate solutions concerning desalination experiments.*

C^{fd} (keq/m^3)	C^{fc} (keq/m^3)
0.01	0.051
0.1	0.513

A batch type operation and a unidirectional operating mode are applied. The ED and CEDI desalination experiments are carried out at the 70% of I_{lim} which is periodically obtained from Cowan plots. The experiments are stopped when the 30-50% of desalination rate is reached. The desalination rate is calculated by Eq. (3.2).

The desalination procedure is followed for a last experiment. Initially the diluate and concentrate solutions are the regenerate wastewater and a 2 M NaCl solution, respectively. The regenerate's characteristics are described in §3.2.1.

During ED and CEDI operations it is tried to combine a 7% of desalination with an operation current density equal to 70% of the i_{lim}. Sample are taken at the start and at the end of experiments treating wastewater to analyse the content of TOC.

CEDI and ED desalination experiments are compared calculating the energy consumption per unit removed ions and the current efficiency, according to the procedure described in §4.2.4.

4.3 Results and discussion

4.3.1 Current-Voltage curve characteristics

Current - voltage relations were obtained by measuring the current passing between the two electrodes for a step-wise increase in applied global voltage of the stack. At the beginning of CEDI, the current raises linearly with the increase in the applied voltage. After the current exceeds the limiting current, the curve slop starts to decrease. Therefore, I_{lim} is evaluated with the tangents crossing in the graph that represents the current versus the voltage, as shown in Figure 4.4.

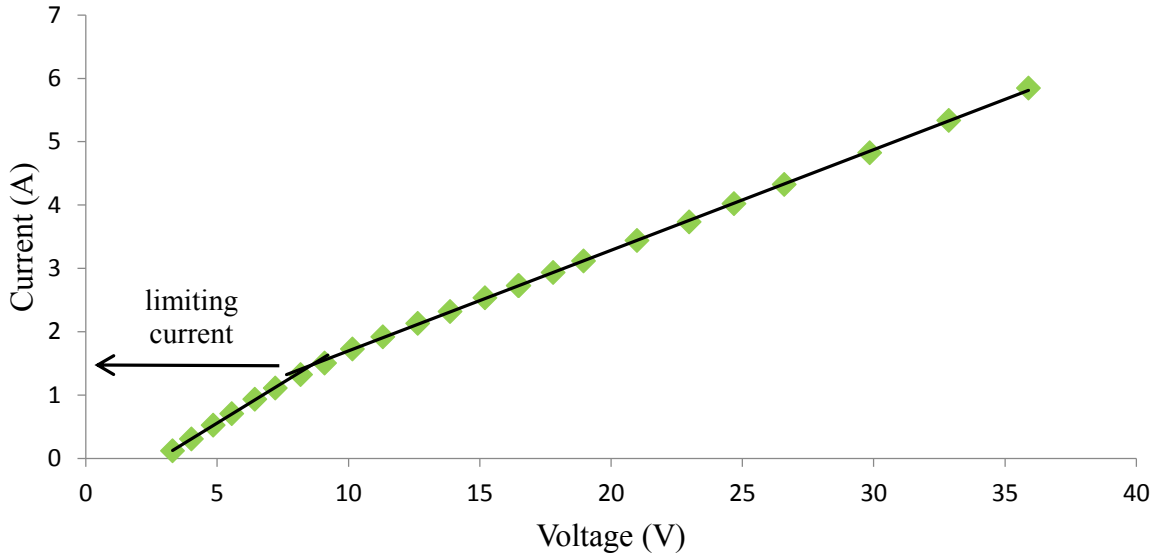

Figure 4.4. *Experimental current versus applied voltage in the CEDI stack (3 cell pairs, cell length and width: 10cm, concentrate cell thickness: 2mm, diluate cell thickness: 4mm). Diluate are NaCl aqueous solution with 0.01 and 0.051 M, respectively. The flow rates of diluate and concentrate are 138 and 108 l/h, respectively. The diluate compartments are filled with CERs and AERs with a volume ration of 30:70.*

In addition, I_{lim} was confirmed by the resistance versus 1/current plot, as discussed in §2.2. When the LCD is exceeded, the increase in resistance in a CEDI operation is mainly due to the water splitting. A requirement in a CEDI process is that water dissociation takes place at the resin beads surface in order to regenerate both AERs and CERs. However, the production of H^+ and OH^- ions at 70% I_{lim} seems to be appropriate to guarantee the continuous regeneration of resins. Thus, the value of 30% below the I_{lim} is selected for both ED and CEDI desalination experiments.

4.3.2 Limiting current density and limiting resistance

Flow condition and stack geometry being equal, CEDI operation allows to increase I_{lim} at diluate's concentration in the range 0.001 - 1 M. Figure 4.5 shows a comparison of obtained I_{lim} between ED and CEDI experiments.

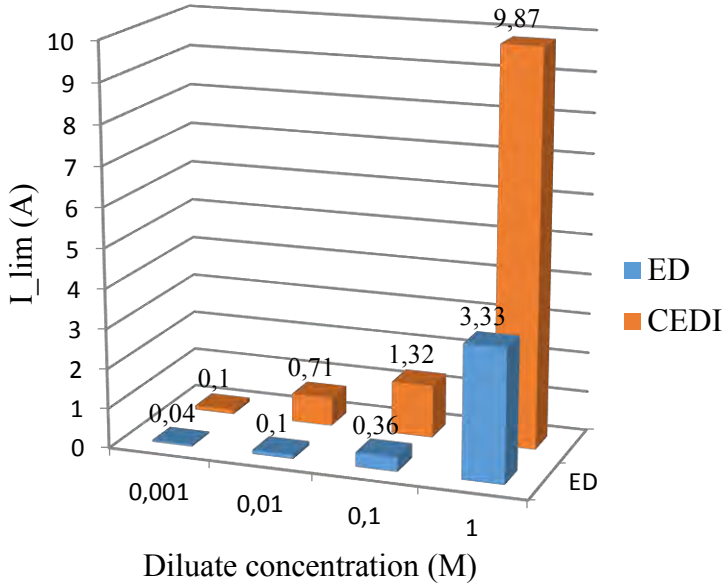

Figure 4.5. *Limiting resistance at different diluate concentrations comparing ED and CEDI processes using the same stack geometry.*

The introduction of resins beads leads to an increase higher than the 150% of the I_{lim} at each investigated concentration value. The highest increase (610%) is obtained at 0.01M concentration. In industry, a very high limiting current density permits to guarantee elevate ionic transports avoiding losses of energy utilization and drastic pH-values shifts.

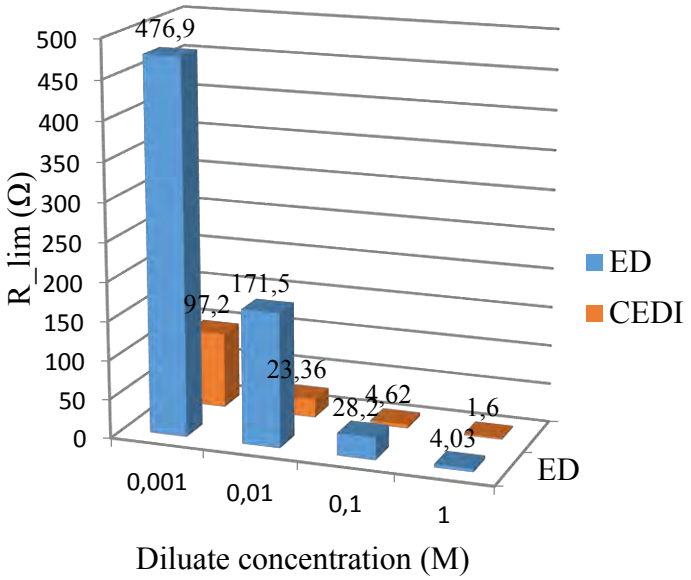

Figure 4.6. *Limiting resistance at different diluate concentrations comparing ED and CEDI processes using the same stack geometry.*

As a consequence of the increase in I_{lim}, the limiting resistance is decreased when diluate compartments are filled with CERs and AERs beads. The obtained R_{lim} for ED and CEDI operations are reported in Figure 4.6. The highest R_{lim} reductions are obtained for 0.001 M and 0.01 M, respectively 80% and 87%. A lower resistance implies a reduction in energy consumption on equal current passing through the stack. Obviously, the cost of resins must be evaluated within total annual costs of an industrial plant. Moreover, in an ED stack the thickness of diluate's compartments can be reduced, since they don't contain the packing bed of resin beads. This aspect has a direct effect on the energy consumption in an ED process, as expressed by Eq. (1.34).

4.3.3 Desalination of NaCl solutions

Considering the desalination experiments, the desalination rate and the duration of operation don't give any indications on efficiency of the process. In fact an identical desalination rate can be reached rapidly with a high imposed voltage drop or slowly using a lower voltage drop across the stack. On the other hand, $\dot{E}$ and Φ allow to compare CEDI and ED operations revealing the efficiency of the process in terms of energy and current.
Table 4.3 resumes experiment duration, desalination rate, energy consumption and current efficiency for each desalination experiment. Data have been obtained using different concentration of NaCl in diluate solutions.

Table 4.3. *Results of desalination experiments with a NaCl solution as diluate at different concentrations, comparing ED and CEDI operations.*

Process	C^{fd} (keq/m^3)	Experiment duration (min)	DR' (%)	$\dot{E}$ (kJ/eq)	Φ (%)
ED	0.01	327	33.14	564.6	56.27
CEDI	0.01	211	49.71	303.6	88.19
ED	0.1	565	38.74	487.4	51.52
CEDI	0.1	385	38.53	231.1	76.93

CEDI experiments are characterised by lower energy consumptions and higher current efficiencies than ED operations for both diluate concentrations. Hence, CEDI operation allows a better use of the imposed current and energy (substantially expressed as current multiplied by voltage drop multiplied by the time).

4.3.4 Behaviour of organic matter in Electrodeionization

In the ED desalination of regenerate wastewater the 7% of *DR'* was achieved in 333 minutes, consuming 426.0 kJ, while in the CEDI operation a period of 308 minutes was required to get. the same desalination rate. The energy consumption was 419.4 kJ.

The estimation of the efficiency of the ED end CEDI experiments using wastewater as diluate solution is quite complex and it was not considered in this study. In fact this specific wastewater contains several ionic components and conductivity data does not provide any information about the ion composition in the water.

Particular importance has to be paid to the removal rate of TOC during a CEDI desalination process. In fact, while in the ED experiment no trace of TOC was detected in the concentrate product, during the CEDI experiment the 7.23% of TOC removal rate was reached.

During the ED desalination experiment described in Chapter 3 the NOM was more or less retained in the diluate, as well. Evidently, the contact between the resin beads and the membranes improves the transfer of organic matter from concentrate to diluate.

The recovery of organic substances by CEDI is described in Ganzi *et al.* (1992), but the simultaneous separation of organic matter and salt ions should be in-depth analysed.

4.4 Conclusions and recommendations for the future

In this study CEDI operations achieved better performances than ED in terms of LCD and in terms of current efficiency and energy consumption, as well. At each investigated NaCl concentration in diluate solution, a significant increase in I_{lim}, and a consequent decrease in R_{lim}, in CEDI operation respect to ED were obtained.

In order to compare the two processes, a lab-scale stack was built with the same geometry of the ED plant and filling diluate compartments with resin beads. In particular, the thickness of dilute compartment was 2 times the concentrate cell thickness. The thickness of the cell influences the resistance of the entire stack. In industrial applications, an ED stack can present very thin cells reducing the energy consumption compared to CEDI. Therefore, an extended design study including economic analysis comparing CEDI and ED industrial plants should be conducted.

The increase in current efficiency and the reduction in energy consumption using a CEDI process respect to an ED process are highlighted carrying out desalination experiments at two different diluate's concentrations.

No particular variations in pH values of solutions were detected during CEDI desalination experiments applying a current equal to 70% of I_{lim}. Instead, other disadvantages were encountered, such as packing difficulty of the resin beads and a consequent decrease in free

flow in the cells during operation. Figure 4.7 shows the different distribution of resin beads found at the start and at the end of a CEDI experiment.

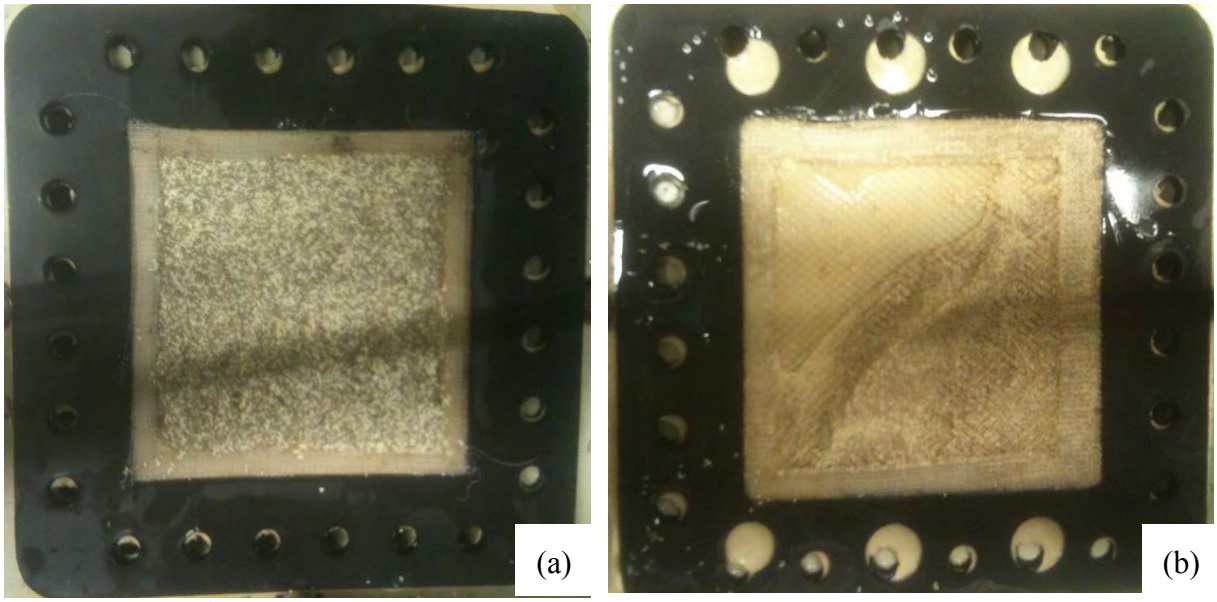

Figure 4.7. *Comparison between the section of a diluate compartment at the start (a) and at the end of a CEDI operation.*

The use of bigger and more manoeuvrable resin beads can theoretically solve these complications. Obviously, eventual changes in I_{lim}, R_{lim}, energy consumption and current efficiency have to be evaluated.

In this work an important capacity of CEDI in removing NOM was detected. In 1991 Katz *et al*. developed an Electrodeionization Reversal (EDIR) process. EDIR utilizes the periodic polarity reversal during the operation to reduce the membrane fouling. Further investigations on the treatment by EDIR of wastewater with high content of NOM should be conducted.

Conclusions

A reliable determination of the LCD is essential for designing and operation of an ED industrial plant. In this study, the LCD was empirically obtained by measuring the relationship between the applied current and the potential in an Electrodialysis pilot equipment. The coefficients of an equation describing LCD as a function of the diluate flow velocity and concentration were obtained by a multi-variables nonlinear regression. The empirical model developed allows to foresee the LCD value, when the operative conditions change. However, the estimated parameters are closely related to the structure of the stack adopted, especially the type of membranes, channel width and spacer geometry.

In this work, a design study of an EDR plant to couple to a deionization by ion-exchange resins system for the production of drinkable water was developed. Industrial regenerate wastewater was used to carry out batch experiments executing unidirectional and reversal operating modes. A reduced dimension stack allowed to investigate on water transport and membrane fouling, caused by NOM phenomena in a relatively short period. In a plant using 13 consecutive stacks to reach a desalination rate of 63%, the water flux was estimated as 15.5% of the water capacity of the entire plant. After a long run process EDR showed limitations in restore the original membrane's resistance. However, a caustic cleaning permits to overcome this drawback. An economical evaluation of a plant with a water capacity of 100 m^3/d was carried out, obtaining a total annual cost of 135620 €/year.

In the last section of this study ED and CEDI operations were compared in terms of I_{lim}, R_{lim}, removal rate and energy efficiency, using the same stack geometry. Generally, CEDI process allows better performances than ED, considering a wide range of diluate concentration. An interesting capacity of CEDI in NOM removal was detected. Further investigations on the treatment by EDIR of wastewater with high content of NOM should be conducted.

CEDI system presented also some disadvantages, such as reduction of the active surface area due to movement of the resins during operation and decreasing free flow in the cells. To mitigate the aforesaid disadvantages, the use of bigger and more manoeuvrable resin beads is suggested.

Nomenclature

$\dot{E}$ = energy consumption per unit removed ions (kJ/eq)
$\dot{F}$ = volume force (N/m^3)
$\bar{I}$ = average current (A)
$\dot{Q}$ = general electrolyte current source term (A/m^3)
$\dot{R}$ = ideal gas constant (8314 J/keq K)
$\dot{T}$ = temperature (K)
$\dot{a}$ = activity of a chemical species
$\tilde{k}$ = mass transfer coefficient (m/s)
$\tilde{n}$ = total number of measured variables
$\dot{p}$ = pressure term (Pa)
a = mathematical modelling parameter (A s^b/keq^n m^{2+b-3n})
A = membrane area surface (m^2)
A_{cross} = cross-sectional area of a cell (m^2)
b = mathematical modelling parameter
b' = physical modelling parameter
C = concentration (keq/m^3)
D = diffusion coefficient (m^2/s)
DR = desalination rate based on mass (%)
DR' = desalination rate based on conductivity (%)
E = energy consumption per unit product volume (J/m^3)
e_i = residual
F = Faraday constant (96485337 C/keq)
I = current (A)
i = current density (A/m^2)
IC = ionic current (A)
I_{lim} = limiting current (A/m^2)
i_{lim} = limiting current density (A/m^2)
J = flux (keq/m^{3}s)
k = number of variables
MW = molecular weight (kg/kmol)
n = mathematical modelling parameter
N = number of cells in stack
P = electric power (W)
p = number of parameters

Q = volumetric flow rare (m^3/s)
r = membrane area resistance ($\Omega\ m^2$)
R = resistance (Ω)
R_{lim} = limiting resistance (Ω)
s = safety factor
T = transport number
TDS = total dissolved solids (mg/l)
u = linear flow velocity (m/s)
U = voltage drop (V)
U_{lim} = limiting voltage (V)
V = volume (l)
W = weight (kg)
$wt\%$ = weight percent
x, y, z = directional coordinates
x_i = independent variable
Y = cell width (m)
y_i = dependent variable
z = species charge number
Δm = total ions removed (keq)
Δp = pressure drop (Pa)
Δt = interval of time (s)
Δz = thickness of boundary layer (m)

Greek letters

$\tilde{\beta}$ = generic parameter
$\tilde{\sigma}$ = standard error
α = volume flow rate correction term
β = shadow effect correction term
Δ = cell thickness (m)
Λ = equivalent conductivity ($S\ m^2/keq$)
μ = dynamic viscosity (Pa s)
μ_Y = nonlinear function
σ = electrical conductivity ($1/\Omega\ m$)
Φ = current efficiency
φ = electrical potential (V)
ψ = permselectivity

η = pump efficiency
ξ = current utilization

Superscripts

0 = intial time instant
am = anion-exchange membrane
b = bulk solution
c = concentrate
cm = cation-exchange membrane
d = diluate
fc = concentrate cell inlets
fd = diluate cell inlets
m = membrane
t = specific time instant
Δ = difference

Subscripts

av = average
c = cation
cell = cell in a stack
co = co-ion
cou = counter-ion
cp = cell pair
D = dliuate solution
dry = dry state
e = electrolyte solution
h = specific interval of time
i = specific component
k = number of variables
m = membrane
pump = pumping
s = salt solution
spec = specific
w = water

wet = wet state

Acronyms

AEM = Anion-Exchange Membrane
AER = Anion-Exchange Resin
CEDI = Continuous Electrodeionization
CEM = Cation-Exchange Membrane
CER = Cation-Exchange Resin
ED = Electrodialysis
EDIR = Electrodeionization Reversal
EDR = Electrodialysis Reversal
LCD = Limiting Current Density
MSE = Mean Square Errors
NOM = Natural Organic Matter
SCD = Secondary Current Distribution
SSE = Sum of Squares of Errors
TCD = Tertiary Current Distribution
TDS = Total Dissolved Solids
TOC = Total Organic Carbon

References

Banasiak, L. J. (2009). Removal of Inorganic and Trace Organic Contaminants by Electrodialysis. *Ph.D. Thesis*, University of Edinburgh (U.K.).

Bouhidel, K. E. and A. Lakehal (2006). Influence of voltage and flow rate on electrodeionization (EDI) process efficiency. *Desalination*, **193**, 411-421.

Brauns E., W. De Wilde, B. Van den Bosch, P. Lens, L. Pinoy, M. Empsten (2009). On the experimental verification of an electrodialysis simulation model for optimal stack configuration through solver software. *Desalination*, **249**, 1030-1038.

Brauns, E., W. De Wilde, B. Van den Bosch, P. Lens, L. Pinoy and M. Empsten (2009). On the experimental verification of an electrodialysis simulation model for optimal stack configuration design through solver software. *Desalination*, **249**, 1030-1038.

Chao, Y. M. and T. M. Liang (2008). A feasibility study of industrial wastewater recovery using electrodialysis reversal. *Desalination*, **221**, 433-439.

Cho, J., G. Amy and J. Pellegrino (2000). Membrane filtration of natural organic matter: factors and mechajection and flux decline with charged ultrafiltration (UF) membrane. *J. Membr. Sci.*, **164**, 89-110.

Cowan, D. A., and J. H. Brown (1959). Effect of turbulence on limiting current density in electrodialysis cells. *Industrial and Engineering Chemistry Research*, **51**, 1445-1448.

Ervan, Y. and I. G. Wenten (2003). Study on the influence of applied voltage and feed concentration on the performance of electrodeionization. *Songklanakarin J. Sci. Technol.*, **24** (Suppl.), 955-963.

Ganzi, G. C., J. H. Wood and C. S. Griffin (1992). Water Purification and Recycling Using the CDI Process. *Ionpure Technologies Corp*., *Environmental Progress*, **11**, 49-53.

Ganzi, G. C., Y. Egozy, A. J. Guiffrida and A. D. Jha (1987). Highly purity water by electrodeionization performance of the Ionpure™ continuous deionization system. *Ultrapure Water J.*, **4,** 43-48.

Ganzi, G.C. (1988). Electrodeionization for High Purity Water Production, *AIChE Symposium Series*, **84**, 73-83.

Graybill, F. A., and H. K. Iyer (1994). *Regression Analysis: Concepts and Applications* (1st ed.), Duxbury Press, Belmont (U.S.A.), pp. 509-607.

Grebenyuk, V. D., R. D. Chebotareva, S. Peters and V. Linkov (1998). Surface modification of anion-exchange electrodialysis membranes to enhance anti-fouling characteristics. *Desalination*, **115**, 313-329.

Ionics Inc., (1984). Electrodialysis-Electrodialysis Reversal Technology, Ionics Inc., Watertown (U.S.A).

Juda, W. and W. A. Mc Rae (1950). Coherent ion-exchange gels and membranes. *J. Am. Chem. Soc.*, **72**, 1044.

Juhasz, E., K. N. Marsh (2009), Recommended reference materials for realization of physicochemical properties. Section: Electrolytic conductivity. *Pure and Applied Chemistry*, **53**, 1841-1845.

Kariduraganavar, M.Y., R. K. Nagarale, A. A. Kittur, S. S. Kulkarni (2006). Methods for electrodialysis and fuel cell applications. *Elsevier B. V.*, **197**, 225-246.

Katz, W. E., I. D. Elyanow, K. J. Sims (1991). Electrodeionization polarity reversal apparatus and process, U.S. Patent 5,024,465.

Kim, D. H., S. H. Moon and J. Cho (2002). Investigation of the adsorption and transport of natural organic matter (NOM) in ion-exchange membranes. *Desalination,* **151***,* 11-20.

Lee, H. J., D. H. Kim, J. Cho and S. H. Moon (2002) Characterization of anion exchange membranes with natural organic matter (NOM) during electrodialysis. *Desalination*, **151**, 43-52.

Lee, H. J., S. H. Moon and S.P. Tsai (2002). Effects of pulsed electric fields on membrane fouling in electrodialysis of NaCl containing humate. *Separation and Purification technology*, **27**, 89-95.

Lee, H.J., H. Strathmann, S. H. Moon (2002). Determination of the limiting current density in electrodialysis desalination as an empirical function of linear velocity. *Desalination*, **190**, 43-50.

Lindstrand, V., G. Sundstrom and A. S. Jonsson (2000). Fouling of electrodialysis membranes by organic substances. *Desalination*, **128**, 91–102.

Meng, H., C. Peng, S. Song and D. Deng (2004). Electro-regeneration mechanism of ion-exchange resins in electrodeionization. *Surface Review and Letters*, **11**, 599-605.

Mihara, K. and M. Kato (1969). Polarity reversing electrode units and electrical switching means therefore, U.S. Patent 3,453,201.

Nagarale, R. K., G. S. Gohil and V.K. Shahi (2006). Recent developments on ion-exchange membranes and electro-membrane process. *Advances in Colloid and Interface Science*, pp. 97-130.

Strathmann, H. (2004). *Ion-exchange membrane. Separation Process*. Elsevier B.V., Amsterdam (The Netherlands), pp. 152-159; 287-300.

Wilinks, F. C. and P. A. McConnelee (1988). Continuous deionization in the preparation of microelectronics-grade water, *Solid State Technology*, 87-92.

Web sites

`http://www.comsol.com/blogs/` (last access: 19/09/2014)

`http://www.lenntech.com/` (last access: 02/09/2014)

`http://www.statsoft.com/Support/Blog/` (last access: 30/07/2014)